

For Reference

NOT TO BE TAKEN FROM THIS ROOM

Ex LIBRIS
UNIVERSITATIS
ALBERTHEAENSIS





Digitized by the Internet Archive
in 2024 with funding from
University of Alberta Library

<https://archive.org/details/Tse1982>

THE UNIVERSITY OF ALBERTA

RELEASE FORM

NAME OF AUTHOR John W. Tse

TITLE OF THESIS Samarium-153 As A Potential Tumor
Localizing Agent

DEGREE FOR WHICH THESIS WAS PRESENTED Doctor of Philosophy

YEAR THIS DEGREE GRANTED Fall 1982

Permission is hereby granted to THE UNIVERSITY OF
ALBERTA LIBRARY to reproduce single copies of this
thesis and to lend or sell such copies for private,
scholarly or scientific research purposes only.

The author reserves other publication rights, and
neither the thesis nor extensive extracts from it may
be printed or otherwise reproduced without the author's
written permission.

THE UNIVERSITY OF ALBERTA

Samarium-153 As A Potential Tumor Localizing Agent

by

(C)

John W. Tse

A THESIS

SUBMITTED TO THE FACULTY OF GRADUATE STUDIES AND RESEARCH
IN PARTIAL FULFILMENT OF THE REQUIREMENTS FOR THE DEGREE
OF Doctor of Philosophy

IN

Pharmaceutical Sciences (Bionucleonics)

Faculty of Pharmacy and Pharmaceutical Sciences

EDMONTON, ALBERTA

Fall 1982

THE UNIVERSITY OF ALBERTA
FACULTY OF GRADUATE STUDIES AND RESEARCH

The undersigned certify that they have read, and recommend to the Faculty of Graduate Studies and Research, for acceptance, a thesis entitled Samarium-153 As A Tumor Localizing Agent submitted by John W. Tse in partial fulfilment of the requirements for the degree of Doctor of Philosophy in Pharmacy and Pharmaceutical Sciences (Bionucleonics).

Abstract

High specific activity samarium-153 of high radionuclidic purity was produced using an (n,γ) reaction. Sm-153 citrate, Sm-153 transferrin and Sm-153 EDTA were prepared. Sm-153 colloid formation was observed for both Sm-153 citrate and Sm-153 transferrin in vitro and in vivo. Liver and spleen uptake of Sm-153 citrate and Sm-153 transferrin were predominant in tissue distribution studies. No significant difference was observed between the two agents during in vitro and in vivo tests. They were also shown to be inferior to Ga-67 citrate and Ga-67 transferrin in tumor localization in vivo.

Little colloidal formation was observed when Sm-153 was complexed with EDTA both in vitro and in vivo. Calcium ions were found to have little ability to displace samarium from its EDTA complex. Sm-153 EDTA also showed greater affinity to tumor culture cells than Ga-67 citrate. In a dual-labelled Sm-153(C-14)EDTA study, Sm-153 was found to be taken up by tumor culture cells independently from C-14 EDTA. A 1:10 samarium-to-EDTA ratio was required to offer optimal stability in vivo. Skeletal uptake of Sm-153 EDTA, especially in joints, was observed in vivo. Sm-153 EDTA showed at least a twenty-two fold higher tumor-to-blood ratio than Ga-67 citrate at 24 and 48 hours post administration in vivo. This ratio could be further improved

to a small extent by lowering the dose administered. Gamma scintillation imaging results indicated that Sm-153 EDTA was superior to Ga-67 citrate in the delineation of Dunning Prostatic tumors. Tissue distribution studies revealed that Sm-153 EDTA localized mainly in bone, liver and kidneys. About 80% of the injected dose was eliminated through urine within the first 6 hours. Elimination of Sm-153 EDTA in feces was found to be negligible. Dual-labelled Sm-153(C-14)EDTA experiments indicated that little C-14 EDTA activity was detected in tumor and the Sm-153 uptake in tumor was found to be independent of the C-14 EDTA during the same period of time in vivo.

Samarium EDTA in intravenously-injected doses of up to 10.9 uMole Sm/Kg did not produce any noticeable changes in the normal weight gain and the histological architecture of body organs such as lung, liver, kidneys and bone. The estimated radiation dose for Sm-153 EDTA administered intravenously at 10.9 nMole Sm/Kg was about 0.38 rads/mCi (0.10 mGy/MBq) for the whole body, 1.52 rads/mCi (0.41 mGy/MBq) for liver, 0.35 rads/mCi (0.09 mGy/MBq) for total bone and 1.21 rads/mCi (0.33 mGy/MBq) for kidneys.

Sm-153 has a suitable decay emission consisting of 28% photons of 103 KeV for imaging, and an optimal physical half-life of 46.8 hours. Sm-153 EDTA is simple to prepare, store and distribute. The high tumor-to-blood ratio offered by Sm-153 EDTA and the possibility of early tumor diagnosis at 6 hours together with the comparative estimated whole

body radiation dose of 0.38 rads/mCi (0.10 mGy/MBq) versus 0.26 rads/mCi (0.07 mGy/MBq) for Ga-67 citrate makes Sm-153 EDTA a good potential tumor imaging agent.

Acknowledgements

I would like to thank the Heavenly Father and Jesus Christ, the Creator of the Universe and the ultimate source of wisdom, for providing such opportunity to His child so that some of the answers are unfold.

I would like to express my deepest gratitude to Dr. A.A. Noujaim and to Dr. L.I. Wiebe for their guidance throughout this project. Their examples and spirit as teachers and researchers inspire their student.

Gratitude is expressed to Dr. U.K. Terner for his help and advice, and to Dr. Shnitka for the pathological examination.

Financial awards in the form of Alberta Heritage Foundation Fund for Medical Research Studentship and Research Allowance are gratefully acknowledged.

DEDICATION

To Lettice, my beloved wife, who shares and bears with
me.

Table of Contents

Chapter	Page
I. Introduction	1
II. Survey of the Literature	4
A. The 'Rare Earth' Elements	4
B. Natural Abundance and Extraction of Samarium ...	5
C. Industrial use of Samarium	7
D. Physical Properties of Samarium	8
E. Chemistry of Samarium	8
F. Common Samarium Compounds	9
1. Oxides	10
2. Oxalate	11
3. Carbonate	12
4. Hydrous oxide (hydroxide)	12
5. Chloride	13
6. Fluoride	13
7. Bromide and Iodide	14
8. Nitrate	14
9. Sulfate	14
10. Sulfides	15
11. Citrates	15
12. Samarium Complexes	16
G. General Analysis	16
H. Natural Isotopes	17
I. Artificially Produced Radioisotopes of Samarium	18
J. Samarium-153	18

K. Physiological Distribution of Samarium and its Derivatives	21
L. Current Use of Samarium in Medicine	23
M. Radioactive Samarium as an X-ray Source	25
N. Samarium-153 as a Skeletal Imaging Agent	25
O. Samarium-153 as a Tumor Imaging Agent	26
P. Toxicity	29
1. Oral	30
2. Parenteral	30
3. Inhalation	31
4. Skin	32
III. Experimental Methods	33
A. Tissue Culture Methods	33
Melanoma 2 AB and EMT-6 Culture Cells	33
B. Animal Tumor Models	34
1. Lewis Lung Tumor Model in BDF, Mice	34
2. Dunning 3327 Prostatic Tumor Model in Copenhagen/Fisher Rats	34
C. Preparation of Radiochemicals	35
1. Production of Samarium-153	35
2. Screening of Potential Samarium Compounds	37
3. Preparation of Samarium-153 Citrate	38
4. Preparation of Samarium-153 Transferrin	38
5. Preparation of Samarium-153 EDTA	39
6. Preparation of Samarium-153(C-14) EDTA	39
7. Preparation of Gallium-67 Citrate	40
8. Preparation of Gallium-67 Transferrin	41

D. Quality Control of Radiochemicals	42
1. Radionuclidic Purity Control	42
2. Radiochemical Purity Control	42
3. Colloid Formation Determination	44
4. Determination of Calcium-45 and Samarium-153 Competition for binding with EDTA	44
5. Determination of Samarium-153 EDTA in Urine	45
E. Studies of Uptake by Culture Cells	45
F. Tissue Distribution Studies	47
G. Whole Body Imaging Studies	48
H. Whole Body Radiochemical Elimination Studies ..	49
1. Whole Body Counting	49
2. Urinary Excretion of Samarium-153 EDTA ..	49
I. Dual-labelled Samarium-153(C-14)EDTA Tissue Distribution Studies	50
1. Tissue Sample Preparation	50
2. Determination of Samarium-153 Radioactivity	50
3. Determination of Carbon-14 Radioactivity	51
J. Toxicity Studies	52
1. Effect on Weight Gain	52
2. Histopathological Studies	52
K. Statistical Methods	53
IV. Results and Discussion	54
A. Quality Control of Radiochemicals	54
1. Radionuclidic Purity	54
2. Radiochemical Purity	58

3. Colloid Formation Determination	59
B. Screening of Potentially Useful Samarium Compounds	62
1. Ultracentrifugation Method	62
2. Imaging of Potentially Useful Samarium Complexes	64
C. Calcium-45 and Samarium-153 Competition	67
D. Determination of Samarium-153 EDTA in Urine ...	69
E. Radiochemical Uptake by Cells in Tissue Culture	71
1. Comparison of Sm-153 Citrate, Sm-153 Transferrin and Ga-67 Citrate Uptake in Melanoma 2AB Cells	71
2. Uptake of Sm-153 EDTA (1:10) in Melanoma 2 AB Cell Cultures	72
3. Mechanism of Uptake of Sm-153 EDTA (1:10) in cell culture	75
4. Uptake of High Specific Activity Sm-153 EDTA(1:10) by EMT-6 Tumor Cells	81
F. Tissue Distribution Studies	82
1. Sm-153 Citrate Distribution in BDF, Mice Bearing Lewis Lung Tumors	82
2. Sm-153(C-14)EDTA (1:10) and Ga-67 Citrate distribution in BDF, Mice	88
3. High Specific Activity Sm-153 EDTA (1:10) Distribution in BDF, Mice Bearing Lewis Lung Tumors	89
G. Whole Body Imaging Studies	97
1. Comparison of Sm-153 Chloride, Sm-153 Citrate and Sm-153 Transferrin Tumor Localization	97
2. Comparison between Sm-153 Citrate and Ga-67 Citrate Tumor Localization	98
3. Comparison of Tumor Localization between Sm-153 Transferrin and Ga-67 Transferrin	100

4. In vivo Disposition of Samarium-153 Citrate	102
5. Effect of EDTA Concentration on Samarium Distribution <u>in vivo</u>	104
6. Tumor Localization of High Specific Activity Sm-153 EDTA (1:10)	108
H. Radiochemical Elimination of Sm-153 EDTA	110
1. Whole Body Elimination of Sm-153 EDTA (1:10)	112
2. Blood Kinetics of Sm-153 EDTA (1:10) in Rats	113
3. Excretion of Sm-153 EDTA in Urine and Feces	117
I. Mechanism of Sm-153 EDTA Tissue Distribution .	120
J. Toxicity Studies	126
1. Effect on Weight Gain	126
2. Histopathological Results	128
K. Absorbed Radiation Dose Calculations for Sm-153 EDTA	129
1. Radiation Dose to the Liver	131
2. Radiation Dose to the Total Bone	138
3. Radiation Dose to the Kidneys	138
4. Radiation Dose to the Whole Body	138
V. Summary and Conclusions	140
Bibliography	143
Appendix 1	149
Appendix 2	150
A. Absorbed Radiation Dose to the Bone	150
B. Absorbed Radiation Dose to the Kidneys	151
C. Absorbed Radiation Dose to Whole Body	152

List of Tables

Table	Page
1 Artificially Produced Radioisotopes of Samarium	19
2 Separation of Sm-153 Complexes by Ascending Liquid Chromatography	60
3 Colloid Formation of Samarium Complexes	63
4 Chromatographic Separation of Samarium and Calcium Complexes	68
5 Chromatographic Separation of Samarium from Urine	70
6 Uptake of Sm-153 Citrate, Ga-67 Citrate and Sm-153 Transferrin by Melanoma 2AB Cells	74
7 Uptake of Sm-153 EDTA (1:10) and Ga-67 Citrate by Melanoma 2AB Cells	77
8 Uptake of Sm-153(C-14)EDTA (1:10) by Melanoma 2AB Cells	80
9 Uptake of Sm-153(C-14)EDTA (1:10) and Ga-67 Citrate by EMT-6 Cells	84
10 A, B: Tissue Distribution Results of Sm-153 Citrate at 3.0 uMole Sm-153/Kg in BDF, Mice Bearing Lewis Lung Tumors	87
11 A, B: Tissue Distribution Results of Sm-153(C-14)EDTA (1:10) and Ga-67 Citrate at 1.09 uMole nuclide/Kg in BDF, Mice Bearing Lewis Lung Tumors	90
12 A, B: Tissue Distribution Results of Sm-153 EDTA and Ga-67 Citrate at 10.9 nMole nuclide/Kg in BDF, Mice Bearing Lewis Lung Tumors	94
13 Distribution of Sm-153 Citrate and Sm-153 Transferrin Activity in Blood	105
14 In Vivo Colloid Formation of Samarium-153 After Injection of Sm-153 Citrate or Sm-153 Transferrin	106
15 Whole Body Elimination of Low Specific Activity Sm-153 EDTA (1:10) and Ga-67 Citrate in Rats	114

Table	Page
16 Whole Body Elimination of High Specific Activity Sm-153 EDTA (1:10) and Ga-67 Citrate in Rats	115
17 Disappearance of High Specific Activity Sm-153 EDTA (1:10) in Blood	118
18 Cumulative Sm-153 EDTA (1:10) Activity in Urine and Feces from Rats	121
19 A, B: Tissue Distribution Results for Dual-labelled Samarium-153(C-14)EDTA (1:10) at 1.09 uMole Sm/Kg in BDF, Mice Bearing Lewis Lung Tumors	124
20 Equilibrium and Absorbed Dose Fraction for various emissions of Sm-153 of uniform distribution in Liver	133
21 Equilibrium and Absorbed Dose Fraction for various emissions of Sm-153 of uniform distribution in Bone	134
22 Equilibrium and Absorbed Dose Fraction for various emissions of Sm-153 of uniform distribution in Kidneys	135

List of Figures

Figure	Page
1 Decay Scheme of Sm-153	22
2 Low Specific Activity Sm-153 Gamma Ray Photopeak Spectrum	55
3 High Specific Activity Sm-153 Gamma Ray Photopeak Spectrum	56
4 Theoretical Calculation of Sm-153 Production in a Nuclear Reactor	57
5 Scintigraphic distribution of Sm-153 Complexes in Normal Rats	66
6 Melanoma 2AB Cell Uptake of Sm-153 Citrate and Ga-67 Citrate	73
7 Uptake of Sm-153 EDTA (1:10) by Melanoma 2AB Cells	76
8 Uptake of Sm-153(C-14)EDTA (1:10) by Melanoma 2AB Cells	79
9 Uptake of High Specific Activity Sm-153(C-14)EDTA by EMT-6 Tumor Cells	83
10 Tumor to Blood Ratios of Sm-153 Citrate in BDF, Mice Bearing Lewis Lung Tumors	86
11 Tumor to Blood Ratios of Sm-153(C-14)EDTA (1:10) and Ga-67 Citrate in BDF, Mice Bearing Lewis Lung Tumors	91
12 Tumor to Blood Ratios of High Specific Activity Sm-153 EDTA (1:10) and Ga-67 Citrate in BDF, Mice Bearing Lewis Lung Tumors	95
13 Tumor to Blood Ratio Comparison of Sm-153 EDTA (1:10) and Ga-67 Citrate at various dosages	96
14 Scintigraphic Images of Samarium Uptake in Dunning Prostatic Tumor Bearing Rats	99
15 Scintigraphic Images of Sm-153 Citrate, Sm-153 Transferrin, Ga-67 Citrate and Ga-67 Transferrin Uptake in the Dunning Prostatic Tumor Bearing Rats	103

Figure	Page
16 Effect of EDTA on the Biodistribution of Sm-153 in the Dunning Prostatic Tumor Bearing Rats	109
17 A, B: Scintigraphic images of High Specific Activity Sm-154 EDTA (1:10) and Ga-67 Citrate in Dunning Prostatic Tumor Bearing Rats	111
18 Whole Body Elimination of Sm-153 EDTA (1:10) in Rats	116
19 Blood Kinetics of High Specific Activity Sm-153 EDTA (1:10) in Rats	119
20 Cumulative Sm-153 EDTA (1:10) Activity in Urine and Feces from Rats	122
21 Tumor to Blood Ratios of Sm-153(C-14)EDTA (1:10) in BDF, Mice Bearing Lewis Lung Tumors	125
22 The Effect of Sm-153 EDTA (1:10) on Normal Weight Gain	127
23 The Percentage Dose Distribution of Sm-153 EDTA (1:10) in Mice	132

I. Introduction

Gallium-67 citrate has been documented as a useful tumor-scanning agent (1-6). The distribution of carrier-free gallium was found to be predominantly in the liver, spleen, kidney and bone of animals. The addition of stable gallium caused a progressive increase in relative concentration within the skeleton and a relative decrease in soft tissue concentration (7). The uptake of gallium-67 in neoplasms, makes it an important tool for the detection of lymphomas, bronchogenic carcinomas, malignant melanomas, primary bone tumors, lung tumors and breast tumors.

However, because gallium-67 has a low abundance of optimal emissions (93 KeV photons, 38%, 184 KeV photons, 20%, 300 KeV photons, 24%, etc.) imaging with a gamma camera is difficult. Scan interpretation has also been a difficult task, as gallium-67 citrate offers low tumor-organ ratios for blood, liver, spleen, kidneys, heart and gastrointestinal tract (GIT). Due to a relatively slow tumor uptake and blood clearance, imaging with gallium-67 citrate must be delayed 48 hours following injection, thus resulting in a loss of potential information due to radiodecay. In addition, gallium-67 citrate does not concentrate in all tumor types nor does it concentrate to the same extent in all tumors of the same type.

Primary tumors are detected more reliably with gallium-67 citrate than metastatic tumors, and reliability seems to be higher in the neck and thorax region. Larson (8) commented that gallium-67 citrate will never be a tool for mass cancer screening because of nonuniform uptake, relatively nonspecific localization, and unsuitable physical characteristics. It is also known that toxic doses of gallium affect the GIT, kidneys, and hematopoetic and lymphatic systems.

Gallium-67, complexed to transferrin, has been proposed and observed to enhance a more rapid uptake by Melanoma 2AB culture cells(9). It was further reported that transferrin might also serve as a facilitating carrier in the uptake of gallium-67 at the tumor cell surface(9). While research towards a gallium-67 carrier vehicle continues, the search for a better tumor imaging agent is a definite need.

Samarium-153 has been shown in a preliminary observation to be tumor-avid in a rabbit tumor model (10). Samarium belongs to the lanthanide group of rare earths. The LD₅₀ of samarium chloride in mice is 585 mg/kg i.p. and greater than 2,000 mg/Kg after oral administration (11). Samarium-153 is an artificial radioactive isotope produced in a nuclear reactor using the Sm-152(n, γ)Sm-153 reaction. Since Sm-152 is of 27% abundance and has a high thermal neutron capture cross-section (approximately 208 barns) for neutron activation, the production of Sm-153 using the (n, γ) reaction is not difficult.

Samarium-153 specific activities of 15-20 mCi/mg have been reported after 6 hours of irradiation in a 100 KW TRIGA reactor, although the thermal neutron flux was not reported (10). Samarium-153 has adequate physical properties for imaging (28% yield of 103 KeV photons). Production, storage and commercial distribution to various locations will not be difficult because of the 46.8-hour deexcitation half-life.

Although preliminary dosimetry calculations on Sm-153 citrate (10) indicate a whole body radiation dose of 0.67 rads/mCi, compared to 0.26 rads/mCi for gallium-67 citrate, further evaluation of samarium-153 is still warranted since a samarium scan might be performed at a much earlier time than the 48-72 hours delay regularly implemented for the gallium-67 scan. Additionally, the samarium-153 dosage might be smaller and the cleansing of the bowel would not be necessary as is required in the case of patients undertaking a gallium-67 scan. The potential use of samarium-153 as a tumor imaging agent, therefore, prompted this research.

II. Survey of the Literature

A. The 'Rare Earth' Elements

Samarium belongs to the lanthanide group of elements which were originally known as the 'Rare Earth' elements because of their occurrence as an oxide mixture in earth. The description 'rare' is misleading in that some (eg. cerium and neodymium) are more plentiful in the earth's crust than lead.

On the conventional periodic table, lanthanum belongs to the transition metals of group III B. Because samarium and other rare earth elements (atomic numbers 58 - 71) have characteristics similar to lanthanum, they may be generally regarded as lanthanide elements.

The rare earth elements are conventionally divided into two groups. The 'light group' (or cerium group) is composed of lanthanum (La), cerium (Ce), praseodymium (Pr), neodymium (Nd), and promethium (Pm). These elements may be separated by conventional crystallization procedures.

The 'heavy group' (or yttrium group) includes yttrium (Y), samarium (Sm), europium (Eu), gadolinium (Gd), terbium (Tb), dysprosium (Dy), holmium (Ho), erbium (Er), thulium (Tm), ytterbium (Yb), and lutetium (Lu). The heavy

lanthanides, samarium through lutetium, are separated by ion exchange. Natural mixtures of the heavy rare earths are found together, with yttrium oxide composing up to 80% (12). Before modern separation techniques were available, the main use of these elements was in the manufacture of mantles for gas lights. However, they are now used in the production of control rods for atomic reactors, in alloys with nickel and chromium, in microwave devices, lasers, masers, and in television screens.

The element samarium was discovered in 1879 by L. de Boisbaudran, the discoverer of gallium. Demarcay resolved and purified the element in 1901 (13). The name samarium was taken from the mineral samarskite, in turn named in honour of a Russian mine official, Colonel Samarski.

B. Natural Abundance and Extraction of Samarium

The rare earth elements as a group constitute about 0.008% of the earth's crust, and samarium generally comprises about 1 to 2 % of the rare earth mixtures.

In general, samarium ranks 62nd in abundance of the earth crust elements. The principle sources of samarium from commercial ores are monazite (4.5% Sm_2O_3) and bastnäsite (0.5% Sm_2O_3) (14). The lanthanides carried by monazite are usually in the 3+ oxidation state (15).

Samarium is concentrated to a various degree by plants, as reported in a Georgia study (16, 17). Concentration in the ash of hickory leaves, dogwood stems, lichens, mosses, horsetail was found to be 200 - 700, 200, 2.6 - 40, 1.8 - 23, 102 ppm respectively. Evidence for the occurrence of samarium in other plants has not been found (16 - 18).

Monazite ores generally are cracked by acid attack (H_2SO_4 or HCl) which converts the rare earth elements to the corresponding soluble sulfates or chlorides. After reaction, the mixture is added to cold water to dissolve the anhydrous rare earth sulfates.

Samarium can then be separated from the other rare earths in its trivalent form by ion-exchange or solvent extraction methods. Samarium can also exist in the divalent form, but the divalent ion in solution is unstable and slowly decomposes in water. Chemical reduction of samarium salts with calcium or alkali metals usually gives the divalent salt.

Pure metallic samarium is silver-gray in colour, retaining a luster in dry air, but only moderately stable in moist air, with formation of an adherent oxide. Finely divided samarium, as well as chips resulting from working the metal are pyrophoric and ignite spontaneously in air, burning at $150^\circ - 180^\circ C$ (14). Samarium oxide is pale yellow and is readily soluble in most acids (15).

C. Industrial use of Samarium

Relatively few important uses have been reported for samarium. However, due to recently expanded research in rare earth chemistry, development of this element's use may be promising.

Samarium has some application in the ceramic industry. Samarium oxide has been used in optical glass filters, sunglasses, etc., to increase the infrared absorption. Samarium is also used as a catalyst for certain organic reactions. Samarium oxide has catalytic activity for the oxidation of acyclic primary alcohols to aldehydes. Various samarium compounds have shown promise as phosphor activators and also as thermionic emitters. Samarium titanate has been used to stabilize the performance of capacitors, and the sulfide salt has been studied for use in thermoelectric generating devices (13, 14).

The samarium isotope mixture has a very high thermal-neutron absorption cross-section (5800 barns at 0.025 eV). This is especially due to samarium-149 which has a very high cross-section of 40,000 barns. No chain reaction exists if samarium is used during the separation of low cross-section isotopes from spent uranium fuel. Therefore, there has been some interest in using samarium in the atomic industry. Nuclear applications such as in the manufacture of control rods, burnable poisons, and in shielding

applications have been implemented (13, 14).

D. Physical Properties of Samarium

Samarium resembles steel in appearance. At room temperature, it crystallizes in the rhombohedral form (α -Sm) with a density of 7.536 g/cc. At 917°C , it is transformed to the centered cubic form (β -Sm) with a density of 7.40 g/cc. The heat of transition is 0.744 kcal/mole. Samarium melts at 1072°C and boils at 1804°C . The heat of vaporization is 46 kcal/mole (13, 14).

E. Chemistry of Samarium

Samarium belongs to lanthanides which are characterized by the successive filling-in of the well-shielded 4f electron shell while maintaining (ideally) the same $5\text{d}^16\text{s}^2$ outer electronic configuration in each element. The fourteen lanthanides following lanthanum in which the fourteen 4f electrons are being successfully added to the lanthanum configuration, are generally electropositive elements and give M^{3+} ions (14).

Samarium has an atomic number of 62 and an atomic weight of 150.35. Because of its position in the series, samarium would ideally have the electronic configuration $4f^55d^16s^2$. However, the more probable configuration is $4f^65s^2$ for the neutral atom and $4f^55s^25p^6$ for the Sm^{3+} ion. A consequence of this configuration is that samarium exhibits valences of 2^+ and 3^+ . As expected from its configuration, the trivalent state is more stable.

The ionic radius for Sm^{+2} is 1.14\AA and Sm^{+3} is 0.964\AA . The first ionization potential is 5.6 eV and the second is 11.4 eV (14).

Samarium metal is an active reducing agent. It will reduce carbon monoxide, carbon tetrachloride, as well as the oxides of many metals including iron, manganese, chromium, silicon, tin, lead, and zirconium. The electrode potential, E° , of samarium is +2.2 volts for $Sm^{+3}+3e^-$.

While samarium metal is an active reducing agent, it is moderately stable in dry air. In moist air an oxide coating develops.

F. Common Samarium Compounds

Many derivatives of samarium such as the nitrides, sulfides, carbides, silicides, phosphides, and hydrides may be formed directly by reacting the metal and corresponding

nonmetal at high temperature. Principal compounds of samarium are the trivalent oxide, hydrous oxide, oxalate, nitrate, chloride, sulfate and carbonate (14).

The compounds of samarium are usually yellowish in colour and include samarium oxide (Sm_2O_3), samarium chloride ($\text{SmCl}_3 \cdot 6\text{H}_2\text{O}$) and samarium bromide ($\text{SmBr}_3 \cdot 6\text{H}_2\text{O}$). Samarium salts generally exhibit an oxidation state of 3^+ . Samarium (II) aqueous solutions are not stable because water is reduced by Sm^{+2} . In addition, all compounds of Sm^{+2} are thermodynamically unstable with respect to oxidation by water or oxygen and are stable indefinitely only in an inert atmosphere (14).

A number of compounds of Sm^{+2} are known including the halides, sulfate, chromate, phosphate, hydroxide, carbonate and oxide, and the structures of some of these are known. SmO has the rock salt structure (14).

1. Oxides

Samarium oxide, Sm_2O_3 , is probably the most common and important compound of the element. It is stable except for a slight tendency to absorb moisture and carbon dioxide from the air. It is insoluble in water but dissolves readily in mineral acids with liberation of a considerable amount of heat (19, 20). It is prepared by calcination of various other salts, some of which are the carbonate, hydrous oxide,

oxalate, nitrate, and sulfate, or by air oxidation of the metal. The oxide is a convenient compound for preparation of other salts and metallic samarium.

(i). reaction with HCl (20, 21),

Samarium oxide dissolves easily in hydrochloric acid, yielding hexahydrated samarium trichloride.



(ii). reaction with H_2SO_4 (20, 21)

Samarium oxide dissolves readily in sulfuric acid, and yields octahydrated samarium sulfate.



(iii). reaction with CH_3COOH (20, 21),



2. Oxalate

Samarium oxalate, $\text{Sm}_2(\text{C}_2\text{O}_4)_3 \cdot 10\text{H}_2\text{O}$, is precipitated from aqueous salt solutions by the addition of oxalic acid or ammonium oxalate. The oxalate is virtually insoluble in water, and slightly soluble in acid. In water, the

solubility is less than 0.01 g/l at 25°C (19, 20).

3. Carbonate

Samarium carbonate, $\text{Sm}_2(\text{CO}_3)_3 \cdot 3\text{H}_2\text{O}$ is prepared by precipitation of aqueous solutions of samarium chloride with solutions of alkali bicarbonates saturated with carbon dioxide or by hydrolysis of a solution of the trichloracetate. The carbonates are insoluble in water, but are readily soluble in acids (19, 20).

4. Hydrous oxide (hydroxide)

Samarium hydrous oxide (hydroxide), $\text{Sm}(\text{OH})_3$, is formed by the addition of an alkali or ammonium hydroxide to an aqueous solution of a samarium salt. The solubility of the hydroxide in water is very low at room temperature. Accordingly, only very low concentrations of OH^- ions are produced in solution even though samarium metal is moderately basic (19, 20).

5. Chloride

Samarium chloride, $\text{SmCl}_3 \cdot 6\text{H}_2\text{O}$, is prepared by dissolving the oxide, hydrous oxide, or carbonate in hydrochloric acid, and crystallizing the chloride by evaporation. Samarium chloride has a high solubility in water, being greater than 1 Kg/l at room temperature. The divalent chloride SmCl_2 is not very stable under normal conditions (20, 22).

Divalent samarium chloride is formed upon reduction of the trivalent salt with hydrogen at about 270°C . The divalent chloride reoxidizes easily in the presence of air. Samarium chloride reacts with sodium hydroxide to form samarium oxide (20, 22).



6. Fluoride

Samarium fluoride, $\text{SmF}_3 \cdot \text{H}_2\text{O}$ is formed as a gelatinous precipitate by the addition of hydrofluoric acid to an aqueous solution of a samarium salt. It can also be prepared by treating the oxalate, hydrous oxide, or carbonate with HF. The fluoride is insoluble in water or acid (19, 20).

7. Bromide and Iodide

Samarium bromide and iodide have been studied much less than the chloride and fluoride. The iodide is especially unstable in moist air, and is difficult to prepare (19, 20).

8. Nitrate

Samarium nitrate, $\text{Sm}(\text{NO}_3)_3 \cdot 6\text{H}_2\text{O}$ is prepared with nitric acid in the same general manner as the chloride is with hydrochloric acid. It is very soluble in water and moderately soluble in some alcohols, ketones, and ethers. Samarium nitrate can be thermally decomposed to the oxide (19, 20).

9. Sulfate

Samarium sulfate, $\text{Sm}_2(\text{SO}_4)_3 \cdot 8\text{H}_2\text{O}$, can be prepared by dissolving the oxide, hydrous oxide, or carbonate in sulfuric acid and is crystallized by evaporation. Water solubility of the hydrated sulfate is quite low, being 0.27g/l H_2O at 20°C. Contrary to normal behavior, the solubility decreases with increasing temperatures, being 0.20g/l H_2O at 40°C. Anhydrous samarium sulfate is formed by

heating the hydrous form to about 400°C. Divalent samarium sulfate can be precipitated from the trivalent sulfate solution by reduction with magnesium amalgam. The divalent sulfate is easily oxidized by air or dilute nitric acid (23).

10. Sulfides

Samarium sulfides, SmS_2 , and Sm_2S_3 , are formed under a variety of conditions at elevated temperatures by reacting solid samarium salts such as the oxide, carbonate, sulfate, or chloride with agents such as sulfur, carbon disulfide, hydrogen sulfide and ammonium sulfide. The sulfides are insoluble and fairly stable in water. In acid, decomposition takes place with the evolution of hydrogen sulfide (19, 20).

11. Citrates

Samarium citrate was prepared by the addition of samarium chloride solution to 0.1 - 1.0 M sodium citrate. Usually, a samarium citrate salt contains 3 molecules of water of crystallization which separate from the compound at about 200 - 250°C (24). Samarium citrate is fairly soluble in water at neutral pH (25).

12. Samarium Complexes

Samarium has been complexed with a number of complexing or chelating agents for in vivo investigations. They include Sm-HEDTA (39, 40), Sm-DTPA (39, 44, 45), Sm-Bleomycin (46) and Sm-Trypsin (38).

Complexing of samarium can be easily achieved by incubating the chelating or complexing agent with the samarium chloride or citrate salt at an optimal pH and temperature in aqueous media. Preparation of some of these complexes are discussed in subsequent sections.

G. General Analysis

Analysis of samarium is carried out mainly by spectrographic and spectrophotometric methods. The bivalence of samarium cannot be taken advantage of by polarographic methods because of certain trivalent cation interference at the reduction potential of Sm^{+3} to Sm^{+2} ($E_{\frac{1}{2}} = -1.80$ V) (19).

Spectrographic analysis is well established for the determination of impurities in samarium, and for the estimation of samarium in the presence of other compounds. Useful arc spectrum lines for samarium are found at 3568.36 Å, 3592.59 Å, and 3634.27 Å. In solution, both valence

states show light absorption at various wavelengths. Divalent samarium is characterized by intense absorption bands in the ultraviolet. Because of its instability, the divalent state is not particularly useful for analysis. The trivalent ion exhibits absorption at 3625 Å, 3475 Å, and 4020 Å in addition to other less intense bands (19). Light absorption enables analysis to be carried out rapidly by spectrophotometric methods. The absorption bands of samarium and most trivalent lanthanons are very sharp in contrast to the broad absorption bands of the transition-metal ions. Such analysis can be utilized with fairly high purity materials (99.9%) and can also be used effectively in crude mixtures. Instrumental analysis such as atomic absorption and neutron activation also offer sensitive analytical methods of great ease. Wet chemical analysis relying on solubility differences, complex formation, etc., have essentially been replaced (19).

H. Natural Isotopes

The naturally occurring isotopes with their respective abundances are listed in the following table (76, 77):

<u>Natural Isotope</u>	<u>Relative Natural Abundances</u>
Sm-144	3.09 %
Sm-147	14.97 %
Sm-148	11.24 %
Sm-149	13.83 %
Sm-150	7.44 %
Sm-152	26.72 %
Sm-154	22.71 %

I. Artificially Produced Radioisotopes of Samarium

A number of samarium isotopes can be produced artificially. Their half-life, major radiations and the principal means of production are listed in Table 1. It is generally agreed that the thermal neutron cross-section for the natural mixture of samarium is 5800 barns (76). This explains the importance of samarium for such applications as the manufacture of nuclear reactor control rods.

J. Samarium-153

Among the artificially produced samarium radioisotopes, Sm-153 and Sm-156 would seem to be the choices for gamma

Table 1

Artificially Produced Radioisotopes of Samarium*

<u>Isotope</u>	<u>Half-Life</u>	<u>Major Radiations (MeV)</u>	<u>Production Means</u>
Sm-143m	64 s.	γ 0.748	Sm-144(n, 2n) Sm-144(γ , n) Sm-144(p, pn)
Sm-145	340 d.	γ 0.061 (13%) e^- 0.016, 0.054	Sm-144(n, γ)
Sm-146	7×10^7 y.	α 2.46	Sm-147(n, 2n)
Sm-151	87 y.	β^- 0.076 max. e^- 0.014, 0.020 γ Eu L X-rays 0.022	Sm-150(n, γ)
Sm-153	46.8 hr.	β^- 0.80 max. e^- 0.022 - 0.101 γ Eu X-rays 0.070 (5.4%) 0.103 (28%) 0.41 to 0.64 (0.6%)	Sm-152(n, γ) Nd-150(α , n)
Sm-155	23.5 m.	β^- 1.53 max. e^- 0.056, 0.097, 0.103 γ Eu X-rays 0.104 (73%) 0.246 (4%)	Sm-154(n, γ)
Sm-156	9.4 hr.	β^- 0.72 max. e^- 0.014 - 0.039 γ Eu X-rays 0.088 (30%) 0.166 (10%) 0.204 (20%)	Fission
Sm-157	0.5 m.	γ 0.57	Gd-160(n, α)

* References (7c, 77)

imaging with our present instrumentation. When consideration is given to the physical half-life, ease of production, storage and transportation, radiation energy, gamma abundances, radionuclidic purity and other radiopharmaceutical considerations, Sm-153 would appear to be the best.

Samarium-153 can be produced in a nuclear reactor using the $\text{Sm-152}(n,\gamma)\text{Sm-153}$ reaction. Since Sm-152 is of 27% abundance and has a high thermal neutron capture cross-section (approximately 208 barns), the production of Sm-153 presents no great difficulty when enriched Sm-152 is bombarded with slow neutrons.

Samarium-153 has a 46.8 hour half-life and decays to Eu-153. Its decay scheme has been reported in Figure 1 (76).

The principal emissions are as follows (76):

β^- 0.80 MeV (max)

e^- 0.022, 0.055, 0.062, 0.095, 0.101 MeV

γ Eu X-rays 0.070 MeV (5.4%)

0.103 MeV (28%)

0.41 to 0.64 MeV (0.6%, 16 γ rays)

The fact that samarium-153 exhibits such an unusually high neutron cross section (208 barns), a reasonably short half-life (46.8 hours) and moderately energetic gamma rays (103 KeV - 28%), makes this isotope a potential addition to the armamentarium of radionuclides used for nuclear medicine

imaging.

K. Physiological Distribution of Samarium and its Derivatives

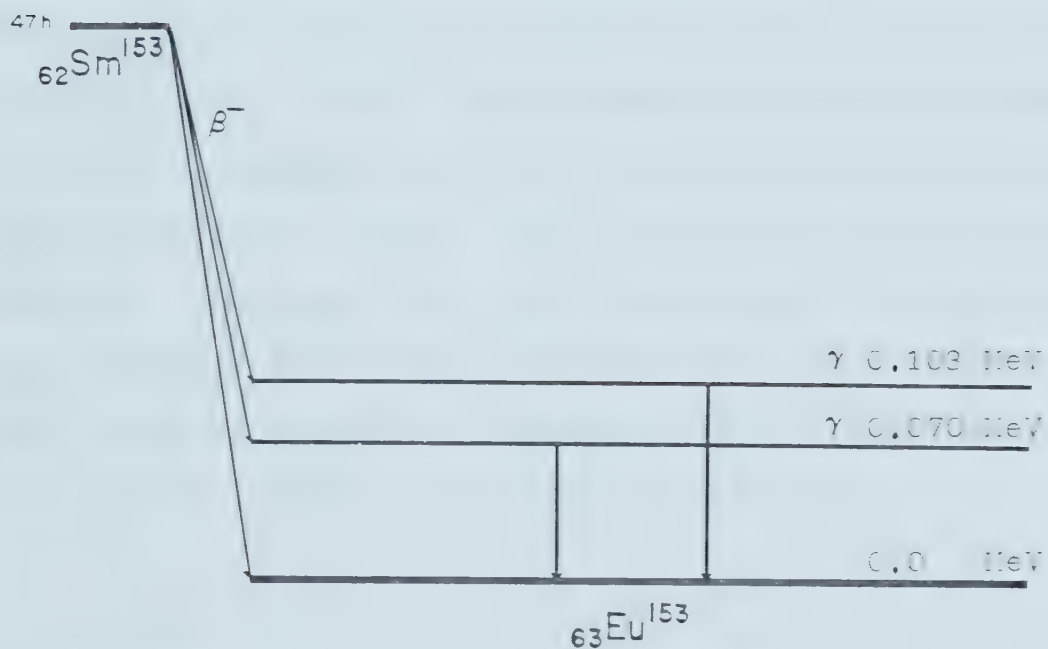
Analysis of the accumulation of natural lanthanides in human organs such as spleen, kidney, liver, pancreas, hypothalamus, thyroid gland, and heart, by spark source mass spectrometry, revealed that the liver did not seem to accumulate samarium and europium to any extent greater than the other organs (26). The presence of samarium and other lanthanides in a given organ was not correlated with age or sex. The contents of Sm and Eu in spleen ash were high in the case of alcoholics as compared to nonalcoholics (26).

When rat strains, differing genetically in their tendency for alcohol consumption, were given 2 combinations of rare earths mixed with their food, there was no difference in the accumulation of lanthanides which could be associated with differences in drinking habits (26).

A different distribution study was conducted by Erametsa et al. Upon autopsy, specimens from 22 human individuals revealed that there was great individual variation in the amount of lanthanides present in the spleen. Samarium was found to be the main lanthanide and the highest content in spleen ash was found to be 194.0 ppm. No

Figure 1 Decay Scheme of Sm-153

(Simplified)



marked differences were noted between males and females (27).

Trace amounts of samarium have also been found in RNA from beef heart tissue using a neutron activation technique (28). However, the report did not give further information on the form of incorporation of Sm in RNA (28).

Matsusaka et al reported that only small amounts of the stable samarium chloride can be absorbed through the gastrointestinal tract. The percentage of oral absorption and retention of samarium might be greater in neonates than in older mice (29). Subcutaneous injection of samarium chloride revealed a slow excretion, mostly by the gastrointestinal route (29). Intravenous injection of samarium chloride into rats showed an accumulation of approximately 50% of the injected dose in the liver and a 25% skeletal deposition. Excretion was via the bile, with a 15-day half-life in the liver (11, 29).

L. Current Use of Samarium in Medicine

Samarium has been employed as part of the therapeutic agent in Phlogosol® solutions for the treatment or inflammations of the oral mucosa (30, 31) and radiation induced skin lesions (32). It has also been used as a tool in studies on the responsiveness of the isolated guinea pig

ventral taenia coli (33 - 36) as samarium and other similar rare earths have often been referred to as specific antagonists to the fraction of calcium which is bound to cell membrane. This property accounts for tension development in the isolated muscle preparation used to study Ca^{+2} mobilization (33 - 36). Maximal tension was strongly reduced by the Sm^{+3} concentration of 8×10^{-5} M in a polarized preparation whereas a potentiation of the maximum response was observed on the depolarized tissue (33, 35).

Samarium and other lanthanide ions have been reported to exhibit an inhibitory effect on the twitching response of skeletal muscle sarcolemma. The exceptions were Tm^{+3} , Er^{+3} and Ho^{+3} which were required in significantly higher concentrations to effect a 50% reduction in the contractile response. This indicates that the sarcolemma has an acute ability to detect the ionic radii of multivalent cations, but samarium somehow interferes with the muscle response mediated by the Ca^{+2} ion (37).

Similar experiments using membrane vesicles of skeletal muscle sarcoplasmic reticulum showed that samarium is responsible for the inhibition of sarcoplasmic reticulum Mg-ATPase activity (37).

Samarium and other trivalent lanthanide ions, and some divalent ions (Mn^{+2} and Cd^{+2}), have been found to bind to the porcine trypsin molecule where the single binding site is usually for Ca^{+2} . The affinity of the ions to trypsin depends strongly on their ionic radius. The smaller the ion,

the higher the binding constant. The affinity of metal ions to trypsin, however, does not depend on their chemical similarity to Ca^{+2} (38).

Samarium and other rare earths have also been known to have anticoagulant property by suppressing thromboplastin formation and interfering with prothrombin (96, 97). However, they are not in wide application because of a possible hemoglobinuria and the availability of highly purified heparin (98).

M. Radioactive Samarium as an X-ray Source

Kastuer et al has reported that Sm-145 might be used as an x-ray source for scanning small bones using its γ rays of 0.061 MeV (13%). Sm-145 has a half-life of 340 days (39).

N. Samarium-153 as a Skeletal Imaging Agent

O'Mara et al reported four different lanthanides as chelates of hydroxyethylenediaminetetraacetic acid (HEDTA) for potential skeletal imaging using the rectilinear scanning technique. He proposed that Sm-153 had the greatest advantage because of its 47-hour half-life and its high

detection efficiency by the gamma camera (40).

Gilyazutdinov et al followed up with another study in which these authors reported that Sm-153 HEDTA was also suitable for radioisotope diagnosis of bone tumors. However, they also added that liver accumulation made Sm-153 HEDTA undesirable for tumor diagnosis in the organs adjacent to the spine (41).

O. Samarium-153 as a Tumor Imaging Agent

In a study of the affinity of lanthanide elements towards malignant tumor tissues, samarium was observed to be significantly accumulated in Yoshida sarcoma-bearing rats after the chloride salt was injected intravenously (42, 43).

Higasi et al also reported that Sm-153 accumulated at remarkably higher concentration than gallium-67 citrate at 48 hours post administration in mice bearing Ehrlich tumors. The samarium used was in the chloride form in dilute hydrochloric acid (44). The accumulation of this rare earth element in liver, kidney and bone was lower than that of gallium-67 which is currently used as a tumor imaging agent.

Higasi postulated that samarium and other rare earth elements whose ionic radius is similar to that of Ca (0.99) or Mg (0.62) which are abundant in the tumor cell membrane, might pass through the tumor cell membrane much more easily

than would the other elements (44).

In a comparative brain scintigraphic examination with indium-113-EDTA and samarium-153-DTPA (diethylenetriamine-pentaacetic acid), Tarjan et al reported that superficial small tumors were more accurately detected with a Sm-153-DTPA complex than with In-113-EDTA. Sm-153 was found to be more suitable for gamma camera imaging due to its soft gamma radiation. Physical and biological properties of the Sm-153 DTPA complex were reported to be good for brain scanning. However, Sm-153 might increase the radiation burden of the patients (45).

Sullivan and Friedman, in their tumor localization studies with radioactive lanthanide and actinide complexes, stated that when samarium(III) was compared to gallium, it exhibited enhanced localization in tumors with a concomitant lower body background (46). The studies involved the intravenous administration of the chemicals to white mice bearing sarcoma-180 tumors. They also suggested that Sm(III) might be a better imaging agent for tumor diagnosis than gallium-67 (46). Samarium-153 was used with citrate and bleomycin as carriers.

During their tumor metabolism studies, Friedman et al (47) found that samarium-153 was in trivalent states and probably bonded to serum proteins in tumor tissue. Autoradiography also showed that the samarium-153 was concentrated in the viable outer layers of the tumor. The animal tumor model used was an ICR strain female mouse

bearing sarcoma-180 tumors. The authors postulated that the first step of samarium-153 (III) citrate metabolism in the animal model is the formation of a complex of $\text{Sm}(\text{H}_2\text{O})_6^{+3}$ ionically bonded to serum proteins. This entity is then transferred into the outer layer of tumor tissue. The higher concentration of the samarium-153 in the tumor could result from a more rapid metabolism of the protein complex by the tumor. In addition, the samarium-153 species may not be excreted from the tumor tissue as rapidly as from other tissues (47).

Additional support to Friedman's interpretation was provided by the work of Thakur et al (48), which demonstrated that the In-111 (III) bleomycin complex in the blood stream was rapidly converted into a complex between In-111 and a serum protein, transferrin. Sullivan et al (46), showed that in the case of samarium-153 citrate, the tumor/tissue ratios were greater at 48 hours than at 24 hours, thus indicating preferential excretion of samarium-153 from the non-tumor tissue.

In a recent study with samarium-153 citrate, Woolfenden et al (10), found that samarium-153 has a higher tumor-to-blood and tumor-to-muscle ratio (13±2 and 72±21 respectively) than gallium-67 citrate (2±0.3 and 36±12 respectively) at 24 hours in the V² carcinoma in the New Zealand White (NZW) rabbit tumor model. They also found that samarium-153 had a higher accumulation in experimental abscesses. Abscess to blood ratio was 8±5 for Sm-153 citrate

and 3±1 for Ga-67 citrate at 24 hours. Abscesses were produced in tumor-free NZW rabbits using intramuscularly implanted fecal pellets.

Considerable uptake also occurred in liver and bone. The plasma clearance half time was approximately 3 hours. This preliminary study indicated that samarium-153 citrate might be a better tumor and abscess imaging agent than gallium-67 citrate (10).

All these reports indicated that samarium-153 has a great potential for use as a radiopharmaceutical for tumor imaging.

P. Toxicity

In general, rare earth elements are considered to be less hazardous than other heavy metals from a toxicologic point of view (49). External exposure to these elements in the industrial, medical or environmental sphere is usually small. In the lanthanide group, only samarium has been reported to be a constituent of urban air in the United States. The level detected was 0.07 ug/m³ (50).

1. Oral

The oral toxicity is low due to poor gastrointestinal absorption. The LD₅₀ of samarium administered orally is greater than 2000 mg/kg in mice with samarium chloride and about 2900 mg/Kg in rats with samarium nitrate (11).

2. Parenteral

Based on scattered acute parenteral toxicity studies, rare earth elements can be considered only slightly toxic (11, 49). The signs of acute toxicity determined in rodents consisted of writhing, ataxia, labored respiration, and sedation. The maximum incidence of death occurred at 48 to 96 hours. There was a tendency for the females to be more sensitive than the males. LD₅₀ for samarium nitrate i.v. in female rats is 8.9 mg/Kg compared to 59.1 mg/Kg for male rats (11). Intravenous injection of various salts of the rare earths (lanthanum through samarium) caused splenic and hepatic degeneration in various rodents (49). Examination in mice and rabbits revealed that those rare earths accumulated mainly in the hepatic Kupffer's cells and spleen pulp cells (51). LD₅₀ in mice i.p. is 585 mg/Kg for samarium chloride and 315 mg/Kg for samarium nitrate (11).

3. Inhalation

Inhalation exposures in man, while infrequent, have caused sensitivity to heat, itching, and an increased awareness of odor and taste (11). Intratracheal administration or inhalation exposure of experimental animals to fluorides or oxides, or a combination thereof, resulted in progressive lung retention, transient pneumonitis, subacute bronchiolitis, and regional bronchiolar stricturing. The formation of granulomas, while rare, has been reported (49). Samarium oxide fumes and dust inhaled might cause headache and nausea (52).

In an observation of samarium deposition in human lungs, Sticher et al., found that samarium ore existed in a hexagonal rod-like crystal in lung tissue. These findings were based on electron diffraction techniques. The same authors postulated that a conversion of the oxides into the phosphate form in the lung had taken place (53).

Gensicke et al. examined the metabolism of $^{153}\text{SmCl}_3$ after inhalation in mice. They reported that reabsorption of samarium from the lung was slow and incorporation of the tracer in the skeleton was observed. They summarized that the retention of radio-samarium from inhalation resembled the same retention pattern after subcutaneous application (54).

4. Skin

Skin damage by the samarium is apparently not an important factor unless the skin is abraded. Applications to abraded skin caused epilation and scar formation. Intradermal injections produced granulomas in guinea pig and man (11). Samarium can irritate the conjunctiva, but not the cornea. However, in rabbits, when the cornea is denuded, samarium caused permanent corneal opacity (49).

III. Experimental Methods

A. Tissue Culture Methods

Melanoma 2 AB and EMT-6 Culture Cells

The human Melanoma 2 AB and the Murine EMT-6 culture cell lines were supplied by W. W. Cross Cancer Institute. All nutritions used were obtained from Gibco, Grand Island, New York.

A human malignant tissue culture cell line (Melanoma 2 AB) was started in 1974 from a primary melanoma at the W. W. Cross Cancer Institute and had been found to be gallium-avid(55, 56). The melanoma cells were maintained as a monolayer in RPMI-1640 growth medium which also contained 15% heat inactivated fetal calf serum (FCS), and 0.29 mg/ml glutamine.

The EMT-6 tumor cells (57, 58) were maintained in a similar manner to the Melanoma 2 AB culture cells with the exception that Waymouth growth medium was used. The EMT-6 cell line was originated from a mouse mammary sarcoma and was maintained in vitro as a monolayer in Waymouth's medium supplemented with 10% FCS and 0.29 mg/ml glutamine.

B. Animal Tumor Models

All animals under investigation were allowed food (Wayne Laboratory Animal Diets, Lab-Brox) and water ad libitum. Ethics of animal experimentation as outlined by the Medical Research Council Guidelines were followed.

1. Lewis Lung Tumor Model in BDF, Mice

The Lewis Lung Tumor Mouse Model for cancer research has been well documented (59 - 63). Mice bearing Lewis Lung Tumors were supplied through the courtesy of the McEachern Cancer Research Laboratory, University of Alberta. A tumor fragment was implanted subcutaneously at the left side of the body close to the thigh of each BDF, mouse (male, 20g). Tumor growth was observed to attain a size of approximately 0.5 cm in diameter within a period of 10 days. All experiments were conducted immediately thereafter.

2. Dunning 3327 Prostatic Tumor Model in Copenhagen/Fisher Rats

Tumor-bearing Copenhagen/Fisher rats were obtained through the courtesy of Dr. J.D. Chapman of the W. W. Cross

Cancer Institute. This transplantable prostatic adenocarcinoma was first reported by Dunning (64) and later recognized as a useful model for immunological host-tumor interaction studies (65, 66). The tumor was transplanted to either right or both sides of the body with cryopreserved cell suspensions.

C. Preparation of Radiochemicals

All chemicals were of ACS standard. Double distilled water was used throughout this investigation. Isotonic sodium chloride injection, U.S.P. (Cutter Laboratory) was used for dilution when required.

1. Production of Samarium-153

Samarium-153 was produced in the University of Alberta SLOWPOKE reactor, using the $\text{Sm-152}(n,\gamma)\text{Sm-153}$ reaction.

Samarium-152 oxide (Sm_2O_3), 98.2% enriched, was purchased from the Oak Ridge National Laboratory, U.S.A.

Activity produced per target at a defined thermal neutron flux was estimated by the following equation:

$$\text{Activity} = N$$

where

N = number of target atoms

σ = reaction cross-section (208 barns)

Φ = neutron flux ($n \cdot cm^{-2} \cdot sec^{-1}$)

λ = decay constant of samarium-153 = $0.693/T_{1/2}$

t_{irr} = irradiation time

With the enriched samarium-152 (98.2%) oxide target (Sm_2O_3), about 2.18 mCi/2mg of the Sm-153 was produced in the SLOWPOKE reactor (SLOWPOKE Reactor Facilities, University of Alberta) with a thermal neutron flux of $10^{12} n/cm^2/sec$, after 4 hours of irradiation at the inner target site. No significant heat was produced ($4.6 \times 10^{-4} cal/mg$) over the entire irradiation period.

For a typical production, two milligrams of enriched samarium-152 oxide were carefully weighed and sealed inside a small plastic capsule enclosed in another sealed outside capsule. The target sample was transported to the irradiation site through the pneumatic transfer system.

Up to 4.8 mCi/2mg samarium-153 had also been produced at the SLOWPOKE Facility using a thermal neutron flux of $2.5 \times 10^{11} n/cm^2/sec$ and a 48 hours irradiation period.

High specific activity samarium-153 was produced by the nuclear reactor at Chalk River (Atomic Energy of Canada Ltd.). Samarium-153 with an activity of 6.8 Ci/2 mg was produced using a thermal neutron flux of $2 \times 10^{14} n/cm^2/sec$ for 168 hours of irradiation. Two milligrams of enriched

samarium-152 oxide were sealed inside a quartz capillary tube which in turn was sealed inside a small aluminium capsule as the final irradiation target.

2. Screening of Potential Samarium Compounds

A large number of potentially useful samarium salts or complexes were screened in order to find a suitable samarium salt or complex for tumor localization. The minimum criterion was that the radiochemical should be stable and would not form a significant amount of colloid at room temperature during one hour incubation in the presence of RPMI growth medium which contained phosphate buffer. Ultracentrifugation at 144,000G for one hour was employed to determine the formation of colloid.

Such a criterion was important as Sm-153 colloid formation had been shown to indicate erroneous high uptake in culture cell experiments. Furthermore, the colloids localize in the reticuloendothelial system in vivo. This colloidal effect significantly decreases the availability of Sm-153 for tumor localization. Therefore, potential agents so gathered were also injected into normal rats for final in vivo visualization. A good potential agent should have very little uptake by the liver even at 48 hours.

3. Preparation of Samarium-153 Citrate

The irradiated samarium oxide target containing samarium-153 was dissolved in 1.0 N HCl to yield a final concentration of 1 mg/ml solution. The samarium chloride solution was then millipore filtered, and mixed with a sterilized solution of sodium citrate (25 mg/ml) to give a final Sm-153 citrate solution of 1:17 (Sm : citrate) molar ratio. The final pH of the citrate solution was adjusted to 6.5 with 1.0 N NaOH, and millipore filtered again. The vial was labelled, and the samarium citrate was ready for investigation.

4. Preparation of Samarium-153 Transferrin

A samarium-153 chloride solution was mixed with a three-fold molar excess of nitrilotriacetate (NTA) in 0.1 N HCl, and incubated for 30 minutes at room temperature. The pH was then adjusted slowly with sodium hydroxide to pH 2.5. A 0.1 M solution of sodium bicarbonate was then added to raise the pH to 5.0. The reaction mixture was diluted with an equal molar of apotransferrin (Sigma, greater than 90% iron free) dissolved in aqueous 0.1 M KCl and 0.05 M HEPES buffer (N-2-hydroxyethylpiperazine-N-2-ethanesulfonic acid), pH 7.4. The pH of the incubate was then adjusted to 7.4 with

0.1 M sodium bicarbonate and allowed to stand at 2°C for 12 hours. Free and non-specifically bound samarium was removed from the solution by passing the mixture through a 1.5 cm diameter Sephadex G-50 column equilibrated with 0.1 M KCl and 0.05 M HEPES. The transferrin fraction eluted first and was confirmed by UV absorption at 280 nm. The percentage of Sm-153 associated with the transferrin fraction was determined. The final samarium-153 transferrin solution was millipore filtered.

5. Preparation of Samarium-153 EDTA

Samarium-153 chloride solution of 1 mg/ml was added slowly to disodium EDTA solution to form a final 1:10 molar ratio solution. The solution was allowed to incubate at room temperature for 30 minutes and the pH was adjusted slowly to 6.5 with sodium hydroxide (1.0 N NaOH). The final solution was sterilized by passage through a 0.22 micron millipore filter.

6. Preparation of Samarium-153(C-14) EDTA

Samarium-153 chloride solution of 1.0 mCi activity was mixed with 10 uCi of C-14 labelled EDTA (108 mCi/mMole, The Radiochemical Centre, Amersham, England). This solution was

allowed to incubate at room temperature for 30 minutes and then added to a disodium EDTA solution such that the final solution achieved a 1:10 molar ratio of samarium ions to total EDTA. The final solution was allowed to incubate for another 30 minutes, pH adjusted to 6.5 and then millipore filtered as described previously.

7. Preparation of Gallium-67 Citrate

Gallium-67 citrate was supplied by Merck Frosst Radiopharmaceuticals, Montreal, Canada, as a sterile, no-carrier-added and non-pyrogenic solution for intravenous use. It was supplied at a specific activity of 2 mCi/ml on the calibration date, as a complex formed from 9 ng of gallium chloride. Due to the need for equal molar dose comparison with the samarium-153 citrate, non-radioactive sterile gallium citrate solution was added to form a final carrier containing gallium-67 citrate solution (1:17 molar ratio of Ga to citrate) of pH 6.5. Non-radioactive sterile gallium citrate solution was prepared by mixing gallium chloride solution (1 mg/ml) with a sodium citrate solution (25 mg/ml) to give a final gallium citrate solution of 1:17 (Ga : citrate) molar ratio. The pH was slowly and carefully adjusted to 6.5 with sodium hydroxide and then millipore filtered.

8. Preparation of Gallium-67 Transferrin

Gallium-67 chloride was supplied by Frosst Radiopharmaceuticals as a sterile and non-pyrogenic solution. It was complexed with transferrin using a modified procedure as described by Terner (55, 56) and Harris (68, 69). Due to the need for equal molar dose comparison with samarium-153 transferrin, non-radioactive sterile gallium chloride solution was added as a carrier to form the desired molar solution. This carrier gallium-67 chloride solution was then mixed with a three-fold molar excess of nitrilotriacetate (NTA). After a 30 minute incubation at room temperature, the pH was raised to approximately 4.5 with sodium hydroxide. The pH was then further raised to 6.5 with a 0.1 M sodium bicarbonate. An additional equal molar apotransferrin in 0.1 M KCl and 0.05 M HEPES (pH 7.4) was then added and mixed. After adjustment of the pH to 7.4, the mixture was incubated at 2°C for 12 hours. The non-protein bound activity was removed by passage through a 1.5 cm diameter Sephadex G-50 column equilibrated with 0.1 M KCl and 0.05 M HEPES (pH 7.4) buffer. The transferrin fraction was eluted first and was confirmed by UV absorption at 280nm. The percentage of Ga-67 associated with the transferrin fraction was determined. This final gallium-67 transferrin solution was sterilized with millipore filtration.

D. Quality Control of Radiochemicals

1. Radionuclidic Purity Control

The radionuclidic purity of Sm-153 was determined by counting an aliquot of the final product using a Ge(Li) detector (Nuclear Diodes, Prairie View, U.S.A.) interfaced to a multichannel analyzer and a minicomputer (Nuclear Data 600, Nuclear Data Inc.). The resulting spectra were plotted using an X-Y plotter. Major samarium-153 photopeaks (Eu X-rays) were expected to be seen at 70 and 103 KeV. Peak searches and identification of the photo peaks as well as the areas under the peaks were determined. A spectrum due to background radiation was also compared. The percentage of radionuclidic impurities and the total radioactivity of Sm-153 were calculated.

2. Radiochemical Purity Control

a. Ascending Paper Chromatography

Ascending paper chromatography using a pyridine: ethanol: water solvent system (1:2:4) and Whatman No. 1 chromatographic paper (5.5 x 1 inches strips) has been

documented for gallium (70). It was shown to be useful for samarium as well. Samarium-153 citrate was found to have an Rf value of 0.75 at the pH of 6.5. Other samarium complexes tended to stay at the origin. The development time was approximately two hours. The chromatographic paper was then hung to dry, cut into 1.0 cm segments and the radioactivity of each determined by Beckman Gamma 8000 NaI(Tl) Well Counter.

b. Ascending Thin Layer Chromatography

Cellulose gel thin layer chromatography (Eastman Kodak 6064) together with a solvent system consisting of pyridine, ethanol, water (1:2:4) was also used, especially for Sm-153(C-14)EDTA, Ca-45 EDTA and Sm-153 EDTA purity determination. The chromatogram was cut into 1.0 cm sections and samarium-153 radioactivity determined by a Beckman Gamma 8000 Well Counter. After most of the samarium-153 activity had decayed (21 days), the 1.0 cm sections were wetted with 1.5 ml double distilled water overnight, then mixed with 15 ml of liquid scintillation fluor (Aquasol II, New England Nuclear Inc.). The C-14 or Ca-45 radioactivity was then determined separately using the liquid scintillation counting technique in a Beckman 9000 Scintillation Spectrometer.

3. Colloid Formation Determination

High speed ultracentrifugation at 144,000 G of 150 ul radiochemical solutions for one hour was used to separate colloids from the solution using an ultracentrifuge (Airfuge, Beckman). The supernatent was removed carefully into separate tubes and radioactivity from both the residual activity in the tube and the supernatent were determined. The amount of colloid formed was expressed as a percentage. The procedure was performed in duplicate for each compound tested.

4. Determination of Calcium-45 and Samarium-153 Competition for binding with EDTA

The stability of samarium-153 EDTA in a calcium-45 environment was determined by adding an equal molar solution of calcium-45 chloride to a samarium-153 EDTA solution. The mixture was incubated for 30 minutes at room temperature. Duplicate samples were spotted at the origin of a thin layer chromatogram (Kodak) and an ascending chromatographic analysis was performed as described previously. Calcium-45 and samarium-153 radioactivity were determined separately as discussed. Calcium-45 was supplied from Amersham as calcium chloride in aqueous solution (2.19 mCi/49.7 ug/ml).

5. Determination of Samarium-153 EDTA in Urine

Urine samples were collected from rats injected intravenously with samarium-153 EDTA. A small sample of the urine was then spotted on a Whatman No. 1 chromatographic paper strip. The presence of samarium-153 EDTA was then determined by the ascending chromatography method described.

E. Studies of Uptake by Culture Cells

Human Melanoma 2AB or EMT-6 cell suspensions were obtained by washing the monolayer cells in the incubation flasks with Versene buffer (Gibco, Grand Island, N.Y.), followed by a brief incubation of about one minute with 0.1 % trypsin (Gibco, Grand Island, N.Y.). Prolonged exposure to trypsin solution was found to alter cell membrane permeability, which might lead to inaccurate results (56, 71). The cells were then washed twice with 10 ml volumes of growth medium; the final cell suspension contained 10^6 cells/ml of growth medium. The number of cells were determined using a haemocytometer.

Viability of the cells was determined by their ability to exclude 0.1% trypan blue. Viability normally exceeded 98%. The cell suspension (10^6 cells) was then incubated in a

gently shaking water bath at 37°C under normal atmosphere with gallium-67 citrate, gallium-67 transferrin, samarium-153 citrate, samarium-153 transferrin or samarium-153 EDTA. At the end of each incubation period, the cells were washed twice with normal saline and the radioactivity of both cell pellets and combined supernatents determined separately. Cell viability was also determined for the control. A minimum of three replicates were conducted in each experiment. Corrections for dead cell uptake were always made for each tube. The correction for uptake of radiochemicals in the presence of dead cells was made using the following equation (Appendix 1):

$$Uv = U_0/V - (Ud \times (100 - v)/V)$$

where Uv = net uptake by 10^6 viable cells

U_0 = percentage uptake by 10^6 viable and dead cells

Ud = percent uptake by 10^6 dead cells

v = viability in percentage

The dead cell uptake was determined by incubating prepared dead cells with various radiochemicals and the uptake was then determined. Dead cells were prepared by incubating cells at 56° for one hour and subsequently tested for viability using trypan blue.

F. Tissue Distribution Studies

The tissue distribution of gallium-67 citrate, gallium-67 transferrin, samarium-153 citrate, samarium-153 transferrin and samarium-153 EDTA were studied mainly in Lewis Lung Tumor-bearing mice (tumor fragment implanted) when the tumor reached the size of about 0.5 to 0.75 cm in diameter. The radioactive solutions being investigated (0.1 to 0.2 ml) were injected via the tail vein at the rate of about 0.02 ml per second and at a somewhat slower rate for samarium-153 EDTA. At specific time intervals after injection the animals were sacrificed by decapitation. A sample of blood was immediately collected and measured using a 1 ml non-heparinized syringe. The sample was then transferred directly into a counting vial. The entire lungs, liver, spleen, kidneys, tumor and right femur bone were excised and a sample of muscle was taken from the right thigh. The tissues and organs were transferred to counting vials and weighed. A minimum of three animal replicates were employed per time interval post-injection.

At the time of injection, duplicate samples of the radioactive solutions, equivalent to the dose administered to the animals, were put into different counting vials. These were counted at the same time as the tissue samples and were used as a standard for the dose administered. Thus, the need for corrections for radioactivity decay of the

isotopes was eliminated.

The organs and tissue samples were counted twice for one minute each in a Beckman Gamma 8000 counter. The tissues were counted without wet ashing as this was found, from past experience in our laboratory (51), to produce count rates not statistically different than those observed using the present technique. The standard doses were counted without dilution as they were found, from past observation, to show less than 1% loss in count rate when 0.05ml of radioactive solution was diluted to a three milliliter volume (51). In all cases, the tail of the animal was counted to ascertain whether any appreciable amounts of radioactivity remained at the site of injection. Radioactivity in the remaining carcass was determined by counting the upper and lower portions separately in a Picker Autowell II Gamma NaI[Tl] Spectrometer.

G. Whole Body Imaging Studies

Pictures of body distribution and tumor uptake of various radiochemicals at various time intervals post-injection in rats bearing Dunning Prostatic Tumor were recorded. Various radiochemical solutions were injected intravenously via the femoral vein, and gamma scintillation pictures were obtained using a Nuclear-Chicago PHO Gamma IV

gamma camera and a collimator designed for Tc-99m. A minimum of a hundred thousand counts were accumulated per picture, using the posterior view.

H. Whole Body Radiochemical Elimination Studies

1. Whole Body Counting

During the gamma scintillation imaging of various radiochemical solutions in rats bearing the Dunning Prostatic Tumor, the number of counts per minute were recorded immediately following the injection of the radiochemical. Background and decay corrections were subsequently made so that information on the radiochemical elimination from the whole body could be obtained at each time interval post-injection.

2. Urinary Excretion of Samarium-153 EDTA

Following the intravenous injection of samarium-153 EDTA, the rats with the Dunning Prostatic Tumor were housed separately in metabolic study cages. Food and water were allowed ad libitum. Urine was collected at different time

intervals post-injection. Radioactivity of samarium-153 EDTA in 100 ul urine samples was determined using a Beckman Gamma 8000 Counter. Correction for background and physical decay were made. Data were expressed as percentage of injected dose when compared to reference dose standards.

I. Dual-labelled Samarium-153(C-14)EDTA Tissue Distribution Studies

1. Tissue Sample Preparation

Samarium-153 (C-14) EDTA was administered intravenously to groups of Lewis Lung Tumor bearing mice. Organs and tissues of interest were excised at different time intervals and weighed. Aliquots (about 60 mg each) of such tissues were blotted to remove any adhering blood, weighed, and transferred to 20 ml liquid scintillation vials for later processing.

2. Determination of Samarium-153 Radioactivity

The radioactivity of samarium-153 in organs and tissue samples was measured using the Beckman Gamma 8000 Well

Counter. Counting windows were adjusted to encompass the 103 KeV energy peak of the radioisotope.

3. Determination of Carbon-14 Radioactivity

Radioactivity from carbon-14 in the above tissues was determined 40 days later by the liquid scintillation method. The delayed period allowed an almost complete decay of Sm-153. Tissue samples for liquid scintillation were prepared using a tissue solubilization technique as follows:

The small aliquot organ or tissue sample was placed in a glass type scintillation vial. 100 ul of double distilled water was added to the sample vial for initial wetting. Then 2.0 ml of Protosol® (New England Nuclear) was added and the vial agitated from time to time until the sample was completely dissolved to form a homogeneous solution. A few drops of 30% hydrogen peroxide were added to bleach any color formed. The sample solution was then neutralized with the addition of 0.1 ml glacial acetic acid. Then 15 ml of scintillation fluor (Aquasol II, New England Nuclear) was added. About 3 drops of stannous chloride (4% in 0.1 N HCl) solution were added to each vial to reduce chemiluminescence. The samples were left to dark adapt for 30 minutes before counting in a Beckman model 9000 Liquid Scintillation Spectrometer. A series of quenched standards were prepared using various amounts of blood and a known

activity of carbon-14 hexadecane standard. The carbon-14 radioactivity was then calculated from the generated quench correction curve using channel ratio method.

J. Toxicity Studies

1. Effect on Weight Gain

Three separate groups of male adult ALAS strain mice (20 - 23g) were intravenously dosed with samarium EDTA solutions at 0.1 umole Sm/Kg, 1.09 umole Sm/Kg and 10.9 umole Sm/Kg respectively. The animals were allowed food and water ad libitum and were also weighed at various time intervals up to 64 days post-administration. The observed weights were compared to those of controls (dosed with normal saline) at each time period.

2. Histopathological Studies

Histopathological studies were done by Dr. Shnika (Department of Pathology, Faculty of Medicine, University of Alberta) on the lungs, liver, kidneys and femur bone of ALAS strain mice that were sacrificed 1, 20, 48 and 64 days after

intravenous injection of samarium EDTA solution at doses of 0.1 umole Sm/Kg, 1.09 umole Sm/Kg or 10.9 umole Sm/Kg. Female pregnant ALAS mice were injected intravenously with a dose of 1.09 umole Sm/Kg and male offspring were sacrificed 48 and 64 days after birth. Histopathological studies were done on lungs, liver, kidneys, and femur bone as before. Samples from normal ALAS mice were used as reference controls.

K. Statistical Methods

Simple statistical techniques were used in the analysis of results. Observations or measurements in the same group are expressed as arithmetic average or mean. The measure of dispersion of results from the mean was expressed as standard deviation which is equal to the square root of the variance (75). The Unpaired t test was used to determine whether the difference between two means was significant. Confidence limits at 95% probability levels were used, which would give a reasonable degree of confidence on whether the difference was considered to be significant (75).

IV. Results and Discussion

A. Quality Control of Radiochemicals

1. Radionuclidic Purity

Samarium-153 with radionuclidic purity of greater than 98.0% was obtained after the bombardment of enriched Sm-152 oxide target in a nuclear reactor. Gamma ray photo peak spectra obtained after irradiation in the SLOWPOKE reactor (Flux 1×10^{12} n/cm²/sec) and the NRX reactor (Flux 2×10^{14} n/cm²/sec) are shown in figures 2, and 3. The characteristic Sm-153 photo peaks of 70 and 103 KeV were identified with no other radionuclidic impurities observed up to 7 days after the end of bombardment (Figure 2, 3). Figure 4 shows the theoretically calculated yield of samarium-153 after the irradiation of a 2.0 mg sample of enriched samarium oxide for 168 hours at a neutron flux of 2×10^{14} .

Figure 2

Low Specific Activity Sm-153 Gamma Ray Photopeak Spectrum

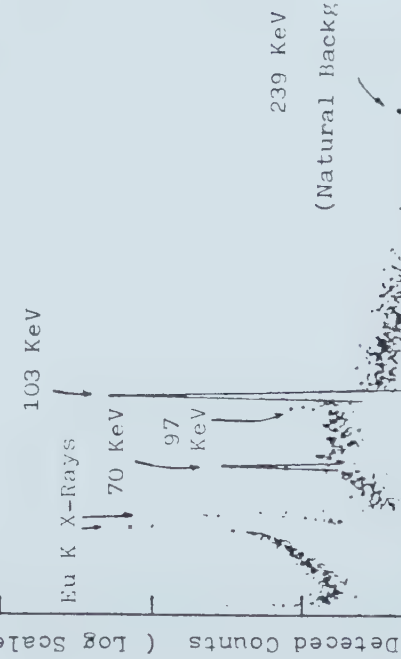
Sm-153 Gamma Ray Photopeak Spectrum

(Low Specific Activity Production)

Detection Geometry : 10 cm distance
with no B shield

Detector Gain: 50

Calibration : 0.159 KeV / Channel
0.295 KeV off set



O

Channe15

4096

Figure 3

High Specific Activity Sm-153 Gamma Ray Photopeak Spectrum

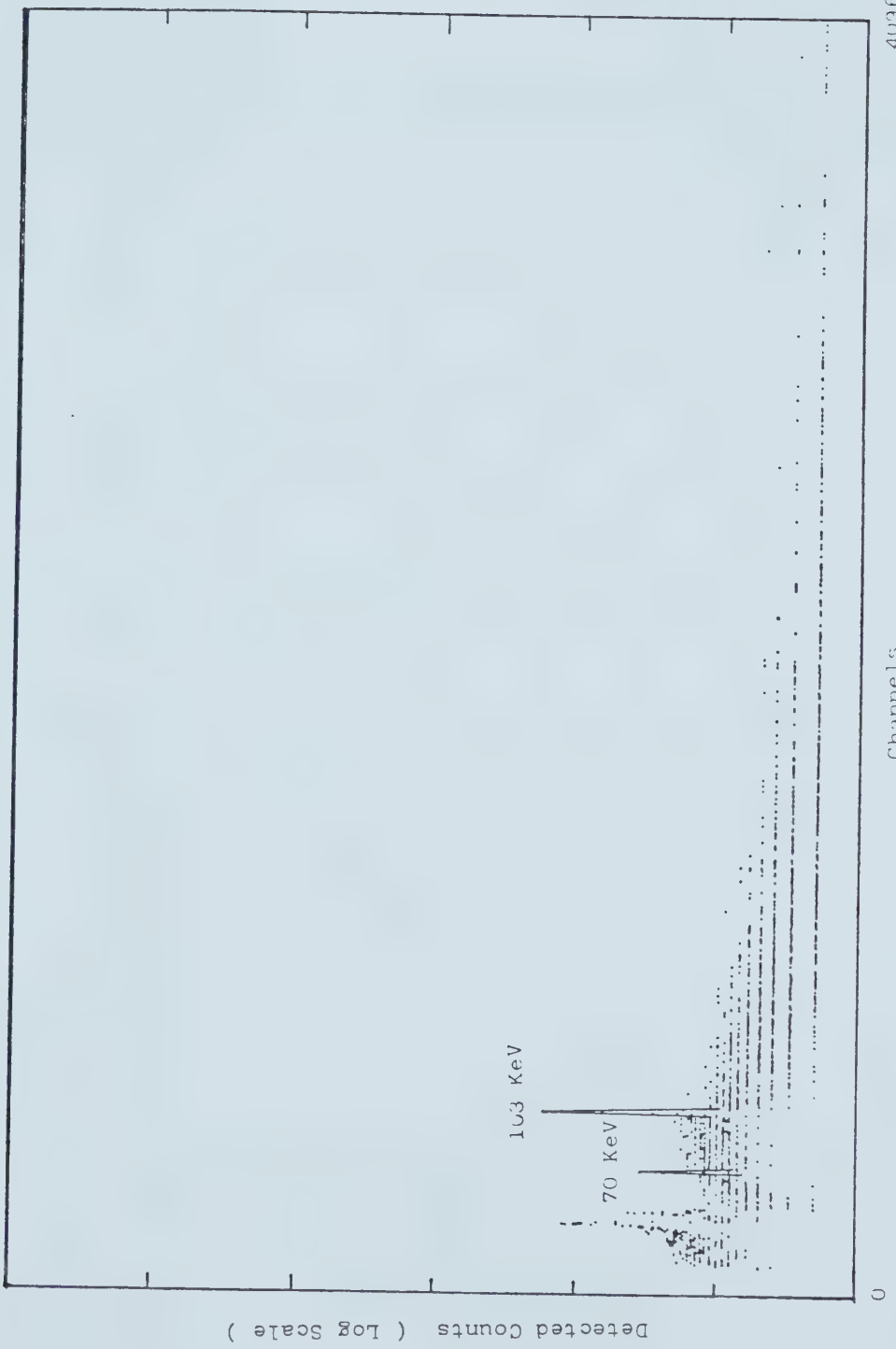
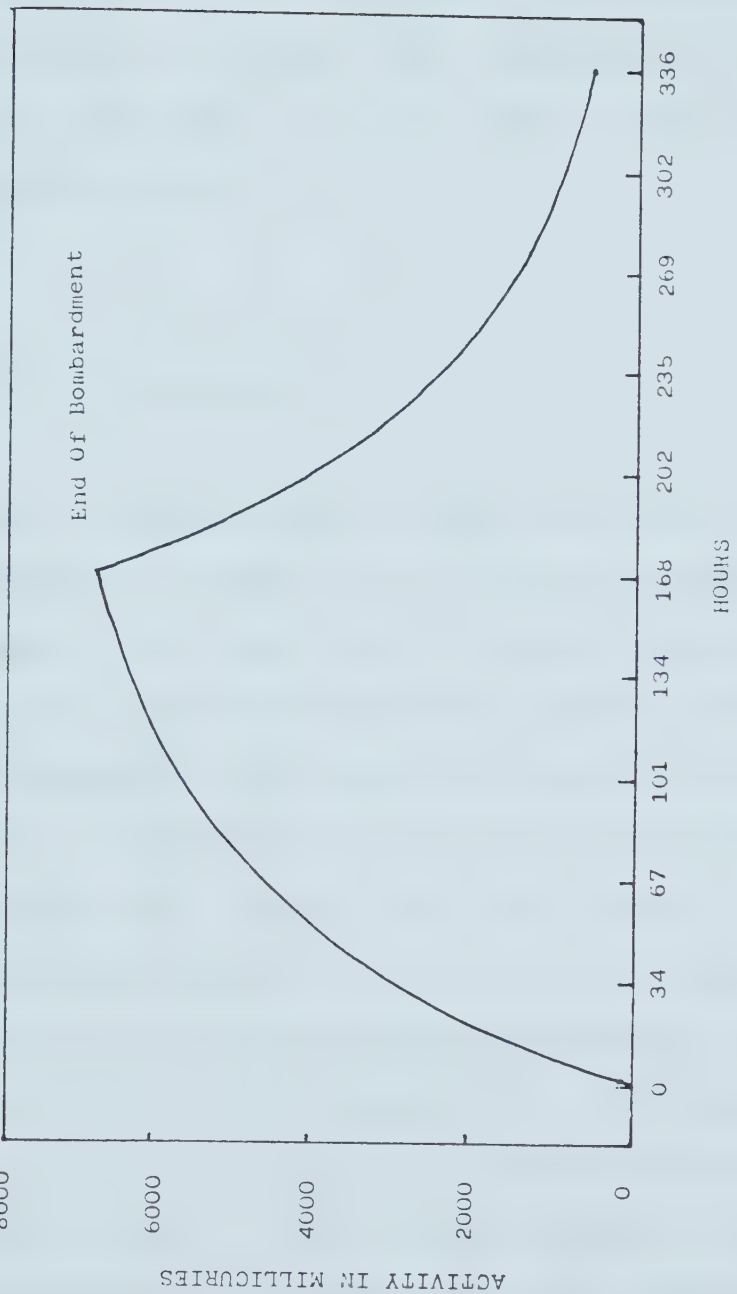


FIGURE 4

Theoretical Calculation of Sm-153 Production in a Nuclear Reactor +



+ based on a flux of $2 \times 10^{14} \text{ n.cm}^{-2} \cdot \text{sec}^{-1}$ bombarding 2.0 mg of $153\text{Sm}_{2}\text{O}_3$

2. Radiochemical Purity

Because of the nature of this project it was imperative to develop radioanalytical methods for ascertaining the purity of the compounds tested. Two types of radiochromatography were used.

a. Ascending Paper Chromatography

Ascending paper chromatography using the pyridine: ethanol:water developing system (1:2:4) and Whatman No. 1 chromatographic paper was found to be very useful in differentiating Sm-153 chloride from Sm-153 citrate. Sm-153 chloride had an Rf value of 0.75 at pH 1.0 and an Rf of 0.1 at pH 6.5. Sm-153 citrate had a constant Rf value of 0.75 at both acidic and alkaline pH (Table 2). This result was similar to that of Kulprathipanja (70) in his observation of the behaviour of gallium chloride and gallium citrate in the same solvent system. After the separation of free and non-specifically bound samarium by the gel filtration method using Sephadex G-50 column, samarium-153 transferrin was found to have an Rf value of 0.1 at the pH of 7.4 (Table 2). Sm-153 chloride, citrate and transferrin had been prepared with greater than 97% radiochemical purity when assayed using these systems. Ga-67 citrate (Merck Frosst) and Ga-67

transferrin had an Rf value of 0.82 and 0.1 respectively (Table 2). Final radiochemical purities of the gallium preparation were about 98%. These results were in agreement with the observation made by Kulprathipanja (70) with the same solvent system.

b. Ascending Thin Layer Chromatography

At a pH of 6.5, Sm-153 chloride, Sm-153 citrate and Ga-67 citrate had an Rf value of 0.1, 0.77 and 0.82 respectively (Table 2). Sm-153 EDTA had an Rf value of 0.9. With varying molar ratio combination of Sm-153 to EDTA, it was observed that a minimum molar ratio of 1:2 was needed to obtain a stable Sm-153 EDTA complex with a purity of about 98%. Close to 100% purity was observed when Sm-153 EDTA was prepared at 1:10 molar ratio. At a molar ratio of 1:1, only 50% of chelation was observed as the activity was equally distributed between two spots having Rf values of 0.1 and 0.9 respectively (Table 2).

3. Colloid Formation Determination

The study of colloid formation under different test conditions is extremely important for the interpretation of in vitro and in vivo observations. We have selected the ultracentrifugation method as it lends itself to quick and

Table 2

Separation of Sm-153 Complexes by Ascending Liquid Chromatography *

<u>Compound</u>	<u>pH</u>	<u>Support⁺</u>	<u>Rf Values</u>
Sm-153 Chloride	1.0	Whatman No.1 Paper	0.75
	6.5	" "	0.1
Sm-153 Citrate	1 to 8	" "	0.75
Sm-153 Transferrin	7.4	" "	0.1
Ga-67 Citrate	6.5	" "	0.9
Ga-67 Transferrin	7.4	" "	0.1
Sm-153 Chloride	6.5	ITLC (Kodak)	0.1
Sm-153 Citrate	6.5	" "	0.77
Ga-67 Citrate	6.5	" "	0.82
Ga-67 Transferrin	7.4	" "	0.1
Sm-153 EDTA(1:1)	6.5	" "	0.1 and 0.9
Sm-153 EDTA(1:2)	6.5	" "	0.9
Sm-153 EDTA(1:10)	6.5	" "	0.9

* Solvent = Pyridine:Ethanol:Water (1:2:4)

accurate results. This technique revealed that both Sm-153 chloride and Sm-153 citrate formed colloid (greater than 98%) with either RPMI growth medium (which contains phosphate buffer), or phosphate buffer alone, after a one hour incubation at room temperature (Table 3). However, no significant amount of colloid formation was observed when Sm-153 citrate was incubated with distilled water, rat serum or Minimal Essential Medium Amino Acid Solution (which does not contain any phosphate buffer). Similarly, Sm-153 chloride and apotransferrin together were found to be stable at room temperature and did not form any substantial amounts of colloid in the Minimal Essential Medium (Table 3).

However, when Sm-153 citrate solution was allowed to stand in an enclosed test tube or was mixed with rat serum at room temperature for 24 hours, a 17.8% and 80.2% colloid formation was observed respectively (Table 3).

Different ratios of citrate to Sm-153 ions also changed the stability of Sm-153 complex when incubated with RPMI growth medium (Table 3). Only 7.6% of colloid formation was observed in the case of Sm-153 citrate (1:80) in the presence of RPMI growth medium. A higher concentration of citrate to samarium seemed to stabilize the tendency of such colloid formation (Table 3). Gallium, which was also found to be stable as the 3⁺ oxidation state in aqueous solution, reacted with citrate in similar manner. Gallium citrate was observed to be stable in the pH range from about 3.0 to 7.5 only at comparable citrate concentrations (70, 82). This

might also explain why a Sm-153 citrate (1: 17) solution alone slowly forms a colloid at room temperature.

In these tests, phosphate buffer was observed to be an immediate cause of colloid formation with Sm-153. Lanthanum had been reported to be able to react with phosphates to form lanthanum phosphate ($\text{LaPO}_4 \cdot 3\text{H}_2\text{O}$) which has a low solubility in water and precipitates out from the solution. The solubility product of LaPO_4 was calculated to be approximately 3.75×10^{-23} (77, 78). Similar reaction had also been reported for gallium with various salts of phosphoric acid (79). Precipitation was observed when the first portions of phosphate were added to a gallium chloride solution. With NaH_2PO_4 , precipitation was reported to be slow and required approximately 48 hours for completion. The resulting solid phases were reported as white gelatinous precipitates which were readily converted into colloidal suspensions (79 - 81).

B. Screening of Potentially Useful Samarium Compounds

1. Ultracentrifugation Method

Various possible salts and complexes of samarium were screened. These include the phosphate, thiosulfate,

Table 3

Colloid Formation of Samarium Complexes

<u>Samarium Salt or Complex *</u>	<u>Reaction Medium or Conditions +</u>	<u>% Colloid ++ Formation</u>
$^{153}\text{Sm Cl}_3$	(alone in 1.0 ml RPMI)	99.8 (a)
+ Sodium Citrate(1:17)	1.0 ml RPMI	98.89 \pm 0.4
+ Sodium Acetate(1:53)	"	99.8 (a)
+ Apotransferrin(1:0.5)	"	87.6 (a)
+ Tartaric Acid (1:29)	"	88.1 \pm 0.6
+ Bis(2-ethylhexyl hydrogen phosphate)(1:10)	"	59.6 \pm 0.2
+ " " (1:5)	"	98.7 \pm 0.3
+ 8 hydroxy-quinoline(1:17)	"	94.7 \pm 6.4
+ Diethyl HIDA (1:10)	"	33.8 \pm 1.9
+ NTA (1:23)	"	3.9 \pm 0.1
+ Disodium EDTA Dihydrate (1:10)	"	3.5 \pm 0.6
+ Sodium Citrate(1:17)	"	98.9 \pm 0.4
+ " (1:20)	"	81.9 \pm 0.1
+ " (1:40)	"	53.9 \pm 0.4
+ " (1:80)	"	7.6 \pm 0.4
+ " (1:160)	"	7.7 \pm 0.1
+ " (1:240)	"	8.6 \pm 0.1
+ " (1:400)	"	9.3 \pm 0.4
+ " (1:800)	"	2.2 \pm 0.6

.... continued

Table 3 (continued)

<u>Samarium Salt or Complex *</u>	<u>Reaction Medium or Conditions +</u>	<u>% Colloid Formation ++</u>
$^{153}\text{Sm Cl}_3$	Phosphate Buffer (0.5M, 1.0ml, pH7.0)	99.3 \pm 0.3
"	Apotransferrin (1:1.0, in 1.0ml HEPES)	6.5 \pm 0.1
"	Apotransferrin (1:1.0) and 1.0 ml Minimal Essential Medium	0.7 \pm 0.2
$^{153}\text{Sm Citrate}$ (1:17)	Distilled Water (1.0ml)	3.3 \pm 2.3
"	Alone, 24hours at room temperature	17.8 \pm 1.9
"	Phosphate Buffer (0.5 M, 1.0ml)	98.8 \pm 0.4
"	Apotransferrin (1:1.0, in 1.0 ml HEPES)	3.7 \pm 1.6
"	Rat Serum (1.0 ml)	2.5 \pm 0.4
"	Rat Serum (1.0 ml and 24 hours incubation at room temperature)	80.2 \pm 0.2
"	Minimal Essential Medium (1.0 ml)	0.9 \pm 0.2

* with $^{153}\text{Sm Cl}_3$ (0.0057ml) and volume of 1.0 ml

+ mean \pm 1 S.D. of 3 determination except (a) which means single determination.

++ all incubations are for 1 hour except where indicated.

carbonate, acetate, succinate, salicylate, dichromate, bicarbonate, citrate, oxalate, tartarate, malonate, glycinate, EDTA, NTA, bis (2-ethylhexyl hydrogenphosphate), 8-hydroxy-quinoline (8 HQ) and diethyl IDA derivatives of samarium. Some of the results were shown in Table 3.

Among the salts and complexes screened, only Sm-153 citrate (1:80), Sm-153 EDTA, and Sm-153 NTA met the criteria and did not form significant amount of colloid in vitro after a one hour incubation with RPMI growth medium (Table 3).

2. Imaging of Potentially Useful Samarium Complexes

A preliminary scan was conducted by imaging the distribution of a number of samarium complexes in rats.

Sm-153 citrate (1:80) and Sm-153 NTA had been shown to be relatively stable in vitro with no significant amount of colloid formation. However, when a 1.09 uMole Sm/Kg dose of either compound was injected intravenously in normal male Wistar rats, a significant uptake by the liver was observed. Gamma scans at 48 hours revealed that a major portion of the radioactivity was concentrated in the liver and spleen for both agents (Figure 5). A similar observation was also noted for both Sm-153 HIDA and Sm-153 complexed with 8 hydroxy-quinoline (Figure 5). Only Sm-153 EDTA (1:10) in rat showed little hepatic concentration and considerable

skeletal localization. Within the skeletal system, uptake by the skull and joints was observed to be predominant for their Sm-153 concentration (Figure 5).

A significant hepatic concentration was also observed by O'Mara (40) after the administration of Sm-153 citrate and Sm-153 NTA in rabbits. However, when Sm-153 HEDTA was used, the same authors also noticed little liver uptake at 24 hours while skeletal uptake consisted of about 45% of the injected dose (40).

In summary, from the in vivo gamma scintillation pictures obtained after intravenous injection of the above agents in normal Wistar rats, only Sm-153 EDTA was found to be suitable (Figure 5). Samarium-153 citrate(1:80), Sm-153 NTA, Sm-153 HIDA and Sm-153 hydroxyquinoline all accumulated in the liver to a great extent after 48 hours. This indicated that these complexes were possibly unstable and that they released samarium which then formed colloid in vivo. On the other hand, Sm-153 EDTA (1:10) exhibited little hepatic accumulation at 48 hours in vivo. Localization of Sm-153 activity in bone and joints was however observed (Figure 5).

Although Sm-153 transferrin did not meet the basic criteria of low liver concentration, it was further evaluated along with Sm-153 citrate and Sm-153 EDTA, as Ga-67 transferrin has been reported to be tumor avid and transferrin itself was suggested to be a potential carrier of the gallium ion (55 - 57).

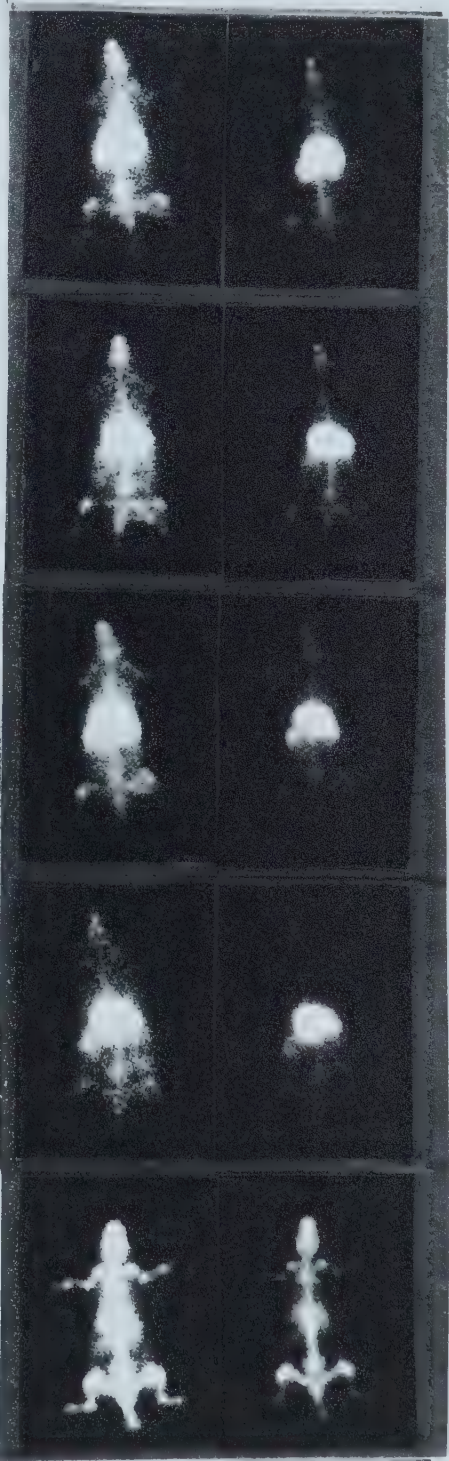
Figure 5

Scintigraphic Distribution of Sm-153 Complexes

in Normal Rats *

Camera exposures #1 & #2

Citrate (1:80)



NTA (1:23)

IDA (1:10)

8-HQ (1:17)

EDTA (1:10)

* Images obtained after collection of 100,000 counts
on a PHO Gamma IV Gamma Camera

C. Calcium-45 and Samarium-153 Competition

Because EDTA complexes of samarium were considered for our study, it was important to determine the extent of calcium competition with the lanthanide. For this, chromatographic procedures were developed to separate the various samarium and calcium complexes.

EDTA labelled with C-14 had an Rf of 0.9 with ascending liquid chromatography using ITLC (Kodak). Ca-45 chloride alone had an Rf of 0.05, which changed to 0.9 when mixed with EDTA, indicating almost 100% complexation (Table 4).

When equimolar amounts of Sm-153 chloride and Ca-EDTA were mixed together, the formation of Sm-153 EDTA was greater than 90% ($Rf=0.9$). On the other hand when equimolar amounts of Ca-45 chloride were mixed with Sm-153 EDTA(1:1), no Ca-45 activity was observed at Rf of 0.9 indicating that Ca-45 could not displace Sm-153 from the Sm-153 EDTA complexes. It was therefore, concluded that Sm-153 had a stronger complexing affinity for EDTA than Ca-45 (Table 4). Calcium disodium EDTA has been known to be able to remove heavy metal ions in clinical application (83 - 85). Samarium was also known to be a competitor for and inhibitor of calcium binding sites (33 - 36, 38, 86, 87). Our results seem to agree with these findings.

Table 4

Chromatographic Separation of Samarium and Calcium Complexes

Sample	Rf Values *
C-14 EDTA (Amersham)	0.9
Ca-45 Chloride (Amersham)	0.05
Ca-45 EDTA (1:1)	0.9
Sm-153 Chloride + Disodium EDTA (1:10)	0.9
Sm-153 Chloride + Disodium EDTA (1:1)	0.1 and 0.9
Sm-153 Chloride + Calcium EDTA (1:10)	0.9
Sm-153 Chloride + Calcium EDTA (1:1)	0.1 and 0.9
Ca-45 Chloride + Sm-153 EDTA (Ca:Sm:EDTA = 1:1:1)	0.05 (Ca-45), 0.1 and 0.9 (Sm-153)

* ITLC (Kodak) used together with a solvent consisting of Pyridine:Ethanol:Water (1:2:4)

D. Determination of Samarium-153 EDTA in Urine

The nature of the samarium derivative in the urine of animals which were administered samarium-153 EDTA was determined by means of chromatography.

Ascending liquid chromatography using Whatman No. 1 paper revealed that Sm-153 EDTA had an Rf of 0.7. However, Sm-153 activity in the urine of rats injected with Sm-153 EDTA had an Rf of 0.1 (Table 5) These results suggested that Sm-153 in urine was not in the form of Sm-153 EDTA. While such changes most likely have happened as a result of in vivo metabolism, the possibility still exists that the change occurred during the chromatographic process in vitro. The pH or other ions in the excreted urine might also be an important factor contributing to such changes.

Table 5

Chromatographic Separation of Samarium from Urine

<u>Sample</u>	<u>Rf Values *</u>
Sm-153 EDTA (1:10)	0.7
Sm-153 radioactivity in urine	0.1

* Whatman No.1 chromatography paper used together
with a solvent consisting Pyridine:Ethanol:Water
(1:2:4)

E. Radiochemical Uptake by Cells in Tissue Culture

1. Comparison of Sm-153 Citrate, Sm-153 Transferrin and Ga-67 Citrate Uptake in Melanoma 2AB Cells

The tumor cell uptake of Sm-153 citrate and Sm-153 transferrin was undertaken in a Melanoma 2AB cell culture. As a comparison, Ga-67 citrate uptake was also tested in the same system. Uptake studies were performed at 1.9 nMole cations per million culture cells. Uptake comparisons were made at various time intervals of incubation.

There were significant differences between the uptake of Sm-153 citrate and Ga-67 citrate by 10^6 Melanoma 2AB cells in RPMI growth medium. The percentage uptake was 93.02 ± 3.75 for Sm-153 citrate and 0.99 ± 0.42 for Ga-67 citrate at 2 hours (Table 6, Figure 6). Since Sm-153 citrate had been shown to form a colloid (over 95%) when mixed with RPMI growth medium, such drastic uptake by 2AB cells might be caused by the surface charge effect between Sm-153 colloid and 2AB culture cells.

The 0.99% uptake of Ga-67 citrate at 2 hours by 2AB cells was consistant with the observations of Terner (55).

Uptake of Sm-153 transferrin by 2AB cells was similar to Sm-153 citrate uptake (Table 6, Figure 6). Since Sm-153 citrate and Sm-153 transferrin had been shown to form

colloid in the presence of RPMI growth medium, such a result was expected. The percentage uptake of Sm-153 citrate and Sm-153 transferrin by 2AB cells at 2 hours were 93.02 ± 3.75 and 91.90 ± 2.00 respectively (Table 6, Figure 6).

When Sm-153 citrate was incubated with RPMI growth medium without 2AB cells, no significant activity was observed on the culture tube wall. This indicated that the Sm-153 colloid so formed was indeed bound, probably due to surface charges, to the culture cell surface instead of the culture tube. Possible formation of samarium phosphates as insoluble colloid had been reported (78, 79) and discussed in previous sections. Sm-153 transferrin offered no observable advantages in preventing colloidal formation in vitro (Table 6, Figure 6). Since the mechanism of culture cell surface adsorption of colloidal particles and the true cell uptake is so different, a comparison between Sm citrate, Sm transferrin and Ga citrate cannot be made. However, this data pointed out that an alternate Sm-153 agent was needed such that availability of Sm-153 ions to the cells is allowed.

2. Uptake of Sm-153 EDTA (1:10) in Melanoma 2 AB Cell Cultures

Since samarium-153 EDTA had been shown, from previous experiments, to be stable both in vivo and in vitro, the

Figure 6

Melanoma 2AB Cell Uptake of Sm-153 Citrate and
Ga-67 Citrate

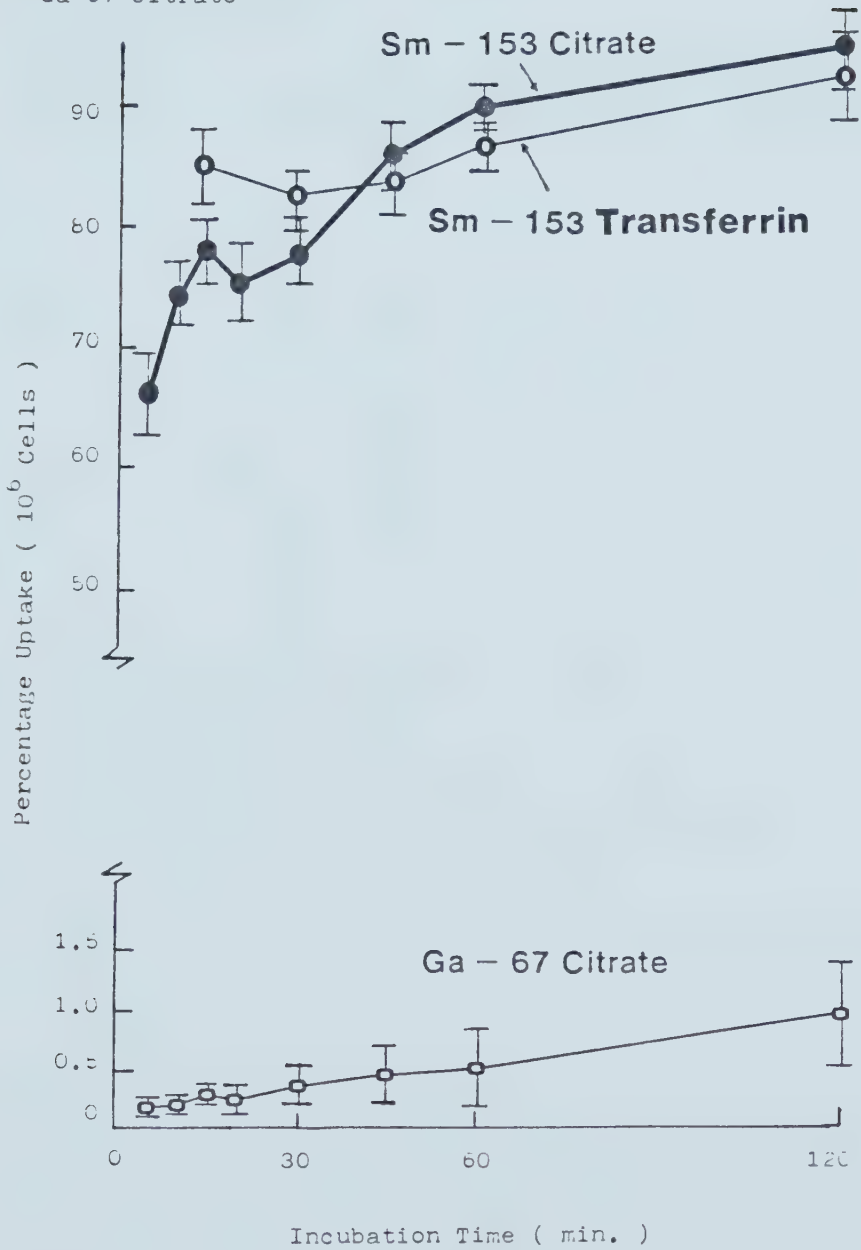


Table 6

Uptake of Sm-153 Citrate, Ga-67 Citrate and Sm-153
Transferrin by Melanoma 2AB Cells *

Incubation Time (min.)	Percent Uptake per incubation tube**		
	Sm-153 Citrate	Ga-67 Citrate	Sm-153 Transferrin
5	66.30 \pm 2.88	0.19 \pm 0.06	--
10	74.20 \pm 1.87	0.22 \pm 0.02	--
15	78.70 \pm 2.80	0.34 \pm 0.02	84.81 \pm 2.90
20	75.30 \pm 2.55	0.29 \pm 0.06	--
30	77.42 \pm 3.38 ⁺	0.42 \pm 0.19 ⁺	81.29 \pm 1.89
45	85.68 \pm 2.63 ⁺	0.47 \pm 0.30 ⁺	82.47 \pm 2.41
60	89.43 \pm 1.53 ⁺	0.55 \pm 0.35 ⁺	87.82 \pm 2.68
120	93.02 \pm 3.75 ⁺	0.99 \pm 0.42 ⁺	91.90 \pm 2.00

* in RPMI medium; 1.9 nmoles of each nuclide added to each tube containing 10^6 cells

** percent uptake per 10^6 cells \pm 1 S.D., each value represents the mean of four determinations except specified with (+) which means seven determinations

uptake of samarium-153 EDTA(1:10) in the Melanoma 2AB cell line was studied at a concentration of 0.6 nMole Sm-153 per million cells. A comparative uptake of Ga-67 citrate (0.6 nMole Ga-67) was also undertaken in the same system.

Sm-153 EDTA was found to have a higher percentage uptake by Melanoma 2AB cells than Ga-67 citrate at a concentration of 0.6 nMole per million cells. Such a difference was observed after 45 minutes of incubation and increased continuously until the end of the experiment (120 minutes). The percentage uptake at 120 minutes was 5.26 ± 0.29 for Sm-153 EDTA and 3.92 ± 0.05 for Ga-67 citrate respectively (Table 7, Figure 7). In this experiment, Sm-153 EDTA was observed to have a 34% higher uptake by the 2AB cells than the same molar concentration of Ga-67 citrate (Table 7), thus indicating that Sm-153 EDTA might be a potentially better tumor localizing agent than Ga-67 citrate.

3. Mechanism of Uptake of Sm-153 EDTA (1:10) in cell culture

In order to reveal whether Sm-153 was taken up by the culture cells as Sm-153 EDTA complex or as individual ions, a cell culture experiment using dual-labelled Sm-153(C-14)EDTA, at 0.6 nMole Sm-153 per million Melanoma 2AB cells and a 1:10 Sm-153 to EDTA molar ratio, was designed. Sm-153 and C-14 activities were determined separately. If the Sm-153(C-14)EDTA complex was incorporated

Figure 7

Uptake of Sm-153 EDTA (1:10) by Melanoma 2AB Cells

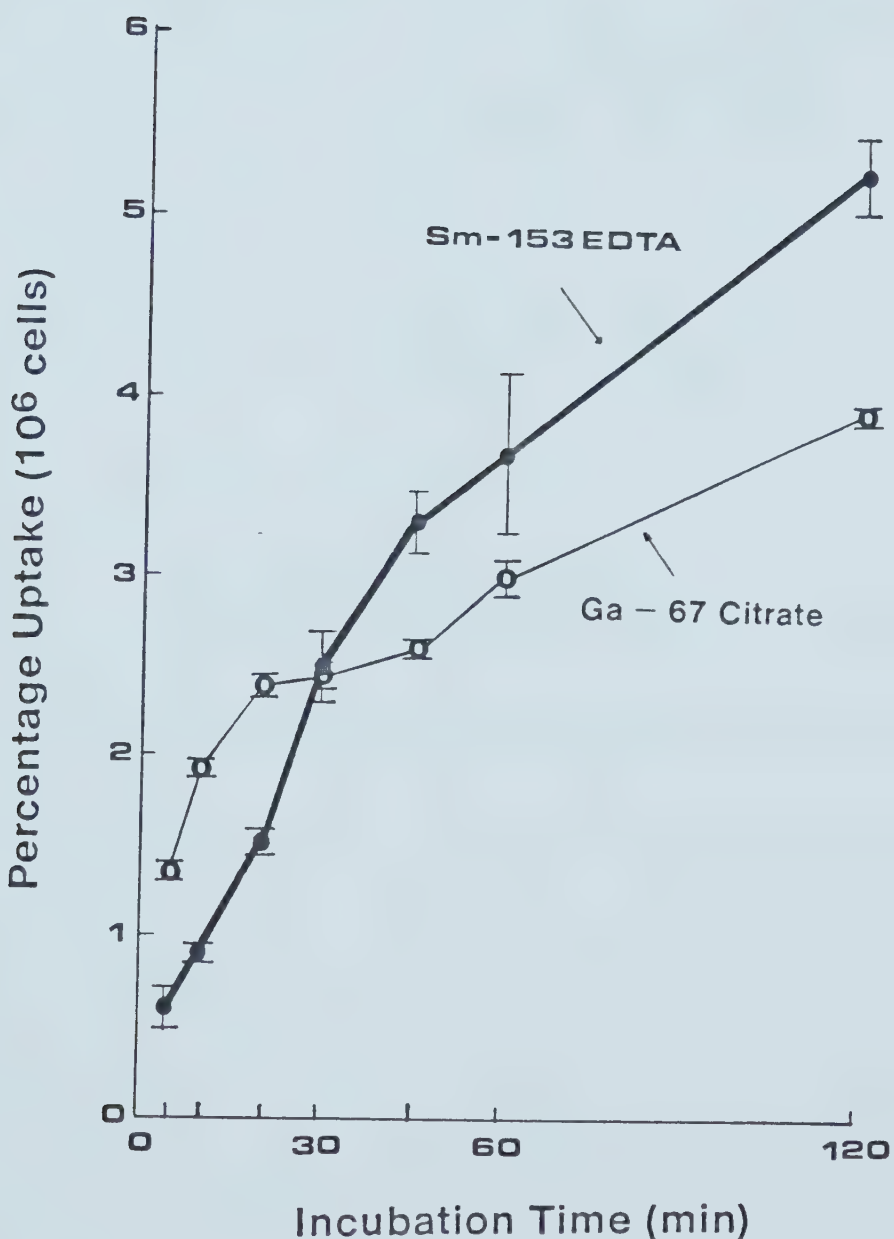


Table 7

Uptake of Sm-153 EDTA (1:10) and Ga-67 Citrate
by Melanoma 2AB Cells*

Time (min.)	Cellular Uptake **	
	Sm-153 EDTA	Ga-67 Citrate ***
5	0.55 ± 0.19	1.45 ± 0.09
10	0.88 ± 0.06	1.93 ± 0.09
20	1.49 ± 0.17	2.43 ± 0.13
30	2.53 ± 0.30	2.46 ± 0.16
45	3.39 ± 0.30	2.69 ± 0.09 ($P < 0.010$)
60	3.64 ± 0.47	3.00 ± 0.24 ($P < 0.100$)
120	5.26 ± 0.29	3.92 ± 0.05 ($P < 0.001$)

* each incubation tube contained 0.6 nmoles of either samarium or gallium

** percent uptake per 10^6 cells, each value represents mean ± 1 S.D. of 3 determinations

*** P values correspond to testing of differences between gallium and samarium values

by cells in an unchanged form, then the cellular ratio of Sm-153 and C-14 radioactivities should be the same as that of the incubation medium.

Sm-153(C-14)EDTA uptake pattern by the Melanoma 2AB Cells varied slightly from the previous experiment in which Sm-153 EDTA was used. This might be the result of differences in the batches of sub-cultured Melanoma 2AB cells or the slight variation in the experimental conditions. Nevertheless, such changes should not affect the purpose of this dual-labelled experiment. The percentage uptake of Sm-153 activity was observed to be 5.49 at 120 minutes. This agreed closely with the previous results. On the other hand, the C-14 activity at 120 minutes was only 2.77 percent of the incubation dose (Table 8, Figure 8). This indicated that the uptake of Sm-153 is somewhat independent of the C-14 labelled EDTA probably through the dissociation of the complex. Since the ratio of the two activities (Sm-153 and C-14) remained fairly constant, it was necessary to investigate the influence of EDTA on the uptake of a different molar concentration of samarium. This was achieved by using a higher specific activity samarium-153 nuclide.

Figure 8

Uptake of Sm-153(C-14)EDTA (1:10) by Melanoma 2AB Cells

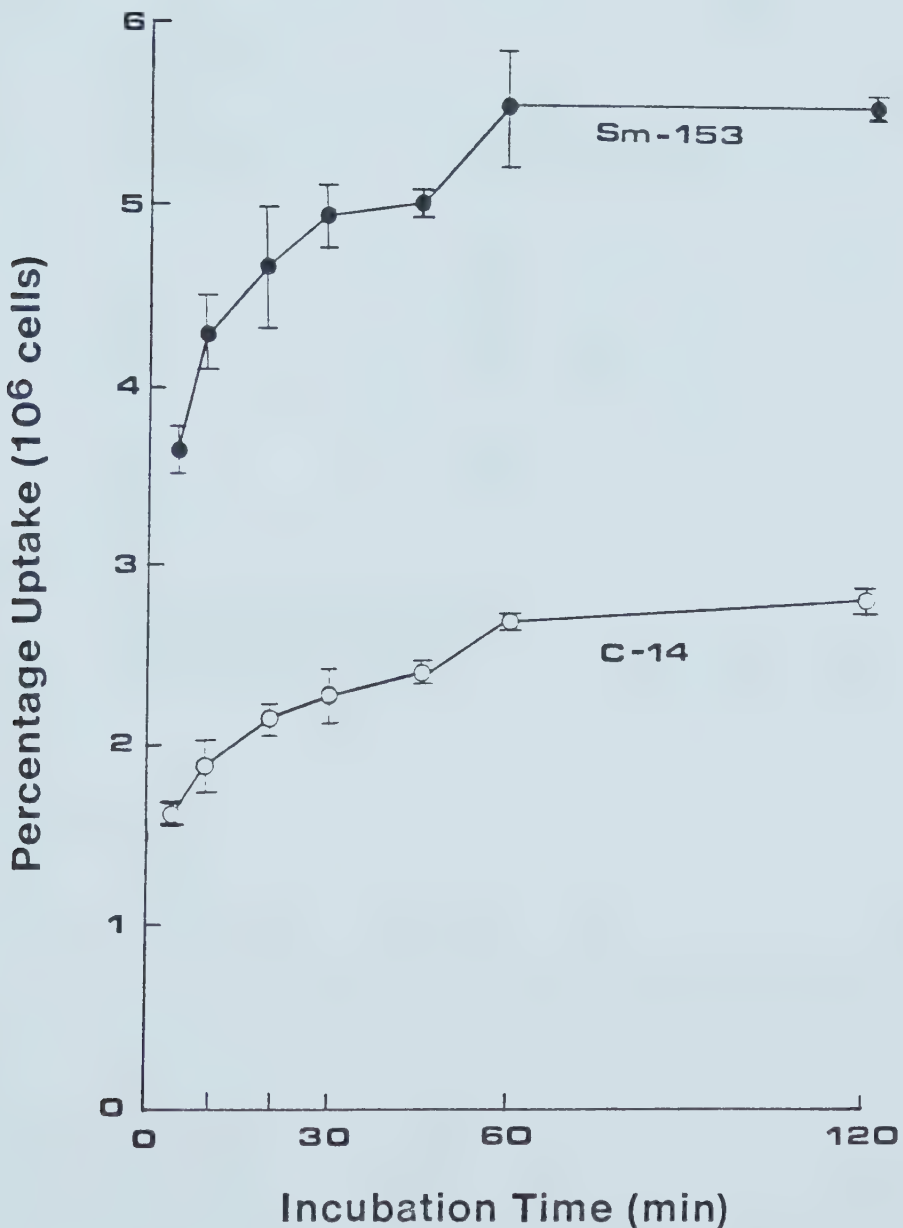


Table 8

Uptake of Sm-153(C-14)EDTA (1:10) by Melanoma
2 AB Cells*

Incubation Time (min.)	Cellular Uptake**		Ratio $^{153}\text{Sm} / ^{14}\text{C}$
	Sm-153	C-14	
5	3.68 \pm 0.18	1.61 \pm 0.10	2.29 \pm 0.21
10	4.30 \pm 0.26	1.88 \pm 0.17	2.29 \pm 0.23
20	4.70 \pm 0.39	2.14 \pm 0.09	2.20 \pm 0.17
30	4.91 \pm 0.14	2.23 \pm 0.12	2.21 \pm 0.14
45	5.02 \pm 0.09	2.30 \pm 0.06	2.18 \pm 0.06
60	5.55 \pm 0.35	2.65 \pm 0.02	2.09 \pm 0.09
120	5.49 \pm 0.06	2.77 \pm 0.08	1.99 \pm 0.05

* each incubation tube contained 0.6 nmoles of samarium

**percentage of uptake per 10^6 cells, each value
represents the mean \pm 1 S.D. of three determinations

4. Uptake of High Specific Activity Sm-153 EDTA(1:10) by EMT-6 Tumor Cells

The uptake of Sm-153(C-14)EDTA at a concentration of 6×10^{-3} nMole was again compared to Ga-67 citrate using 10^6 EMT-6 cell culture and Waymouth growth medium under the same conditions. A significant difference in uptake between Sm-153 EDTA and Ga-67 citrate was again observed. The differences became pronounced at 10 minutes and continued thereafter to 120 minutes. While the percent uptake of Sm-153 at 120 minutes was 20.78, and that of Ga-67 was 4.08. The C-14 EDTA activity, however, was similar to that of previous experiment and the percent uptake by the cells was found to be 3.16 at 120 minutes (Table 9, Figure 9). The reduction in radiochemical concentration of samarium seemed to cause a considerable increase in the percent uptake by culture cells for both Sm-153 EDTA and Ga-67 citrate. At 2 hours, the Sm-153 EDTA was shown to have a five fold uptake increase by the EMT-6 culture cells than the Ga-67 citrate under the same conditions. The uptake of Sm-153 activity by culture cells was also observed to be independent of the C-14 activity. The interesting aspect of this experiment is that the Sm-153/C-14 ratio seemed to increase progressively as a function of incubation time thus lending evidence to the dissociation theory previously proposed. One might also speculate that a saturable transport mechanism exists at the

cellular membrane which explains the noticeable differences in uptake between the low and high specific activity preparations. While it may not be entirely valid to intercompare uptake between different cell lines solely on mechanistic assumptions, experience in our laboratory has demonstrated that radiogallium uptake by the two different cell cultures was essentially identical (99). Of even greater importance is our observation that the samarium uptake was so much higher than radiogallium in the same cell line. This can be explained on the basis of either increased cellular membrane transport or simply a greater tumor metabolic affinity for samarium.

F. Tissue Distribution Studies

1. Sm-153 Citrate Distribution in BDF, Mice Bearing Lewis Lung Tumors

Despite our observation that Sm-153 citrate may form a colloid under certain conditions in vitro, the testing of such a complex in vivo was necessary to ascertain the true biological behaviour of the compound.

When a 3.0 umole Sm/Kg dose of Sm-153 citrate was injected intravenously into BDF, mice bearing Lewis Lung

Figure 9

Uptake of High Specific Activity Sm-153(C-14)EDTA
by EMT-6 Tumor Cells

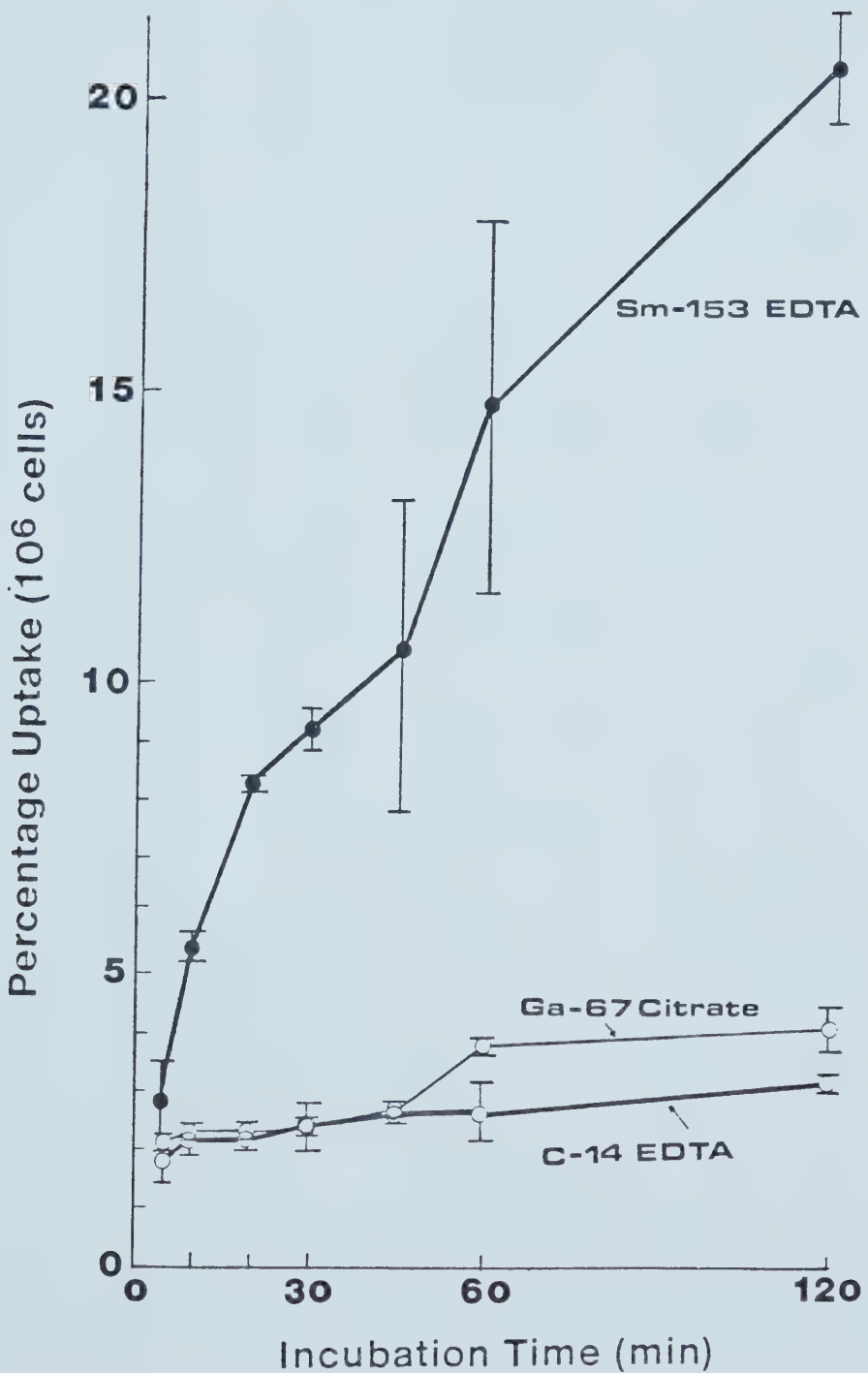


Table 9

Uptake of Sm-153(C-14)EDTA (1:10) and Ga-67 Citrate by EMT-6 Cells*

Incubation Time (min.)	Sm-153	Cellular Uptake**		
		C-14	Ratio 153Sm/14C	Ga-67 ***
5	2.80 ± 0.72	1.80 ± 0.34	1.56 ± 0.25	2.13 ± 0.07 (P < 0.200)
10	5.46 ± 0.23	2.15 ± 0.20	2.54 ± 0.18	2.29 ± 0.07 (P < 0.050)
20	8.21 ± 0.13	2.16 ± 0.12	3.80 ± 0.16	2.27 ± 0.05 (P < 0.005)
30	9.13 ± 0.29	2.35 ± 0.34	3.89 ± 0.56	2.34 ± 0.05 (P < 0.010)
45	10.47 ± 2.90	2.61 ± 0.07	4.01 ± 1.05	2.68 ± 0.12 (P < 0.005)
60	14.88 ± 3.01	2.52 ± 0.55	5.90 ± 1.39	3.84 ± 0.05 (P < 0.001)
120	20.78 ± 0.86	3.16 ± 0.12	6.58 ± 0.70	4.08 ± 0.34 (P < 0.001)

* each incubation tube contained 6×10^{-3} nmoles of either samarium or gallium** percent uptake per 10^6 cells, and each value represents mean ± 1 S.D. of three determinations

*** P values correspond to testing of differences between gallium and samarium values

Tumor, a high percent of the injected dose was found to localize in the liver (52.65% at 6 hours and 75.03% at 48 hours respectively). The percent of injected dose in other organs such as spleen, bone(femur), lungs or kidneys was less than 7% throughout the 48 hour period of observation (Table 10A). Radioactivity measurement per milliter of blood revealed a rapid disappearance of Sm-153 citrate from 9.39% of the dose at 6 hours to 0.11% of the dose at 48 hours (Table 10A). Although tumor-to-blood ratio had reached 52.38 at 48 hours (Figure 10), liver-to-blood ratio was 634.89 and spleen-to-blood ratio was 137.29 at the same period (Table 10B). These distribution results were similar to the observation made by Matsusaka (29), in which approximately 50% of injected samarium chloride localized in the liver. Durbin (88), also observed substantial localization of lanthanide complexed with citrate in the reticuloendothelial system. Considerable hepatic uptake of samarium-153 citrate in rabbit was also reported by Woolfenden (10).

The tissue distribution result suggested that Sm-153 citrate might be a potential tumor imaging agent in view of the high tumor-to-blood ratio at 48 hours (Figure 10). However, the extensive localization of Sm-153 citrate in the liver might limit the usefulness of this tracer in delineating small tumors in the abdominal area. One might also speculate that the possible formation of Sm-153 colloid in vivo might be a factor causing such substantial hepatic uptake.

Figure 10

Tumor to Blood Ratios of Tim-153 Citrate in BDF₁
Mice Bearing Lewis Lung Tumors

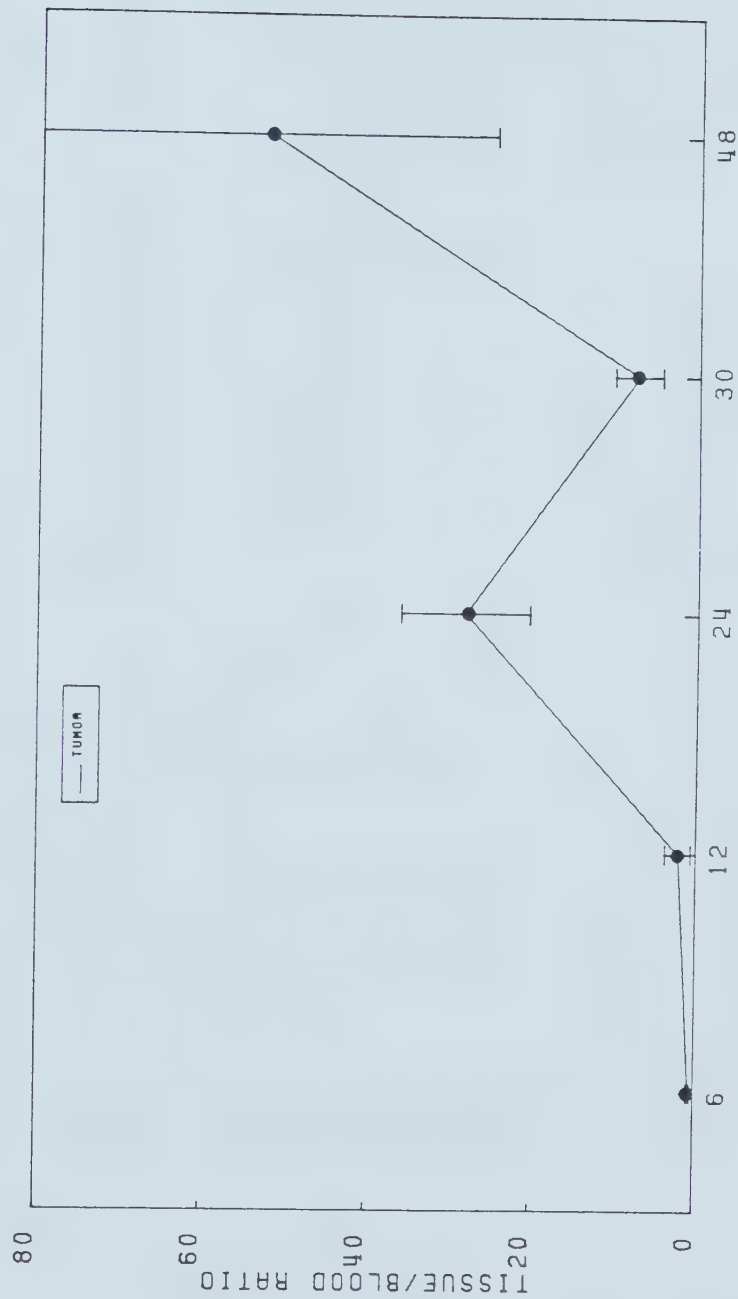


Table 1UA

Tissue Distribution Results of Sm-153 Citrate at 3.0 uMole Sm-153 / Kg
in BALB₁ Mice Bearing Lewis Lung Tumor (a,b)

Tissue	Time after Administration			
	6 Hours	12 Hours	24 Hours	30 Hours
Blood (c)	3.39 ± 2.84	5.44 ± 2.99	0.38 ± 0.09	0.68 ± 0.35
Muscle (d)	0.49 ± 0.21	0.56 ± 0.14	0.74 ± 0.35	0.42 ± 0.09
Tumor	11.16 ± 6.29	18.17 ± 1.99	17.15 ± 4.71	9.73 ± 4.18
Liver	52.65 ± 8.25	56.46 ± 10.43	63.92 ± 7.86	69.58 ± 8.78
Kidneys	2.64 ± 0.57	1.38 ± 0.44	1.31 ± 0.27	1.54 ± 0.26
Lung	1.58 ± 0.58	0.63 ± 0.11	0.58 ± 0.18	1.39 ± 1.27
Spleen	2.15 ± 0.19	2.76 ± 1.27	3.79 ± 0.78	3.05 ± 0.68
Bone (d) (Femur)	1.94 ± 1.19	2.88 ± 1.38	6.16 ± 2.66	3.97 ± 1.74

- (a) Expressed as mean ± 1 S.D. of four animals
- (b) Percentage of injected dose in whole tissue except as indicated
- (c) Percentage of injected dose per milliliter of blood
- (d) Percentage of injected dose per gram of tissue

Table 1Gii

Tissue Distribution Results of Sn-113 Citrate at 3.0 uMole Sn-113 / Kg in
BDF₁ Mice Bearing Lewis Lung^a Tumor (a,e)

Tissue	Time after Administration			
	6 Hours	12 Hours	24 Hours	30 Hours
Muscle	0.05 ± 0.02	0.14 ± 0.11	1.87 ± 0.66	0.88 ± 0.71
Tumor	0.64 ± 0.19	2.18 ± 1.56	28.25 ± 7.80	7.38 ± 2.89
Liver	3.44 ± 1.44	14.15 ± 17.92	140.37 ± 27.92	84.04 ± 56.33
Kidneys	0.74 ± 0.49	0.72 ± 0.74	9.80 ± 1.62	6.75 ± 5.67
Lung	0.92 ± 0.84	0.93 ± 0.85	9.27 ± 1.37	17.21 ± 29.47
Spleen	0.94 ± 0.47	2.85 ± 3.32	31.44 ± 4.56	17.57 ± 10.51
Bone (Femur)	0.25 ± 0.24	0.99 ± 1.28	16.99 ± 8.34	10.33 ± 12.62
				28.59 ± 12.00

(a) Expressed as mean ± 1 S.D. of four animals

(e) Expressed as tissue(gm) / Blood(ml) ratio.

2. Sm-153(C-14)EDTA (1:10) and Ga-67 Citrate distribution in BDF, Mice

Previous observations in cell culture studies indicated that Sm-153 EDTA (1:10) had a higher tumor cell uptake than Ga-67 citrate. An in vivo tissue distribution study was therefore designed for further investigation.

Tissue distribution comparison was made between Sm-153(C-14)EDTA (1:10) and Ga-67 citrate in BDF, mice bearing Lewis Lung Tumors. A dose of 1.09 uMole nuclide/Kg was administered intravenously to separate groups. The goal was to determine (a) whether or not Sm-153 EDTA concentrates better in tumor than Ga-67 citrate and (b) the tissue distribution of Sm-153 in vivo.

The percent dose distribution result is reported in Table 11A and the tissue-to-blood ratio is reported in Table 11B. Hepatic and bone uptake of Sm-153 EDTA was substantially lower than that of Ga-67 citrate at the same time period. The percent dose uptake in liver was 4.76 for Sm-153 EDTA compared to 15.85 for Ga-67 citrate at 48 hours (Table 11A). Bone uptake at 48 hours was 5.02% of the dose for Sm-153 EDTA compared to 15.84 for Ga-67 citrate (Table 11A).

The results also indicated that Sm-153 EDTA had a higher tumor-to-blood ratio than Ga-67 citrate. The tumor-to-blood ratio for Sm-153 EDTA was 37.22 at 24 hours

and 65.49 at 48 hours (Table 11B, Figure 11). However, the tumor-to-blood ratio for Ga-67 citrate was only 1.69 at 24 hours and 1.54 at 48 hours (Table 11B, Figure 11).

Although the Sm-153 EDTA dose used in this experiment was about one-third of the previous Sm-153 citrate dose, the percentage dose to liver at 48 hours was only 4.76% compared to 75.03% for Sm-153 citrate (Table 10A, 11A). This indicated that Sm-153 EDTA might be a better tumor imaging agent than Sm-153 citrate. The result also indicated that Sm-153 EDTA had a substantially better tumor avidity than Ga-67 citrate. Sm-153 EDTA had a twenty-two and forty-two fold higher tumor-to-blood ratio than Ga-67 citrate at 24 and 48 hours respectively (Figure 11). The high tumor to blood ratio and low percentage dose in liver as seen in Sm-153 EDTA in vivo distribution suggested that Sm-153 EDTA (1:10) might be a potentially better tumor imaging agent than Ga-67 citrate as well.

3. High Specific Activity Sm-153 EDTA (1:10) Distribution in BDF₁ Mice Bearing Lewis Lung Tumors

Because of our previous observation in cell culture studies indicating the importance of high specific activity on the uptake of samarium by tumor cells, an in vivo study was designed with the above in mind.

Table 11A

Tissue Distribution Results of Sm-153(C-14)EDTA (1:10) and Ga-67 citrate
at 1.09 uMole nuclide/Kg in BLF₁ Mice Bearing Lewis Lung Tumors (a,b)

Tissue	Time after Administration (Sm-153 EDTA Results)		
	1 Hour	6 Hours	24 Hours
Blood (c)	0.22 ± 0.06	0.04 ± 0.01	0.02 ± 0.00
Tumor	1.79 ± 1.14	0.82 ± 0.61	0.40 ± 0.15
Liver	5.25 ± 1.97	6.36 ± 1.11	5.25 ± 0.86
Kidneys	1.02 ± 0.45	0.97 ± 0.25	0.46 ± 0.17
Lung	0.16 ± 0.06	0.14 ± 0.02	0.09 ± 0.02
Spleen	0.15 ± 0.03	0.10 ± 0.03	0.05 ± 0.01
Bone (d) (Femur)	12.16 ± 2.49	17.12 ± 3.21	12.88 ± 2.41

... continued

Table 11A (continued)

Tissue	Time after Administration (⁶⁷ Ga-Citrate Results)		
	1 Hour	6 Hours	24 Hours
Blood (c)	3.40 ± 0.29	1.89 ± 0.25	0.81 ± 0.05
Tumor	2.43 ± 0.62	0.60 ± 0.27	2.04 ± 0.60
Liver	4.24 ± 0.45	5.11 ± 0.81	14.42 ± 1.39
Kidneys	1.95 ± 0.99	0.74 ± 0.36	0.73 ± 0.27
Lung	0.26 ± 0.05	0.14 ± 0.04	0.11 ± 0.02
Spleen	0.64 ± 0.28	0.43 ± 0.14	0.63 ± 0.03
Bone (d) (Femur)	20.08 ± 1.94	10.29 ± 2.89	12.88 ± 2.66
			15.84 ± 0.65

(a) Expressed as mean ± 1 S.D. of four animals
 (b) Percentage injected dose in whole tissue except as indicated
 (c) Percentage injected dose per milliliter of blood
 (d) Percentage injected dose per 1.0 gram of tissue

Table 11b

Tissue Distribution Results of Sm-153(C-14)EDTA (1:10) and Ga-67 Citrate
at 1.09 uMole nuclide/Kg in BDF₁ mice Bearing Lewis Lung Tumors (a,e)

Tissue	Time after Administration (Sm-153 EDTA Results)		
	1 hour.	6 hours	24 hours
Tumor	3.86 ± 0.96	30.67 ± 6.86	37.22 ± 5.19
Liver	22.22 ± 8.37	154.49 ± 59.15	279.67 ± 42.60
Kidneys	14.50 ± 5.26	75.41 ± 37.09	77.60 ± 21.68
Lung	4.48 ± 1.72	22.00 ± 6.93	36.10 ± 7.36
Spleen	2.00 ± 0.65	11.84 ± 4.02	27.30 ± 8.39
Bone (Femur)	56.20 ± 15.28	442.29 ± 157.36	723.98 ± 170.95

••• continued

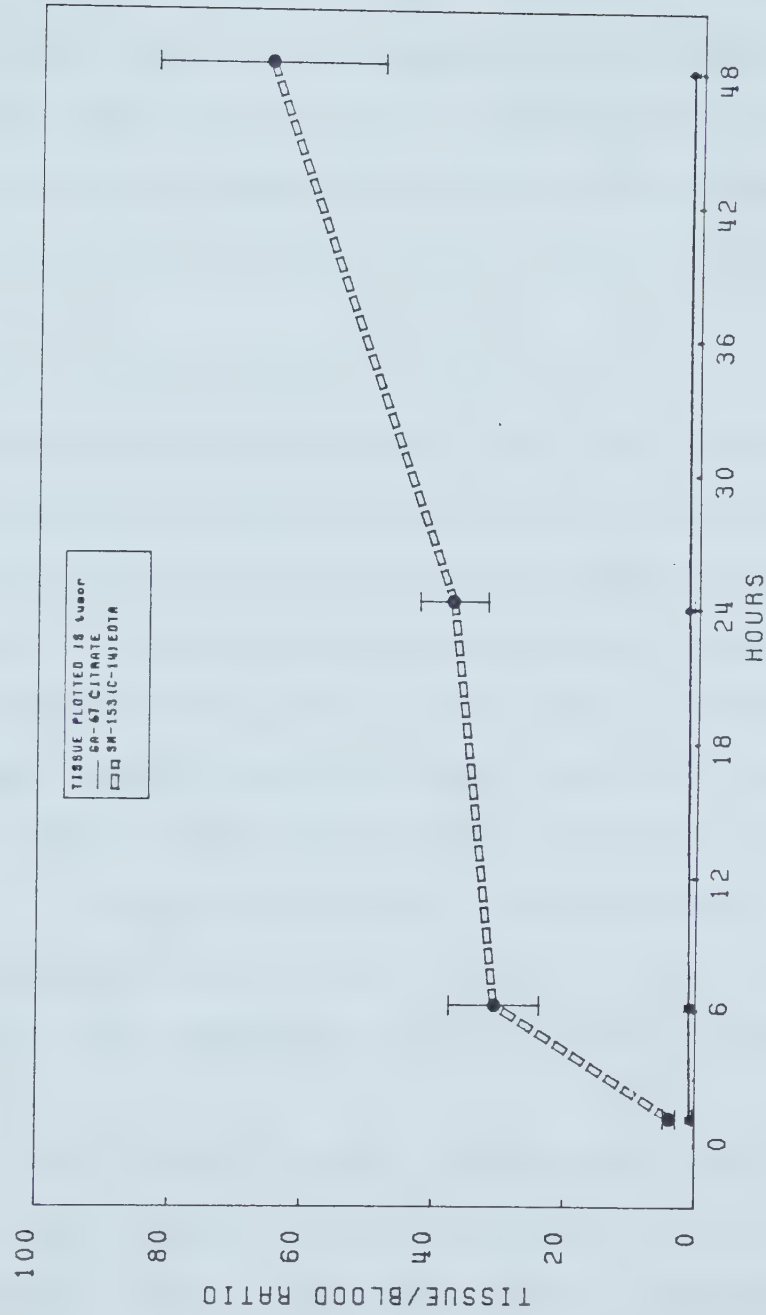
Table 11B (continued)

Tissue	Time after Administration (Ga-67 Citrate Results)		
	1 hour	6 hours	24 hours
Tumor	0.26 ± 0.02	0.40 ± 0.07	1.69 ± 0.86
Liver	0.91 ± 0.20	2.45 ± 0.39	21.41 ± 1.79
Kidneys	1.49 ± 0.38	1.24 ± 0.56	2.69 ± 0.37
Lung	0.43 ± 0.02	0.48 ± 0.06	0.86 ± 0.07
Spleen	0.40 ± 0.13	0.93 ± 0.24	3.62 ± 1.67
Bone (Femur)	5.93 ± 0.85	5.57 ± 2.07	15.84 ± 2.26

(a) Expressed as mean ± 1S.D. of four animals
 (e) Expressed as tissue (μm)/blood (ml) ratio

Figure 11

Tumor to Blood Ratios of SM-153(C-14)EDTA (1:10) and Ga-67 Citrate in
BDF₁ Mice Bearing Lewis Lung Tumors



Sm-153 of a specific activity of 1.0 uCi per 1.09 uMole Sm/Kg is the highest dose achievable through the production by a SLOWPOKE reactor under our irradiation conditions. In a clinical situation, however, a much higher specific activity of Sm-153 is desirable. Tissue distribution studies using a dose of 10.9 nMole Sm/Kg was therefore undertaken. A high specific activity Sm-153 was obtained using the high thermal neutron flux reactor at Chalk River (Atomic Energy of Canada Ltd.).

Tissue distribution results indicated that the percentage dose in liver at 48 hours was 9.59% for Sm-153 EDTA (Table 12A) compared to 15.06% for Ga-67 citrate (Table 12A). The tumor-to-blood ratio at 48 hours increased from an average of 65.49 to 71.54 by reduction of dose from 1.09 uMole Sm/Kg to 10.9 nMole Sm/Kg. The 1/100 dose reduction increased the tumor-to-blood ratio by about 36% at 24 hours and 9% at 48 hours (Table 11B, 12B). Tumor-to-blood ratio for Ga-67 citrate at 48 hours was shown to be an average of 2.18 (Table 12B). Bone-to-blood ratio reached 750.24 for Sm-153 EDTA (Table 12B) compared to 9.25 for Ga-67 citrate (Table 12B).

When compared with Ga-67 citrate, Sm-EDTA was found to be superior in its availability to tumor sites. At 24 and 48 hours post injection, Sm-153 EDTA had shown a respective forty-seven and twenty-five fold higher tumor to blood ratio than Ga-67 citrate (Table 12B, Figure 12). Although statistical analysis of Sm-153 EDTA tumor to blood ratio did

not reveal any significant differences between 10.9 nMole Sm/Kg dose and 1.09 uMole Sm/Kg dose at 48 hours, significant differences existed at 24 hours (P<0.025) (Figure 13).

Sm-153 EDTA (1:10) has also shown greater stability from possible colloidal formation in vivo than Sm-153 citrate. Both 1.09 uMole Sm/Kg and 10.9 nMole Sm/Kg doses of Sm-153 EDTA in BDF₁ mice revealed that less than 10% of the dose is accumulated in the liver at 48 hours (Table 11A, 12A). The high bone-to-blood ratio of 750.24 at 48 hours also suggested that Sm-153 EDTA might also be a good potential skeletal localizing agent.

O'Mara et al (40) had similar observations in rabbits with Sm-153 HEDTA. Although actual dosage used was not identified, they reported that the percentage dose in whole skeleton at 24 hours was 45.70% and in liver was 2.51%. They also suggested that Sm-153 HEDTA might be a good skeletal imaging agent.

Table 12A

Tissue distribution results of Sm-153 EDTA and Ga-67 Citrate
at 10.9 nCiole nuclide/Kg in BDF₁ Mice Bearing Lewis Lung Tumors (a,b)

Tissue	Time after Administration (Sm-153 EDTA Results)			
	1 hour	6 Hours	12 hours	24 hours
Blood (c)	1.60 ± 0.21	0.37 ± 0.08	0.03 ± 0.01	0.02 ± 0.01
Muscle (d)	1.00 ± 0.41	0.40 ± 0.16	0.24 ± 0.09	0.30 ± 0.20
Tumor	9.76 ± 2.24	6.55 ± 1.10	4.21 ± 0.86	1.41 ± 0.29
Liver	13.25 ± 2.21	13.82 ± 1.86	13.99 ± 1.52	12.68 ± 1.77
Kidneys	2.91 ± 0.35	1.50 ± 0.17	0.58 ± 0.05	0.57 ± 0.10
Lung	0.45 ± 0.29	0.23 ± 0.03	0.11 ± 0.01	0.12 ± 0.01
Spleen	0.16 ± 0.11	0.06 ± 0.01	0.07 ± 0.03	0.05 ± 0.01
Bone (d) (Femur)	12.40 ± 2.20	18.60 ± 8.09	17.96 ± 3.86	15.87 ± 4.89

... continued

Table 12A (continued)

Tissue	Time after Administration (Ga-67 Citrate Results)			
	1 Hour	6 Hours	12 Hours	24 Hours
Blood (c)	24.51 ± 12.09	12.21 ± 0.21	6.92 ± 0.46	2.84 ± 0.77
Muscle (d)	2.01 ± 0.56	1.45 ± 0.04	3.95 ± 5.07	0.68 ± 0.24
Tumor	8.44 ± 7.45	5.20 ± 0.65	3.69 ± 0.83	2.85 ± 3.60
Liver	18.74 ± 6.31	18.08 ± 1.97	18.73 ± 2.21	15.27 ± 2.16
Kidneys	4.18 ± 0.66	2.55 ± 0.27	2.20 ± 0.35	1.78 ± 0.32
Lung ^a	4.26 ± 2.44	1.74 ± 0.48	1.12 ± 0.18	0.65 ± 0.11
Spleen	2.33 ± 1.65	1.24 ± 0.07	1.08 ± 0.04	1.19 ± 0.75
Bone (d) (Femur)	10.65 ± 1.19	7.25 ± 1.65	8.39 ± 0.37	7.43 ± 0.77
				8.77 ± 2.35

(a) Expressed as mean ± 1 S.D. of four animals
 (b) Percentage of injected dose in whole tissue except as indicated
 (c) Percentage of injected dose per milliliter of blood
 (d) Percentage of injected dose per 1.0 gram of tissue

Table 12b

Tissue Distribution Results of Sm-153 EDTA and Ga-67 Citrate
at 10.9 milie nuclide/kg in BDF₁ Mice Bearing Lewis Lung Tumors (a,e)

Tissue	Time after Administration (Sm-153 EDTA Results)			
	1 hour	6 hours	12 hours	24 hours
Muscle	0.63 ± 0.28	1.12 ± 0.52	7.25 ± 2.05	16.04 ± 9.51
Tumor	1.72 ± 0.11	4.58 ± 0.66	34.17 ± 5.93	50.44 ± 5.49
Liver	8.01 ± 0.38	35.51 ± 4.34	332.04 ± 43.28	604.62 ± 129.23
Kidneys	0.63 ± 1.48	16.19 ± 3.41	72.07 ± 13.81	77.92 ± 50.20
Lung	2.10 ± 0.97	5.56 ± 1.10	48.51 ± 24.82	79.85 ± 37.45
Spleen	0.42 ± 0.13	4.18 ± 1.40	13.17 ± 7.12	48.15 ± 26.36
Bone (Femur)	8.55 ± 5.04	51.22 ± 19.46	541.52 ± 20.40	852.91 ± 87.35
				750.24 ± 124.65

*** continued

Table 12B (continued)

Tissue	Time after Administration (Ga-67 Citrate Results)			
	1 Hour	6 Hours	12 Hours	24 Hours
Muscle	0.10 ± 0.05	0.12 ± 0.00	0.57 ± 0.72	0.27 ± 0.13
Tumor	0.29 ± 0.23	0.44 ± 0.17	0.59 ± 0.13	1.07 ± 0.12
Liver	0.64 ± 0.19	1.14 ± 0.02	2.22 ± 0.19	4.41 ± 0.31
Kidneys	0.67 ± 0.49	0.58 ± 0.04	0.95 ± 0.08	2.20 ± 1.31
Lung	0.97 ± 0.21	0.79 ± 0.18	0.80 ± 0.01	1.34 ± 0.22
Spleen	0.56 ± 0.34	0.73 ± 0.19	1.27 ± 0.05	2.21 ± 1.16
Bone (Femur)	0.59 ± 0.47	0.60 ± 0.15	1.22 ± 0.14	2.75 ± 0.82

(a) Expressed as mean ± 1 S.D. of four animals
 (b) Expressed as tissue (gm)/blood (ml) ratio

Figure 1?
Tumor to Blood Ratios of High Specific Activity
 Sm-153 EDTA (1:10) and Ga-67 Citrate in BDF₁
Mice Bearing Lewis Lung Tumors

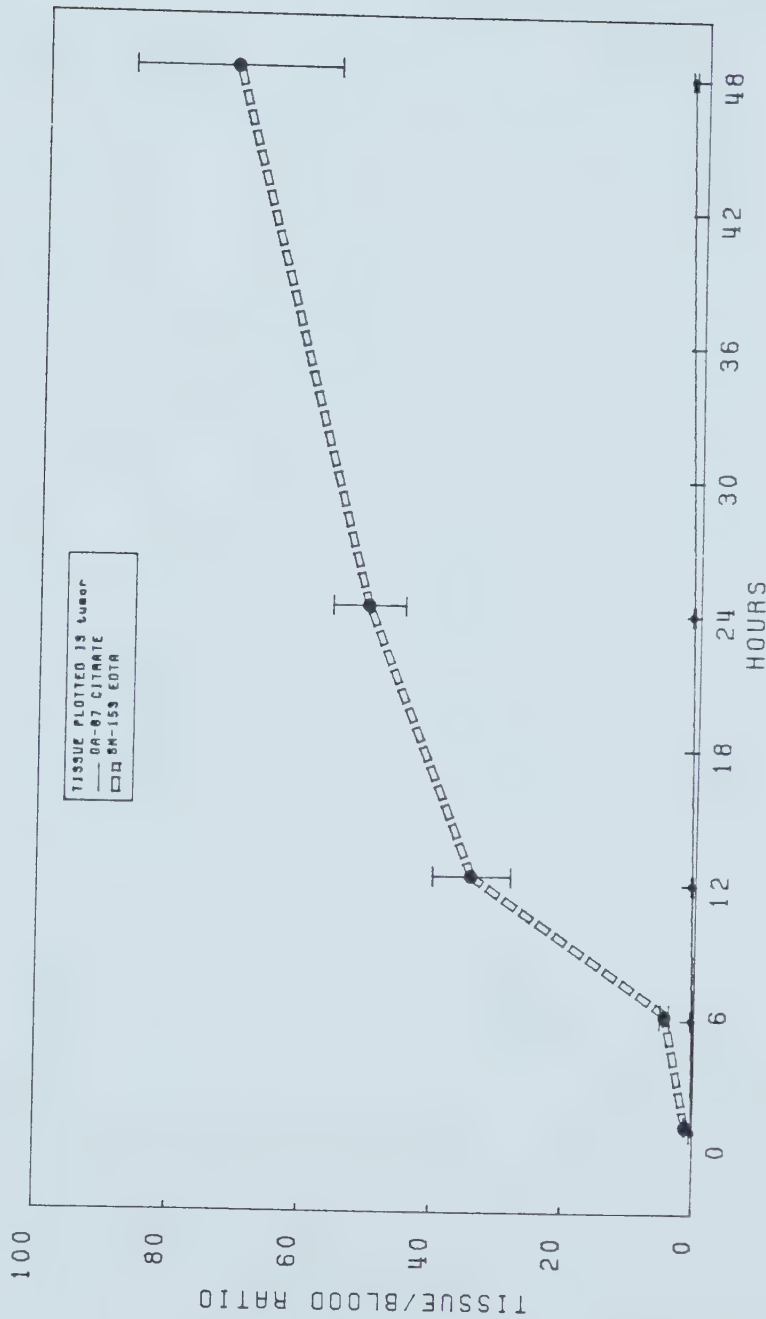
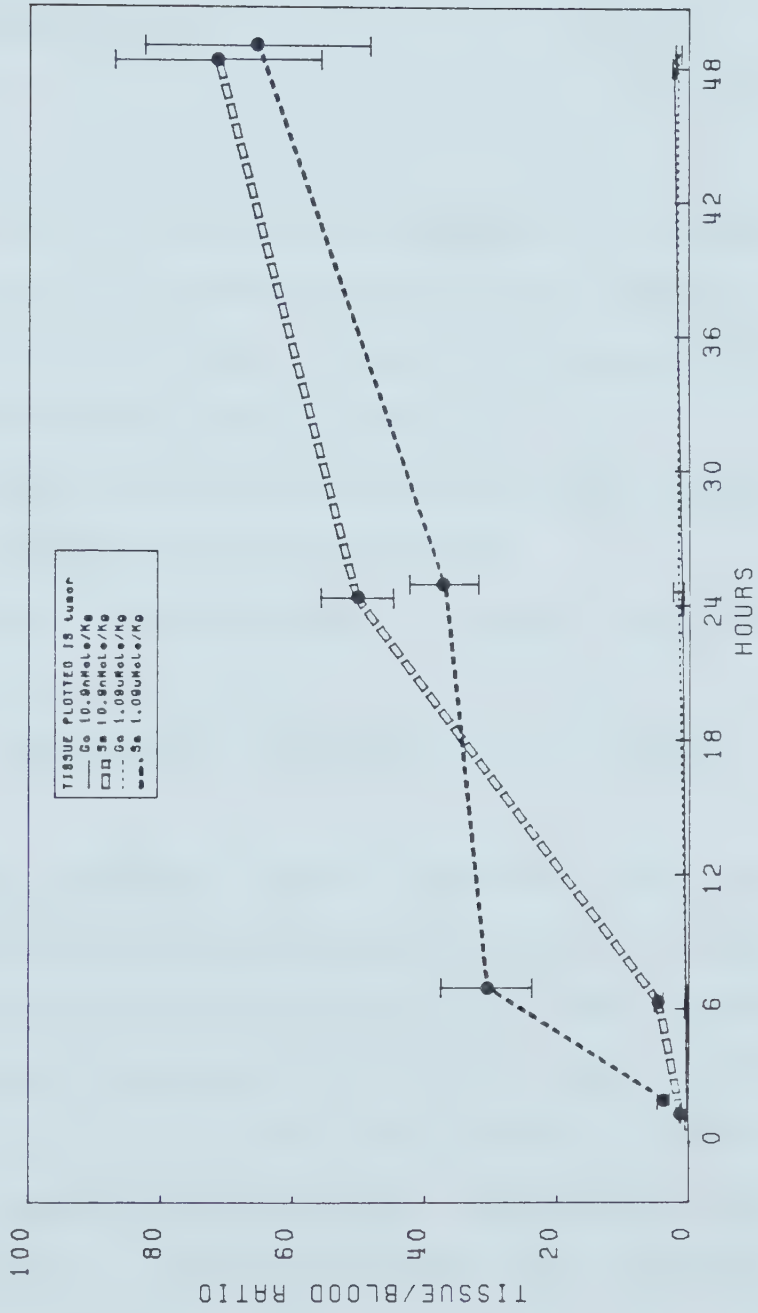


Figure 13
Tumor to Blood Ratio Comparison of Sm-153 EDTA (1:10) and
Ca-67 Citrate at various dosages



G. Whole Body Imaging Studies

1. Comparison of Sm-153 Chloride, Sm-153 Citrate and Sm-153 Transferrin Tumor Localization

The ultimate test of a radiopharmaceutical from the oncological standpoint is the measurement of its uptake by tumor. Our basic criteria in the selection of an appropriate tumor model for the study of samarium were:

1. that the tumor be of such a size that overcomes the limits of the gamma camera spacial resolution,
2. that the tumor bearing animals be readily available for a large number of tests, and
3. that the tumor show an avidity for the element of interest.

Copenhagen rats bearing Dunning prostatic tumors met such criteria and were used throughout this section of the investigation. Rats bearing tumors on both the left and the right flanks were dosed intravenously with 3.0 uMole Sm/Kg body weight with either Sm-153 chloride, Sm-153 citrate or Sm-153 transferrin. Gamma scans were taken immediately after injection, at 6 hours, 24 hours and 48 hours. The heart, liver and tumors were observed to accumulate radioactivity immediately following injection and at 6 hours for all three agents. Cold spots within the tumor were also observed

probably delineating the necrotic area in the tumor (Figure 14). Both Sm-153 chloride and Sm-153 citrate showed a significant concentration in liver at 24 hours while activity in heart and tumor diminished substantially. A similar distribution was observed for Sm-153 transferrin at 48 hours (Figure 14). These observations suggested that initial localization of the three tracers in tumor was mainly due to the vascularity of tumor. Hepatic concentration of tracers from blood circulation possibly continued through the period of observation leading to a 'hot liver' at 24 and 48 hours. Similar observations of samarium distribution were reported by Matsusaka (29), O'Mara (40) and Gilyazutdinov (41).

2. Comparison between Sm-153 Citrate and Ga-67 Citrate Tumor Localization

Since gallium-67 citrate is routinely used for clinical tumor imaging, a comparative study between Sm-153 citrate and Ga-67 citrate was conducted.

Rats bearing Dunning prostatic tumors on both the left and right flanks were intravenously injected with 3.0 uMole nuclide/Kg dose of either Sm-153 citrate or Ga-67 citrate. Although hepatic uptake of both agents was observed at 48 hours, the extent of uptake of Sm-153 citrate by liver was found to be predominant. Delineation of the tumor at 24 and

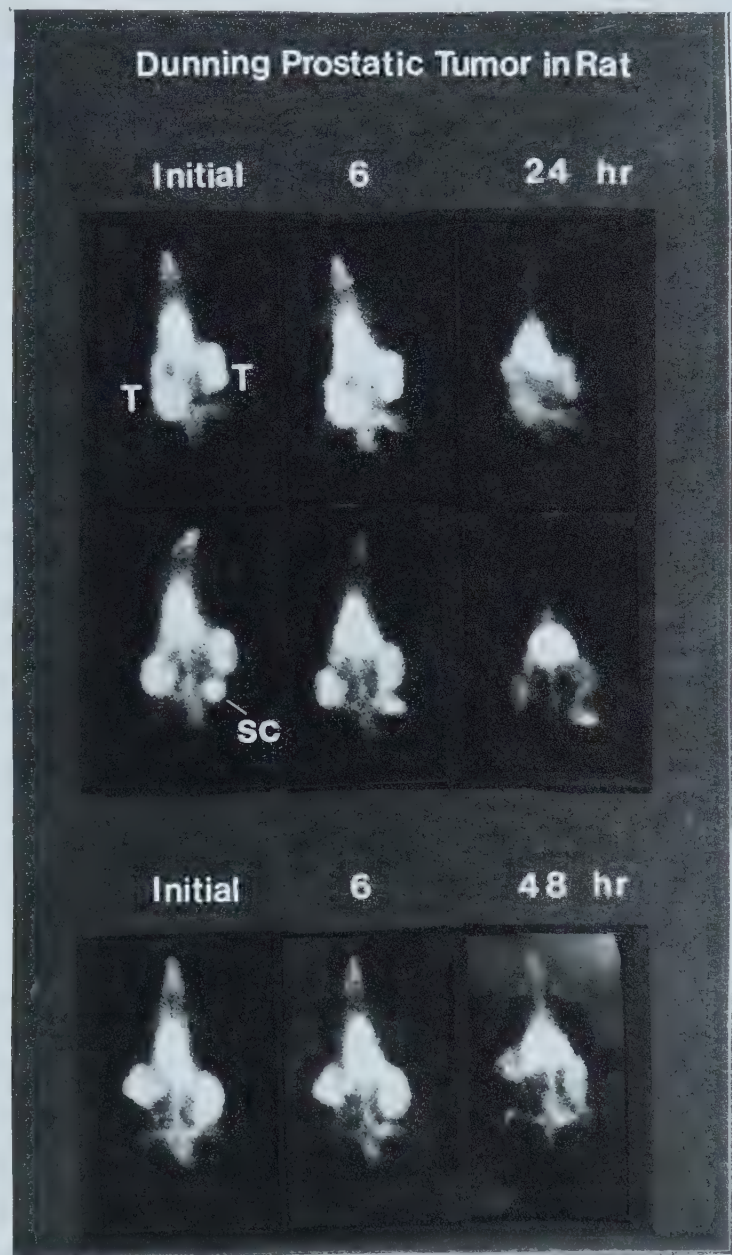
Figure 14

Scintigraphic Images of Samarium Uptake in Dunning Prostatic Tumor Bearing Rats*

**Sm-153
Chloride**

**Sm-153
Citrate**

**Sm-153
Transferrin**



SC : indicates point of partial subcutanious injection

T : indicates location of tumor

* Administered at Dose of 3.0 μ Mole Sm/Kg intravenously

48 hours was difficult when Sm-153 citrate was administered (Figure 15). Scintigraphic results suggested that Sm-153 citrate was inferior to Ga-67 citrate in its tumor affinity. Our observations from this experiment seem to contradict the recommendation made by Sullivan and Friedman (46) as well as Woolfenden (10). Such contradiction might be explained on the basis that these investigators have used different species of animals and tumor models.

3. Comparison of Tumor Localization between Sm-153 Transferrin and Ga-67 Transferrin

Gallium-67 transferrin had been proposed as a potential tumor imaging agent since transferrin receptors were associated with tumor cell membranes (3, 8, 56, 57). Thus, a study was conducted to compare this agent with a samarium-transferrin complex.

Rats bearing Dunning prostatic tumor on both flanks were injected intravenously with either Sm-153 transferrin or Ga-67 transferrin at 3.0 uMole cations/Kg dose. Observation of the resulting scans indicated that they were very similar to those noted for the citrate derivatives of both tracers (Figure 15). Sm-153 transferrin was found to be inferior to Ga-67 transferrin in tumor localization. Small tumor affinity differences were observed in the scans with both isotopes in either their citrate or transferrin form.

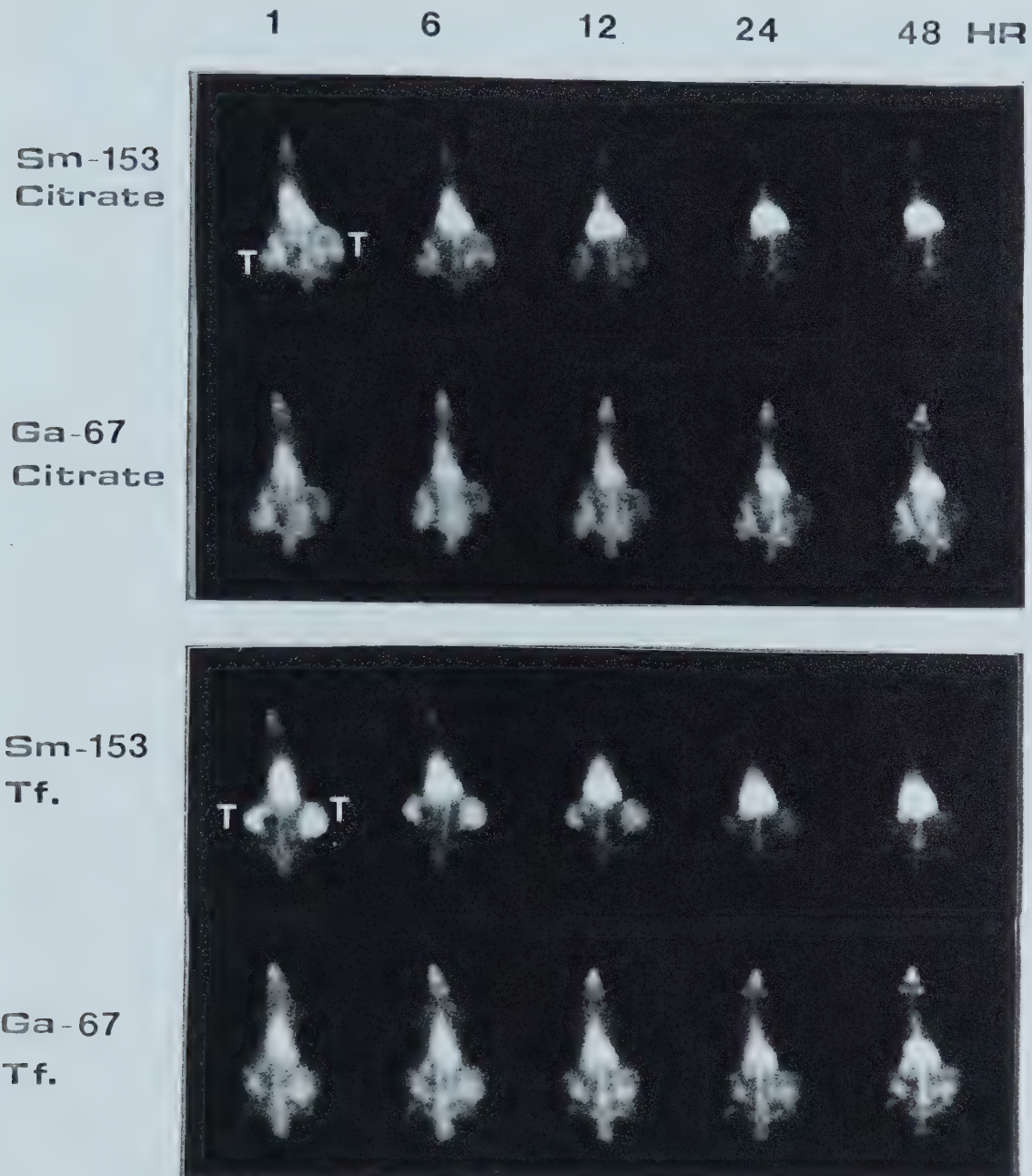
(Figure 15). Hepatic concentration of both agents was also predominant.

4. In vivo Disposition of Samarium-153 Citrate

Since both Sm-153 citrate and Sm-153 transferrin were shown to form a colloid under certain experimental conditions in vitro, and because both agents localized mainly in the liver in vivo, an experiment was designed to investigate the possibility of colloid formation in vivo. Male Wistar rats (weight 300 gm) were injected intravenously via femoral vein with a 3.0 uMole Sm/Kg dose of either Sm-153 citrate or Sm-153 transferrin. One hundred microliters blood samples were collected at different time intervals from a vena cava cannula. The cannula consisted of a PE-50 capillary polyethylene tube surgically implanted in the rat one week earlier. The tube was filled with 10% heparinized normal saline and sealed at one end. The open end of the tube was implanted in a parallel fashion inside the superior vena cava. The tube was brought through the abdominal wall, circled around the body underneath the fur and the sealed end sutured at the posterior side of the neck. Surgical silk (4-0) was used for fastening and surgical chromic gut (4-0) was used for suturing throughout the cannula implantation procedure. About 0.1 ml of sterile normal saline was injected into the tube before the collection of blood took place. The plasma and red cells were separated by centrifugation and activities of both fractions were determined separately. Results from both

Figure 15

Scintigraphic Images of Sm-153 Citrate, Sm-153 Transferrin (Tf), Ga-67 Citrate and Ga-67 Transferrin (Tf) Uptake in the Dunning Prostatic Tumor Bearing Rats*



* Administered at Dose of 3.0 μ Mole Nuclides/Kg

T : Indicates location of Tumor

Sm-153 citrate and Sm-153 transferrin indicated that more than 90% of the activity in blood (1 - 12 hours) remained in the plasma fraction (Table 13). No significant binding with the red cells was evident.

The collected plasma specimens were also diluted to 150 ul with normal saline and ultracentrifuged at 144,000 G for 60 minutes to determine the percentage of colloid formation as a function of time. Both Sm-153 citrate and Sm-153 transferrin exhibited nearly 31% of plasma activity in the form of colloid in the first hour. This percentage increased to more than 75% at 6 hours for both agents (Table 14).

These results correlated well with the scans observed previously. They also confirmed that Sm-153 colloid formation in vivo was one of the major reasons for significant hepatic localization by both Sm-153 citrate and transferrin.

5. Effect of EDTA Concentration on Samarium Distribution in vivo

EDTA was observed in previous experiments to prevent colloidal formation of samarium in vitro. However, the relative quantity of the complexing agent on the stability of the final complex as well as the presence of other interfering ions may play a very drastic role on the bioavailability of the samarium in vivo. For this reason, an

Table 13

Distribution of Sm-153 Citrate and Sm-153 Transferrin Activity in Blood

<u>Hours post injection</u>	<u>Percentage of Blood Activity in plasma</u>	
	<u>Sm-153 Citrate *</u>	<u>Sm-153 Transferrin *</u>
1	93.4	98.2
2	96.1	92.5
3	92.5	-
4	90.5	99.0
5	93.2	99.0
6	91.1	99.0
12	-	99.0

* Each point represents a single observation

Table 14

In Vivo Colloid Formation of Samarium-153 After
Injection of Sm-153 Citrate or Sm-153 Transferrin

<u>Hours post injection</u>	<u>Percentage of Colloid in Plasma</u>	
	<u>Sm-153 Citrate*</u>	<u>Sm-153 Transferrin*</u>
1	31.0	30.8
2	33.5	28.3
4	58.4	42.9
5	60.4	60.9
6	75.0	87.0
12	-	85.7

* Each point represents a single observation

experiment was designed to examine the two different ratios of EDTA added to similar concentrations of samarium-153 chloride. Sm-153 EDTA (1.09 uMole Sm/Kg) with molar ratio of (1:10) and (1:2) were injected, separately, intravenously into groups of rats bearing Dunning prostatic tumors. Little hepatic uptake was observed right after injection for Sm-153 EDTA (1:10). Visualization of kidneys and bladder in the scans indicated a possible fast elimination of Sm-153 EDTA through the kidneys with the final accumulation in the bladder (Figure 16). This would normally be expected for EDTA chelated metals (90, 91). Up to 98% of an EDTA complex of calcium was known to be eliminated within six hours by glomerular filtration and tubular secretion (90, 91). However, starting from 1 hour to 30 hours, gradual hepatic uptake was observed, indicating a possible shift of some Sm-153 from the EDTA complex toward colloid formation or other chemical form with greater avidity for the liver (Figure 16). Skeletal uptake was also noticed at 1 hour, 6 hours and 30 hours. Delineation of tumor was especially clear at 30 hours due to a low body background in the surrounding tissue (Figure 16).

The distribution of Sm-153 EDTA (1:2) was similar to Sm-153 citrate in that the hepatic uptake was already predominant at 1 and 6 hours. Kidney and bladder activities were observed immediately after injection (Figure 16) indicating that renal excretion had taken place. However, the intensive hepatic uptake soon after injection, as

observed in gamma scans, also suggested that Sm-153 EDTA (1:2) did not form a very stable complex and did not offer any great advantage over Sm-153 citrate.

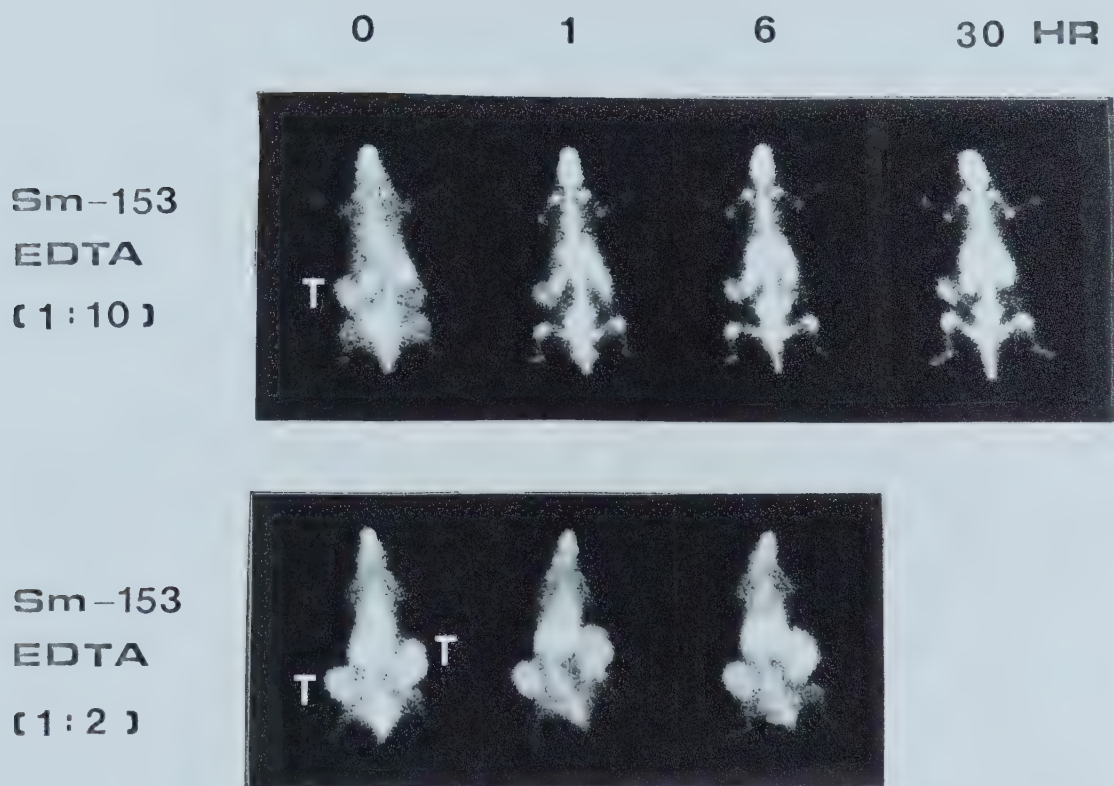
6. Tumor Localization of High Specific Activity Sm-153 EDTA (1:10)

Since high specific activity Sm-153 EDTA (1:10) is desirable in a clinical situation, the effect of high specific activity on the biodistribution of samarium was investigated. A comparison was also conducted with gallium citrate of the same molar concentration.

Rats bearing Dunning prostatic tumors only on the right flank were dosed intravenously with a 10.9 nMole Sm/Kg dose of Sm-153 EDTA (1:10). A series of gamma scans were made at 15 minutes, 30 minutes, 1 hour, 6 hours, 12 hours, 24 hours and 48 hours. The tumor was about 1.5 cm in diameter. Clear tumor delineation was observed starting at 6 hours (Figure 17A). The same animal was injected again with Ga-67 citrate (10.9 nMole Ga/Kg) twelve days later. The tumor was about 3.0 cm in diameter then. A series of scans were made and were compared to the Sm-153 EDTA. Although the tumors were of different size, Sm-153 EDTA was observed to be superior to Ga-67 citrate in tumor localization as the tumor could be identified easier against a low body background once the Sm-153 EDTA activity in the bladder was voided (Figure 17A).

Figure 16

Effect of EDTA on the Biodistribution of Sm-153
in the Dunning Prostatic Tumor Bearing Rats*



*Administered at 1.09 μ Mole Sm/Kg Dose intravenously
T : indicates location of Tumor

Similar procedures were carried out on another two rats bearing Dunning prostatic tumors on both flanks. The tumors were about 1.0 to 1.5 cm diameter. One rat was administered with Sm-153 EDTA and the other with Ga-67 citrate. Comparisons were made simultaneously under the same conditions. Sm-153 offered a good delineation of tumors against a low body background starting at 6 hours while Ga-67 citrate still had a fairly high soft tissue activity. Even at 48 hours, Sm-153 EDTA was found to be superior in tumor localization than Ga-67 citrate (Figure 17B). Results suggested that Sm-153 EDTA (1:10) was a better tumor localizing agent than Ga-67 citrate in this experiment. The low body background made tumor delineation easier for Sm-153 EDTA. Tumor scans using Sm-153 EDTA could be started at 6 hours post injection. Voiding of urine within 6 hours would also decrease bladder activity and improve the delineation of tumors.

H. Radiochemical Elimination of Sm-153 EDTA

Because of the promising results obtained after the administration of Sm-153 EDTA, it was necessary to acquire further information with regard to the whole body retention of the complex, the course of disappearance of Sm-153 EDTA radioactivity in blood, and the route of the Sm-153 EDTA excretion in vivo. Three sets of investigations were therefore designed with these purposes in mind.

Figure 17A

Scintigraphic Images of High Specific Activity
Sm-153 EDTA (1:10) and Ga-67 Citrate in Dunning
Prostatic Tumor Bearing Rats*

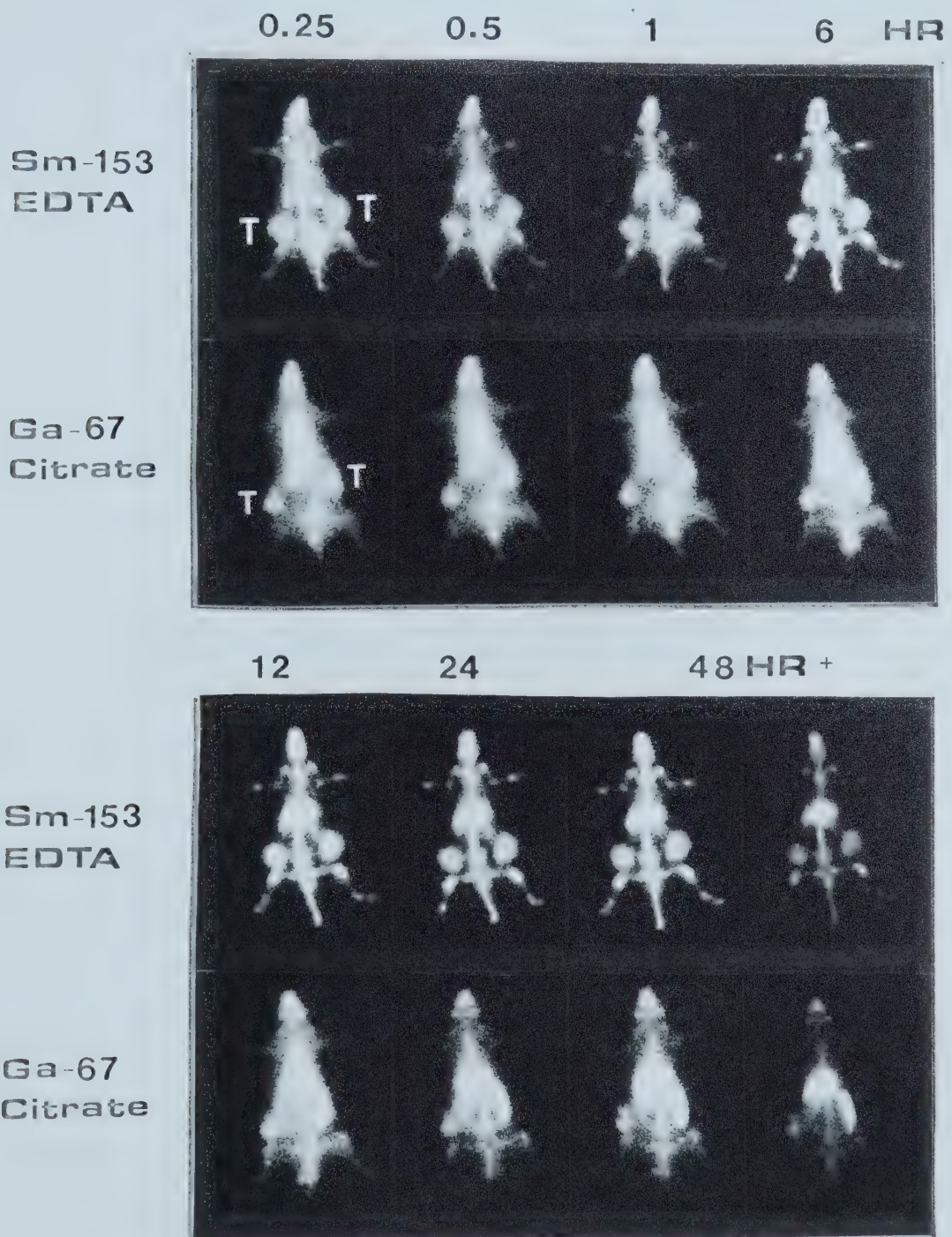


+ Camera exposures #1 & #2

* Administered Dose at 10.9 n Mole Sm/Kg intravenously

Figure 17B

Scintigraphic Images of High Specific Activity
Sm-153 EDTA (1:10) and Ga-67 Citrate in Dunning
Prostatic Tumor Bearing Rats *



+ Camera exposures #1 & #2

* Administered Dose at 10.9 nMole Sm/Kg intravenously

1. Whole Body Elimination of Sm-153 EDTA (1:10)

The percentage of injected dose remaining in the whole body was determined for both Sm-153 EDTA and Ga-67 citrate (which was used as a control) injected rats bearing Dunning prostatic tumors. Each group consisted of three animals. It was observed that an average of 18.9% of the injected Sm-153 EDTA (1:10) of low specific activity (1.09 uMole Sm/Kg) remained in the body at 6 hours. This was probably due to the rapid excretion of Sm-153 EDTA through the urinary system in the first 6 hours. However, from 6 hours to 48 hours, the Sm-153 radioactivity in whole body remained at a constant plateau and no significant changes were observed (Table 15, Figure 18).

Ga-67 citrate, on the other hand, showed a gradual decline over the 48 hour period and decreased to 44.7% at the end of the experiment. At 6 hours, the percentage dose remaining in whole body was 83.6%.

These results correlated well with the scans shown previously. The low tissue background observed in Sm-153 EDTA scans can be explained by the low whole body dose remaining.

When the high specific activity Sm-153 EDTA (1:10) complex (10.9 nMole Sm/Kg) was administered, little change was observed in the percentage dose remaining in the body at 48 hours as compared to the 1.09 uMole Sm/Kg dose. It was

23.7% for Sm-153 EDTA and 40.5% for the same dosage of Ga-67 citrate. However, the percentage of Sm-153 EDTA remaining in the body at 6 hours was 47.0% which was higher than expected (Table 16, Figure 18).

Results from these two experiments indicated that over 50% of the Sm-153 EDTA would be eliminated in the first 6 hours, possibly through the urinary system. The percentage dose of Sm-153 EDTA remaining in the body throughout the 48 hours were observed to be consistently smaller than that of Ga-67 citrate.

2. Blood Kinetics of Sm-153 EDTA (1:10) in Rats

Sm-153 EDTA (1:10) (1.09 uMole Sm/Kg) was injected intravenously through the left femoral vein into six rats bearing Dunning prostatic tumor. Blood samples of 20 ul each were collected from the right femoral vein immediately after injection, at 1 minute, 5 minutes and up to 120 minutes. The dose remaining was then calculated for each sample as a percent of the original sample collected immediately after injection. Disappearance of Sm-153 EDTA progressed in a sharp rate during the first 30 minutes post injection. It was observed that only 9.9% of the administered dose remained at 25 minutes, and only 1.9% of the Sm-153 EDTA dose remained at 120 minutes (Table 17, Figure 19). These results indicate a fast redistribution of Sm-153 EDTA from

Table 15

Whole Body Elimination of Low Specific Activity
 Sm-153 EDTA (1:10) and Ga-67 Citrate in Rats*

<u>Time (hours) post injection at</u>	<u>Percent Dose in Body</u>	
<u>1.09 uMole Sm/Kg</u>	<u>Sm-153 EDTA</u>	<u>Ga-67 Citrate</u>
0.1 - 0.5	100 \pm 0.0	100 \pm 0.0 - 99.4 \pm 0.2
1.0	100 \pm 0.0	98.9 \pm 0.5
6.0	18.9 \pm 2.5	83.6 \pm 1.9
12.0	18.8 \pm 2.1	74.3 \pm 3.1
24.0	19.2 \pm 2.7	59.4 \pm 0.8
48.0	19.2 \pm 4.4	42.7 \pm 0.3

* Each point represents mean \pm 1 S.D. of three determinations

Table 16

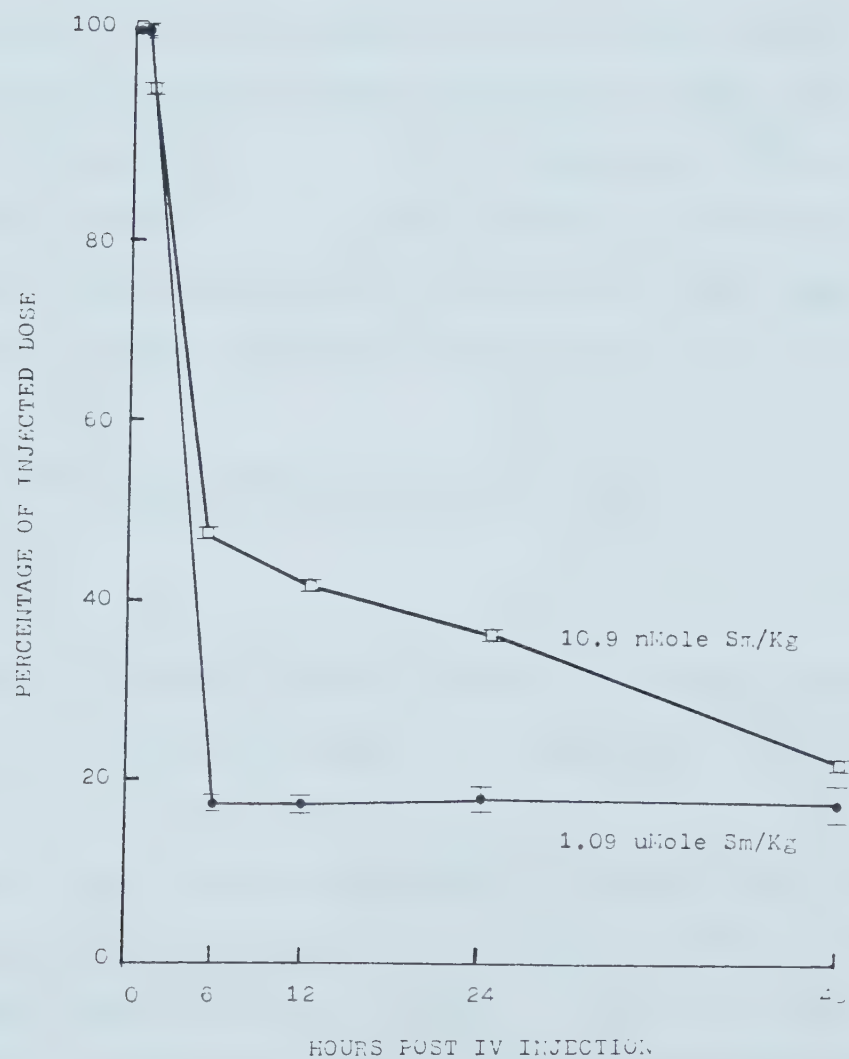
Whole Body Elimination of High Specific Activity
Sm-153 EDTA (1:10) and Ga-67 Citrate in Rats *

<u>Time (hours) post</u> <u>injection at</u> <u>10.9 nMole Sm/E.P.</u>	<u>Percent Dose in Body</u>	
	<u>Sm-153 EDTA</u>	<u>Ga-67 Citrate</u>
0.1	100 \pm 0.0	100 \pm 0.0
0.2	97.9 \pm 0.8	100 \pm 0.0
0.5	97.2 \pm 0.9	99.9 \pm 0.0
1.0	95.6 \pm 0.5	99.6 \pm 0.3
6.0	47.0 \pm 0.9	61.6 \pm 0.9
12.0	42.5 \pm 1.1	75.2 \pm 2.4
24.0	36.5 \pm 0.9	57.2 \pm 0.9
48.0	23.7 \pm 0.5	40.5 \pm 0.4

* Each point represents mean \pm 1 S.D. of three determinations

Figure 18

Whole Body Elimination of Sm-153 EDTA (1:10) in Rats*



* Each point represents mean \pm 1 S.D. of three determinations

the blood compartment to other organs such as kidneys, liver and tumor. One might speculate that the fast redistribution of Sm-153 EDTA from blood to other organs would probably result in a high organ-to-blood ratio such that early organ or tumor visualization would be made possible. Since Sm-153 activity was detected in kidneys and bladder in previous scintigraphic observations, excretion of Sm-153 through urine was suspected. If that speculation is true, then the fast elimination of Sm-153 EDTA, especially in the first 15 minutes, would probably be via the glomerular filtration mechanism as observed in the case of EDTA by Foreman (91, 92), with Cr-51 EDTA by Myers (93, 94) and in the case of other metals chelated with EDTA by Hosain(95).

3. Excretion of Sm-153 EDTA in Urine and Feces

In order to confirm whether Sm-153 was indeed excreted through urine, a direct radioactivity measurement in urine is required.

Three rats bearing Dunning prostatic tumors were dosed intravenously with 1.09 uMole Sm/Kg of Sm-153 EDTA (1:10). Urine and fecal material were collected quantitatively and the cumulative radioactivity of the samples determined over a period of 48 hours.

Results revealed that over 80% of the injected dose was excreted in the urine in the first 6 hours. This confirmed

Table 17

Disappearance of High Specific Activity Sm-153 EDTA (1:10)
in Blood *

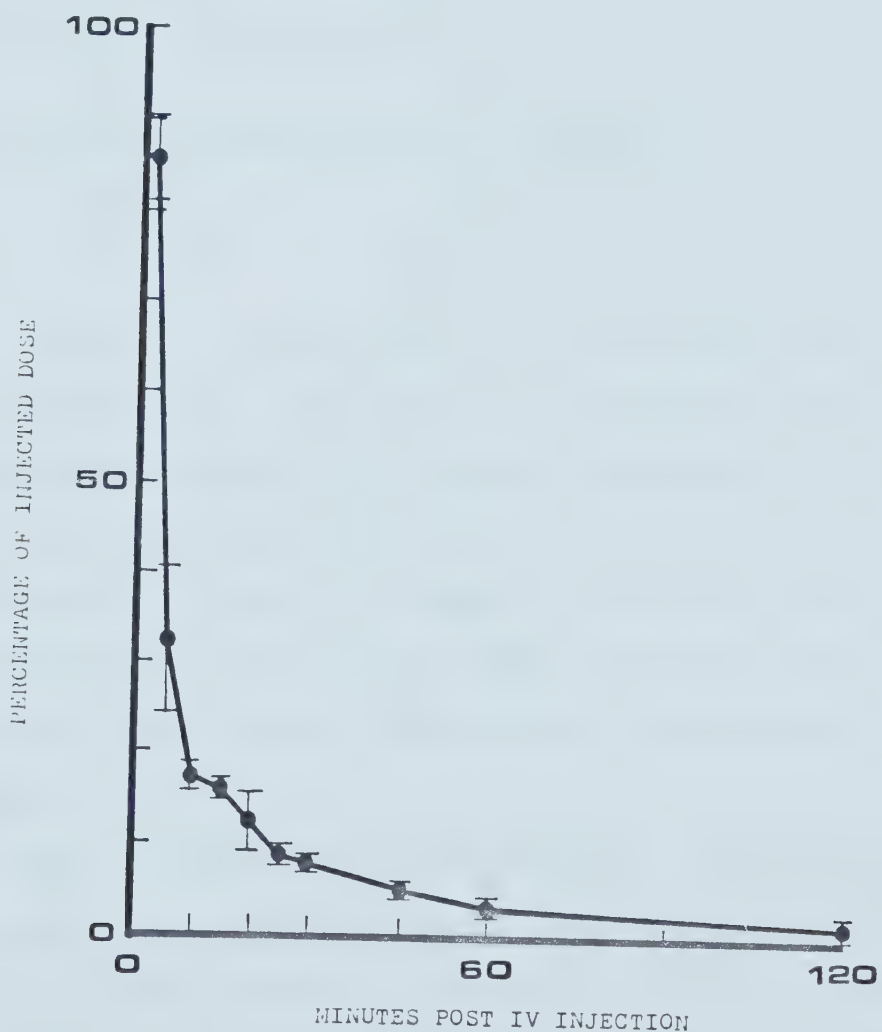
<u>Time (min.)</u> <u>post injection</u>	<u>Percent Dose Remaining**</u>
1	86.0 \pm 4.4
5	32.6 \pm 8.6
10	18.0 \pm 1.4
15	16.1 \pm 0.9
20	12.6 \pm 3.0
25	9.9 \pm 0.9
30	8.8 \pm 0.5
45	5.9 \pm 0.4
60	3.5 \pm 0.5
120	1.9 \pm 0.5

* Each animal was dosed at 1.09 uCi/ Kg intravenously.

** Each value represents mean \pm 1 S.D. of six animals

Figure 13

Disappearance of High Specific Activity Sm-153 EDTA(1:10) in blood *



* Each point represents mean \pm 1 S.D. of six animals
and each animal was dosed at 1.09 uMole Sm/Kg i.v.

that the early and major elimination of whole body Sm-153 radioactivity was indeed through the excretion in urine. Radioactivity in feces was less than 1% over the 48 hours of observation (Table 18, Figure 20). This also indicated that major excretion of Sm-153 EDTA into GIT within the first 48 hours was very minor.

I. Mechanism of Sm-153 EDTA Tissue Distribution

Since early in vitro tumor culture cell studies indicated that the uptake of Sm-153 was independent of the C-14 labelled EDTA through the probable dissociation of the complex, it was necessary to investigate whether such mechanism existed in vivo. A tissue distribution study of Sm-153(C-14)EDTA (1.09 uMole Sm/Kg dose intravenously) in mice bearing Lewis Lung tumors was therefore implemented for such confirmation.

Sm-153 EDTA tissue distribution results in the form of tissue percentage dose distributions and tissue-to-blood ratios were already reported in Tables 11A, 11B and Figure 11. The C-14 EDTA results are reported in Tables 19A, 19B and Figure 21. If the Sm-153(C-14)EDTA complex was incorporated by tissue or tumor in an unchanged form, then the tissue or tumor uptake ratio of Sm-153 and C-14 radioactivities should be the same.

Table 18

Accumulated Sm-153 EDTA (1:10) Activity in Urine and Feces from Rats*

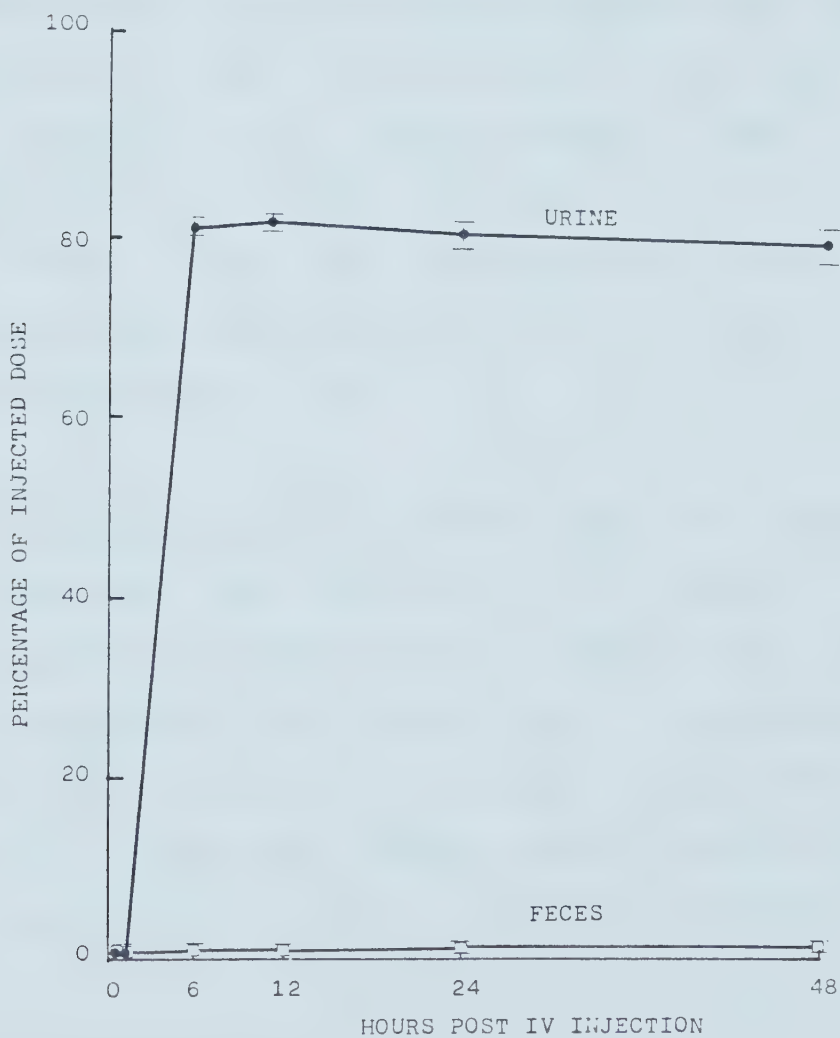
<u>Time (hours)</u> <u>post injection</u>	<u>Accumulated Percent Dose</u>	
	<u>Urine**</u>	<u>Feces**</u>
0.1 - 0.5	0.0 \pm 0.00	0.0 \pm 0.00
1	0.0 \pm 0.00	0.0 \pm 0.00
6	80.95 \pm 2.49	0.11 \pm 0.01
12	81.25 \pm 2.12	0.11 \pm 0.01
24	80.43 \pm 3.07	0.36 \pm 0.37
48	79.98 \pm 4.23	0.95 \pm 0.50

* Each rat was dosed at 1.09 micro curie Sm-153, intravenously

** Each value represents mean \pm 1 S.D. of three animals

Figure 20

Accumulated Sm-153 EDTA (1:10) Activity in Urine and Feces from Rats*



* Each rat was dosed at 1.09 uMole Sm/Kg intravenously and each point represents mean \pm 1 S.D. of three animals

When tissue distribution patterns were compared between Sm-153 activity and C-14 activity in the dual-labelled Sm-153(C-14)EDTA study, little correlation was observed (Table 11A, 19A). C-14 EDTA tumor-to-blood ratio was 4.27 at 24 hours and 0.61 at 48 hours compared to 37.22 and 65.49 respectively for Sm-153 activity (Figure 21). The tissue-to-blood ratio in the C-14 EDTA study did not reveal any preference of C-14 EDTA localization in one or two particular organs. The bone-to-blood ratio and liver-to-blood ratio at 48 hours was only 0.43 and 0.52 respectively (Table 19B). The corresponding ratios for Sm-153 activity at the same period of time were 867.37 and 696.93 respectively (Table 11B).

The dual-labelled Sm-153(C-14)EDTA tissue distribution experiment confirmed that localization of Sm-153 in the tumor was independent of EDTA. Such a pattern was also observed in organs such as liver and bone. It is therefore possible that the intracellular transport mechanism for Sm-153 does not involve EDTA. These results lended further evidence to the dissociation theory previously proposed.

Table 19A

Tissue Distribution Results for dual-labelled Samarium-153 (C-14) EDTA (1:10)
at 1.09 uMole Sm / Kg in BDF₁ mice Bearing Lewis Tumors (a,b)

Tissue	Time after Administration (C-14 EDTA Results)		
	1 Hour	6 Hours	24 Hours
Blood (c)	0.54 ± 0.15	0.08 ± 0.04	0.05 ± 0.02
Tumor	1.11 ± 0.73	0.14 ± 0.10	0.11 ± 0.03
Liver	0.82 ± 0.43	0.24 ± 0.02	0.37 ± 0.13
Kidneys	1.25 ± 0.82	0.32 ± 0.09	0.24 ± 0.07
Lung	0.10 ± 0.00	0.08 ± 0.04	0.04 ± 0.01
Spleen	0.25 ± 0.11	0.24 ± 0.06	0.06 ± 0.03
Bone (d) (Femur)	0.56 ± 0.16	0.13 ± 0.08	0.36 ± 0.29

- (a) Expressed as mean ± 1 S.D. of four animals
- (b) Percentage of injected dose in whole tissue except as indicated
- (c) Percentage of injected dose per milliliter of blood
- (d) Percentage of injected dose per 1.0 gram of tissue

Table I_{2B}

Tissue Distribution Results for dual-labelled Samarium-153((β -14)PrTx (1:10)
at 1.09 uMole Sm-153/Kg in BDF₁ Mice Bearing Lewis Lung Tumors (a,e)

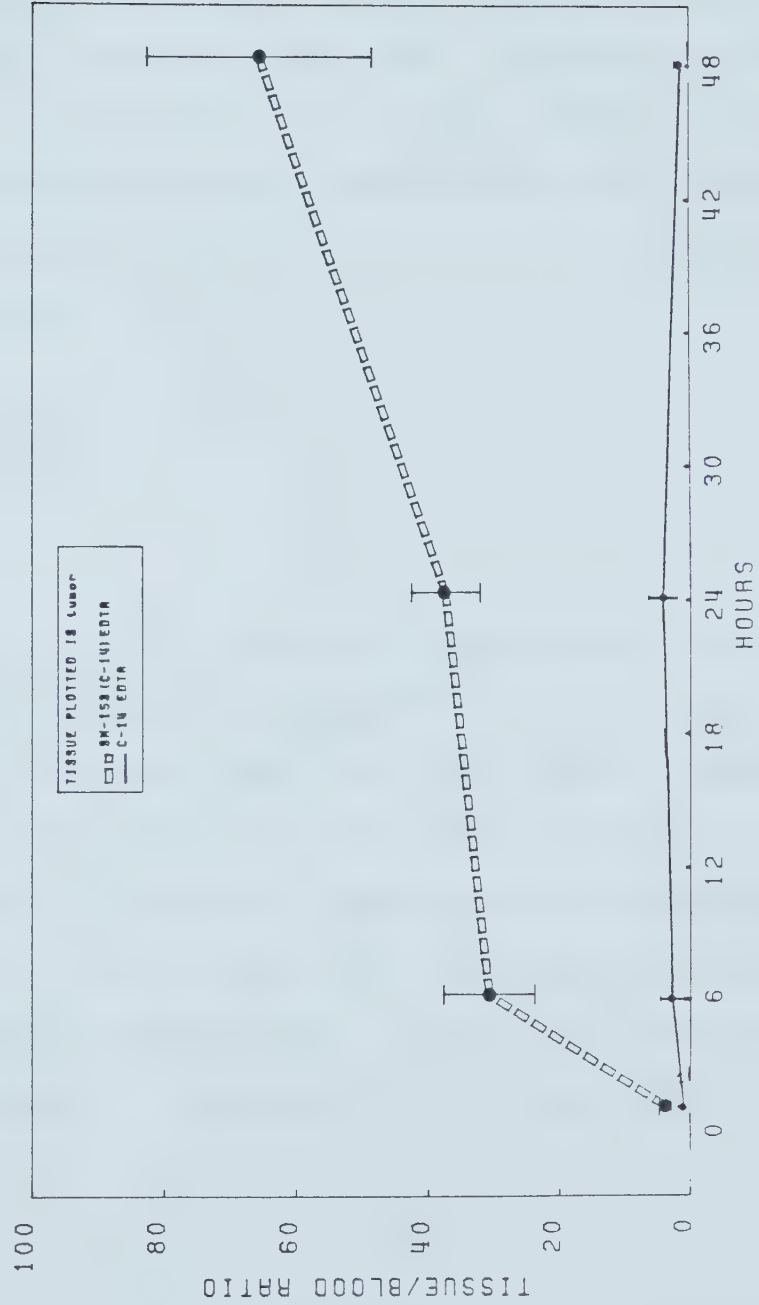
Tissue	Time after Administration (C-14 FPPA I.C.U.)		
	1 Hour	6 hours	24 hours
Tumor	1.15 ± 0.55	2.94 ± 1.97	4.27 ± 2.17
Liver	1.34 ± 0.34	3.44 ± 1.92	8.66 ± 4.97
Kidneys	8.17 ± 6.84	15.91 ± 13.60	17.61 ± 9.53
Lung	1.23 ± 0.49	7.84 ± 7.34	6.44 ± 1.33
Spleen	1.34 ± 0.46	18.56 ± 13.06	10.62 ± 2.45
Bone (Femur)	1.13 ± 0.51	2.01 ± 1.80	8.63 ± 7.71

(a) Expressed as mean ± 1 S.D. of four animals

(b) Expressed as tissue (gm)/blood (ml) ratio

Figure 21

Tumor to Blood Ratios of Sm-153(C-14)EDTA (1:10)
in BDF₁ Mice Bearing Lewis Lung Tumors



J. Toxicity Studies

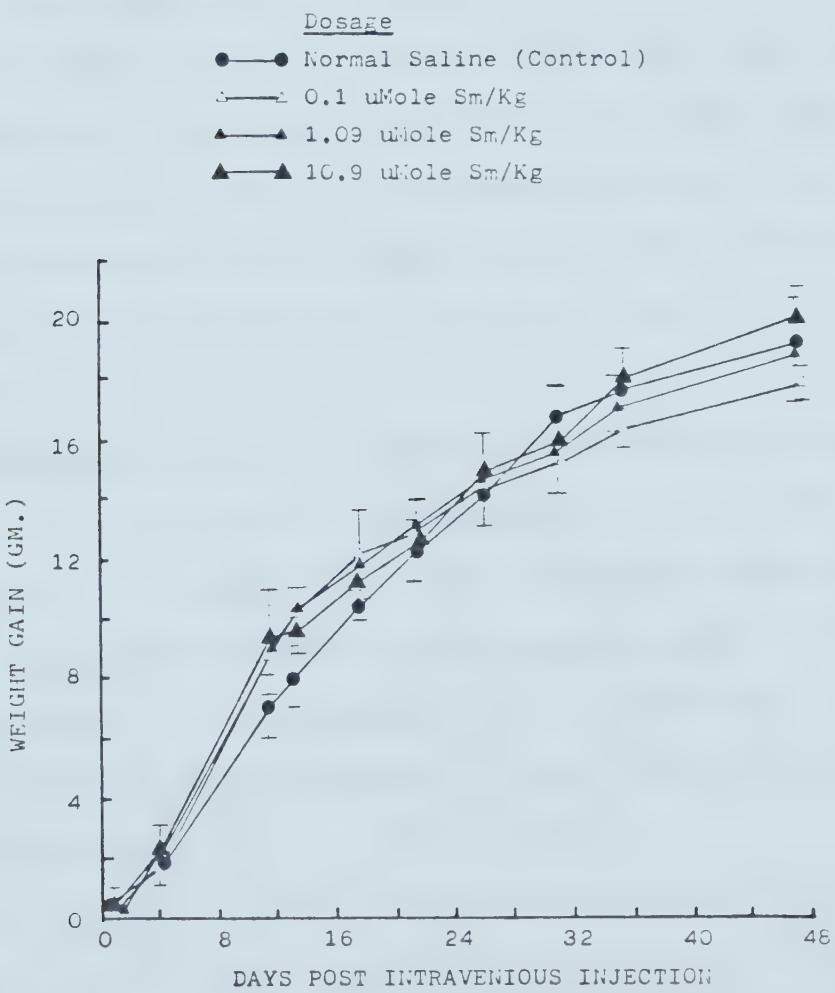
A good radiopharmaceutical should present little undesirable or toxic effects to the physical and histological well being of the body. Weight gain measurements and histopathological examinations of major organs of animals which received intravenous Sm-153 EDTA were therefore important.

1. Effect on Weight Gain

Mice in groups of four injected intravenously with normal saline (normal control), Sm-153 EDTA (1:10) in doses of 0.1 uMole Sm/Kg, 1.09 uMole Sm/Kg and 10.9 uMole Sm/Kg were examined. None of the animals died during the 64-day period of observation. In addition, there was no statistical difference ($P < 0.05$) in the weight gain among the injected groups and the controls within 64 days. Figure 22 depicts the observed weight gain of the animals during the period of experimentation.

Figure 22

The Effect of Sm-153 EDTA (1:10) on Normal Weight Gain*



* Each point represents mean \pm 1 S.D. of four animals (mice).

2. Histopathological Results

The histopathology of samples from lung, liver, kidneys and femur bone were compared for mice receiving Sm-153 EDTA (1:10) and normal mice over a 64-day period. First generation offsprings from female mice injected with 1.09 uMole Sm/Kg dose were also compared.

No observable abnormalities were noticed in all groups when compared to normals. Results also indicated that histological changes were not observed in either the mice injected with Sm-153 EDTA at dosages up to 10.9 uMole Sm/Kg. or the offsprings of female mice injected with 1.09 uMole Sm/Kg doses.

Insignificant number of hylaine casts were observed in the proximal tubules of some mice at 24 hour post administration of Sm EDTA dosed at 1.09 uMole Sm/Kg and 10.9 uMole/Kg. Isolated histopathological samples also revealed a slight increase in the number of bi and tri nuclea regenerating liver cells. However, these were all considered to be insignificant.

These results agree with the low toxicity reported by Haley (11). It is to be noted that in a clinical situation, high specific activity Sm-153 EDTA will be employed and the dose administered would probably be in the nanomole range.

K. Absorbed Radiation Dose Calculations for Sm-153 EDTA

Since Sm-153 EDTA appeared to be of potential value in diagnostic medicine, estimates were made of the radiation dose delivered to the whole body, liver, bone and kidneys. These calculations were based on the following assumptions:

1. internal distribution and elimination found in animal studies using mice can be applied to the human body,
2. 10.9 nMole Sm/Kg dose of Sm-153 EDTA (1:10) is used,
3. the human body has a total bone mass of 10 Kg, liver mass of 1833 g and kidneys mass of 310 g and a total body mass of 70 Kg (71),
4. radiation dose from the internal conversion electrons is not included as detailed information is not available at the time of these calculations,
5. beta radiations are considered as nonpenetrating (72), that they are nearly fully absorbed within a source volume, and the energy which escaped from the volume to other organs of interest is considered to be small in estimating the mean absorbed dose.

Based on the animal distribution and elimination studies certain generalities were made:

1. the uptake in liver, bone and kidneys were observed immediately after injection and little uptake

differences were observed at 1, 6 and 12 hours, therefore, their uptake half-time was considered as negligible (Table 12A, Figure 23),

2. the biological elimination half-times in the liver, bone and kidney were 57.34, 33.57 and 26.94 hours respectively,
3. the biological half-time observed in bone sample (femur) is representative of the whole skeletal system and the original dose concentration in the femur represents one-tenth of the total bone (71),
4. the original dose concentration in liver, total bone and kidneys were 13.99%, 21.30% and 2.91% respectively (original dose concentration in femur was estimated as 2.13%, based on the observed 2.13 ± 0.24 mean percentage dose in femur at 6 hours),

These generalities are not strictly true on the basis of the results of the distribution studies (Table 12A, Figure 23). However, it is believed that they represent the estimated situation in which the radiation dosage would be the highest.

The absorbed dose calculations are based on the equation (71):

$$\bar{D}(v + r) = \frac{\tilde{A}_r}{M_v} \sum \Delta_i \phi_i(v + r) \text{ rad}$$

where $\bar{D}(v + r)$ = dose to volume v from a uniform

distribution of radioactivity throughout region r;

Δ_i = equilibrium dose constant for radiation of type $i = 1, 2, 3, \dots$, with a fractional frequency N_i per disintegration and a mean energy \bar{E}_i in MeV

$$= 2.13 n_i \bar{E}_i \left[\frac{\text{g-rad}}{\mu\text{Ci-hr}} \right]$$

$\phi_i(v + r)$ = the absorbed dose fraction in volume v

\tilde{A}_r = the cumulative activity ($\mu\text{Ci-hr}$)

M_v = mass of volume under consideration

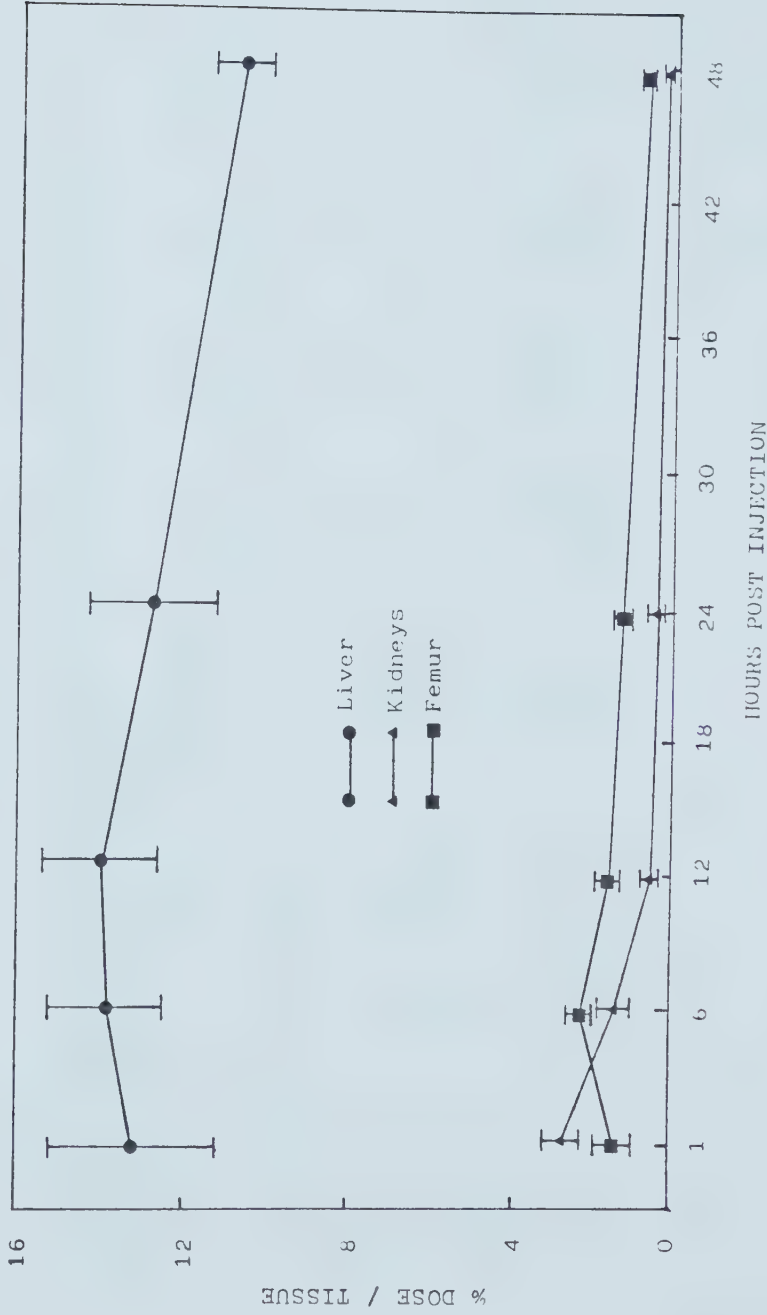
Equilibrium values and absorbed dose fraction values are listed in Tables 20, 21 and 22.

1. Radiation Dose to the Liver

Based on the assumptions previously stated, the radiation dose delivered to the liver is composed of the dose from the radioactivity distributed in the liver plus any contributions from the bone and kidneys. The radioactivity in the liver was initially 13.99% of the administered dose and was cleared from the liver with a biological half-time of 57.34 hours (Figure 23).

Figure 23

The Percentage Dose Distribution of Sm-153 EDTA(1:10) in Mice*



* Lewis lung tumor bearing mice administered intravenously at 10.9mole Sm/Kg

Equilibrium (Δ_i) and Absorbed Dose Fractions (ϕ_i) for various emulsions of Sm-153 of uniform distribution in Liver

Radiation (i)	n_i	\bar{E}_i (MeV)	$\Delta_i \left[\frac{\text{g-rad}}{\text{uCi-hr}} \right]$	ϕ_i Liver	ϕ_i Bone	ϕ_i Kidneys	ϕ_i Whole Body
Beta							
1	0.20	0.27	0.1150	1.0	0	0	0
2	0.50	0.24	0.2556	1.0	0	0	0
3	0.30	0.21	0.1342	1.0	0	0	0
Gamma							
1	0.054	0.070	0.0081	0.2790	0.0780	0.0060	0.0650
2	0.28	0.103	0.0014	0.1675	0.0490	0.0049	0.0550
3 - 19	0.06	0.64	0.0818	0.1622	0.0250	0.0040	0.4130
$\sum_{\Delta_i \phi_i}$				$\sum_{\Delta_i \phi_i}$	$\sum_{\Delta_i \phi_i}$	$\sum_{\Delta_i \phi_i}$	$\sum_{\Delta_i \phi_i}$
				0.5309	0.0056	0.0034	0.0671

Table 21

Equilibrium (Δ_i) and Absorbed dose fractions (ϕ_i) for various combinations of Sm-153 of uniform distribution in bone

Radiation (1)	n_1	\bar{E}_i (MeV)	Δ_i [$\frac{\text{g-rad}}{\text{uCi-hr}}$]	ϕ_i Liver	ϕ_i lone	ϕ_i Kidneys	ϕ_i Whole Body.
<hr/>							
Beta							
1	0.20	0.27	0.1150	0	1.0	0	0
2	0.50	0.24	0.2556	0	1.0	0	0
3	0.30	0.21	0.1342	0	1.0	0	0
Gamma							
1	0.054	0.070	0.0081	0.0044	0.0750	0.0010	0.6510
2	0.28	0.103	0.0614	0.0048	0.1810	0.0090	0.3990
3 - 19	0.06	0.64	0.0818	0.0044	0.1190	0.0010	0.3430

$$\sum_{\Delta_i \phi_i} \sum_{\Delta_i \phi_i} \sum_{\Delta_i \phi_i} \sum_{\Delta_i \phi_i}$$

$$0.00017 \quad 0.5203 \quad 0.00006 \quad 0.0579$$

Table 24

Equilibrium (Δ_i) and Abiotrobed bone fractions (ϕ_i) for various distributions of Sr-153 of uniform distribution in Kidneys

Radiation (i)	n_i	\bar{E}_i (MeV)	$\Delta_i \left[-\frac{B_{i-\text{rad}}}{w_{i-\text{hr}}} \right]$	ϕ_i Liver	ϕ_i Bone	ϕ_i Kidneys	ϕ_i Whole body
<hr/>							
Beta							
1	0.20	0.27	0.1150	0	0	0	0
2	0.50	0.24	0.2556	0	0	0	0
3	0.30	0.21	0.1342	0	0	0	0
Gamma							
1	0.054	0.070	0.0081	0.0360	0.1030	0.1720	0.6300
2	0.28	0.103	0.0614	0.0280	0.0640	0.0730	0.4550
3	0.06	0.64	0.0818	0.0253	0.0340	0.0760	0.4060
<hr/>							
				$\sum_{\Delta_i \phi_i}$	$\sum_{\Delta_i \phi_i}$	$\sum_{\Delta_i \phi_i}$	$\sum_{\Delta_i \phi_i}$
				0.0041	0.0076	0.5167	0.1067

Sm-153 has a physical half-life of 46.8 hours.

Therefore,

$$1/T_{\text{eff}} = 1/T_{\text{phys}} + 1/T_{\text{biol}} = 1/46.8 \text{ hr} + 1/57.34 \text{ hr}$$

$$1/T_{\text{eff}} = 0.0388 \text{ hr}^{-1}$$

where T_{eff} is the effective half-time of Sm-153 in the liver.

$$\lambda_{\text{eff}} = 0.693 \times 1/T_{\text{eff}} = 0.0269 \text{ hr}^{-1}, \text{ and}$$

$$\bar{A}_r = \bar{A}_r [1/\lambda_{\text{eff}}]$$

when there is only one component to the biological clearance (72).

It was found that 13.99% of the dose concentrates initially in the liver; therefore, for each mCi administered, 139.9 uCi will go to the liver.

$$\bar{D}(v + r) = \frac{\bar{A}_r}{M_v} \left[\frac{1}{\lambda_{\text{eff}}} \right] \sum \Delta_i \phi_i (v + r)$$

Therefore,

$$\begin{aligned} D(v \leftarrow r) &= (139.9 \text{ uCi} / 1833 \text{ g}) \times (1 / 0.0269 \text{ hr}^{-1}) \times \\ &\quad (0.5309 \text{ g-rad/uCi-hr}) \\ &= 1.5063 \text{ rads/mCi} \end{aligned}$$

Radiation dose to liver from radioactivity originally in total bone was :

For 1 mCi administered, there were 213 uCi originally in the bone:

$$\begin{aligned}
 1/T_{\text{eff}} &= 1/T_{\text{phys}} + 1/T_{\text{biol}} = 1/46.8 \text{ hr}^{-1} + 1/33.57 \text{ hr}^{-1} \\
 &= 0.0214 \text{ hr}^{-1} + 0.0298 \text{ hr}^{-1} = 0.0512 \text{ hr}^{-1} \\
 \lambda_{\text{eff}} &= 0.693 \times (1/T_{\text{eff}}) = 0.0355 \text{ hr}^{-1}
 \end{aligned}$$

$$\begin{aligned}
 \bar{D}(v+r) &= \frac{A_r}{M_v} \left[\frac{1}{\lambda_{\text{eff}}} \right] \sum \Delta_i \phi_i (v+r) \text{ rad} \\
 &= (213 \text{ uCi} / 10,000 \text{ g}) \times [1/0.0355 \text{ hr}^{-1}] \\
 &\quad \times [0.0007 \text{ g-rad/uCi-hr}] \\
 &= 0.0004 \text{ rad per mCi}
 \end{aligned}$$

Radiation dose to liver from radioactivity in kidney was :

For 1 mCi administered, there were 29.1 uCi originally in the kidneys:

$$\begin{aligned}
 1/T_{\text{eff}} &= 1/T_{\text{phys}} + 1/T_{\text{biol}} \\
 &= 1/46.8 \text{ hr}^{-1} + 1/26.94 \text{ hr}^{-1} \\
 &= 0.0214 + 0.0371 \\
 &= 0.0585 \text{ hr}^{-1} \\
 \lambda_{\text{eff}} &= 0.693 \times (1/T_{\text{eff}}) = 0.0405 \text{ hr}^{-1}
 \end{aligned}$$

$$\begin{aligned}
 \bar{D}(v+r) &= \frac{A_r}{M_v} \left[\frac{1}{\lambda_{\text{eff}}} \right] \sum \Delta_i \phi_i (v+r) \\
 &= (29.1 \text{ uCi} / 310 \text{ g}) \times [1/0.0405] \\
 &\quad \times [0.0041 \text{ g-rad/uCi-hr}] \\
 &= 0.0095 \text{ rad per mCi}
 \end{aligned}$$

The total radiation dose to the liver was estimated to be $1.5063 \text{ rads} + 0.0004 \text{ rads} + 0.0095 \text{ rads} = 1.5162 \text{ rads}$ per millicurie of administered radioactivity.

2. Radiation Dose to the Total Bone

Detailed calculations of the radiation dose to the total bone are shown in Appendix 2. The total radiation dose to the total bone was estimated to be 0.3493 rads per millicurie of radioactivity administered.

3. Radiation Dose to the Kidneys

Detailed calculations of the radiation dose to the kidneys are also shown in the Appendix 2. The total radiation dose was estimated to be 1.2076 rads per millicurie of administered radioactivity.

4. Radiation Dose to the Whole Body

The radiation dose to the whole body was estimated to be 0.3785 rads per millicurie of Sm-153 EDTA administered. Detailed calculations are given in Appendix 2 as well.

Based on the results of tissue distribution studies in mice, the radiation dosage for Sm-153 EDTA was estimated to be 1.52 rads per mCi (0.41 mGy/MBq) to the liver, 0.35 rads per mCi (0.09 mGy/MBq) to total bone, 1.21 rads per millicurie (0.33 mGy/MBq) to the kidneys and 0.38 rads per millicurie (0.10 mGy/MBq) to the whole body of the human model. Present estimations indicate that some consideration of radiation doses to liver and kidneys are needed before using Sm-153 EDTA in vivo.

Woolfender et al (10) reported preliminary dosimetry calculation for Sm-153 citrate based on the results of tissue distribution studies in rabbits. Whole body radiation dose was estimated to be 0.67 rads per millicurie (0.18 mGy/MBq) (10). Since a detailed calculation method and procedure was not expressed and the tracers were different, comparison is difficult. However, it appears that Sm-153 EDTA possibly offers a lesser radiation burden to the patients and better tumor availability than Sm-153 citrate.

When compared to the whole body radiation absorbed dose of Ga-67 citrate (0.26 rads/mCi or 0.07 mGy/MBq) as estimated by Cloutier et al (100), Sm-153 EDTA showed a higher radiation dose to the body per unit radioactivity of Ga-67 citrate. However, Sm-153 EDTA had shown several advantages over Ga-67 citrate in the previous investigation. These advantages, which include higher tumor avidity and the potential of earlier tumor imaging, would help to compensate the higher radiation burden as estimated above.

V. Summary and Conclusions

Experiments conducted throughout this thesis have shown that:

1. High specific activity samarium-153 was produced after the bombardment of enriched Sm-152 via the (n,γ) reaction with no significant radionuclidian impurities.
2. Sm-153 citrate, Sm-153 transferrin and Sm-153 EDTA can be prepared. The amount of complexing agent added determined the physical and biological characteristics of the compound.
3. Sm-153 colloid formation was prominent for Sm-153 citrate and Sm-153 transferrin both in vitro and in vivo.
4. The in vivo uptake of Sm-153 citrate and Sm-153 transferrin was predominantly in the liver and spleen - a result of in vivo colloid formation. No significant difference was observed between the two in vitro and in vivo.
5. Both Sm-153 citrate and Sm-153 transferrin revealed to be inferior imaging agents than Ga-67 citrate and Ga-67 transferrin for tumor localization in vivo.
6. When complexed with EDTA, Sm-153 was prevented from significant colloidal formation both in vitro and in vivo.

7. Calcium ions could not displace samarium from its EDTA complex.
8. Sm-153 EDTA (1:10) showed a greater tumor affinity in tumor culture cell studies than Ga-67 citrate.
9. Sm-153 was taken up by tumor cultured cells independently from EDTA due to possible dissociation of Sm-153 from EDTA complex at the cell surface.
10. A molar ratio of 1:10 of Sm-153 EDTA was needed to offer optimal stability from colloid formation in vivo. Skeletal uptake of Sm-153 EDTA (1:10), especially at joints, was observed.
11. Sm-153 EDTA (1:10) had shown at least a twenty-two fold higher tumor to blood ratio than Ga-67 citrate at 24 and 48 hours in vivo. This ratio could be improved to a small extent by lowering the dose administered.
12. Sm-153 EDTA (1:10) was superior to Ga-67 citrate in the delineation of the Dunning tumor using gamma scintillation imaging.
13. Tissue distribution studies revealed that Sm-153 EDTA localized mainly in bone, liver and kidneys. About 80% of the injected dose was eliminated through urine within the first 6 hours. Elimination of Sm-153 EDTA (1:10) in feces was found to be negligible.
14. Dual-labelled Sm-153(C-14)EDTA (1:10) experiments indicated that little C-14 EDTA activity was

detected in the tumor and that Sm-153 uptake in the tumor was independent of the EDTA during the same period of time in vivo. These results confirmed the possible dissociation of Sm-153 from EDTA during the uptake process as observed previously in vitro.

15. An intravenously injected dose of up to 10.9 uMole Sm/Kg of Sm-153 EDTA did not result in any noticeable changes in normal total body weight gain and histological well being of body organs such as lung, liver, kidneys and bone.
16. For a 10.9 nMole Sm/Kg dose of Sm-153 EDTA (1:10) administered intravenously, the estimated radiation dose to the whole body was about 0.38 rads/mCi or 0.10 mGy/MBq. Estimated radiation dose to liver, total bone and kidneys were 1.52, 0.35 and 1.21 rads/mCi (0.41, 0.09 and 0.33 mGy/MBq) respectively.
17. Sm-153 EDTA (1:10) is a potentially useful tumor imaging agent.

Bibliography

1. HIGASI, T., NAKAYAMA, Y., MURUTA, A., NAKAMURA, K., SUGIUAMA, M., KAWAGUCHI, T. and SUZAKI, S., J. Nucl. Med. 13: 196 - 201, 1972.
2. LANGHAMMER, H., GLAUBITT G., GREBE, S.F., J. Nucl. Med. 13: 25 - 30, 1972.
3. LARSON, S.M., JAMA 222: 321 - 323, 1972.
4. LAVENDER, J.P., LOWE, J. and BARKER, J. R., et al., Br. J. Radiol., 44: 361 - 366, 1971.
5. VAIDYA, S.G., CHAUDHURI, M. A. and MORRISON, R., Lancet 2: 911 - 914, 1970.
6. WINCHELL, H.S., SANCHEZ, P.P., WATANABE, E.K., HOLLANDER, L., ANGER, H.D. and McRAE, J., J. Nucl. Med. 11: 459 - 466, 1970.
7. BRUNES, H.D., Radiology 61: 602 - 612, 1953.
8. LARSON, S.M., Radiopharmaceuticals, Soci. Nucl. Med. 413, 1975.
9. NOUJAIM, A.A., LENTLE, B.C., HILL, J.R., TERNER, U.K. and WONG, H., Int. J. Nucl. Med. and Biol., 6: 193 - 199, 1979.
10. WOOLFENDEN, J.M., BRADFORD BARBER, H., HALL, J. and WACKS, M.E., Proceeding 3rd Ann West Reg Meeting, Society of Nucl. Med., 1978.
11. HALEY, T.J., J. Pharm. Sci., 54: 663, 1965.
12. ROSCINA, T.A., International Labour Office Encyclopaedia of Occupational Health and Safety, McGraw-Hill, II: 1202, 1972.
13. McGRAW-HILL Encyclopaedia of Science and Technology, McGraw-Hill, 12: 19, 1977.
14. CONSIDINE, D.M., Van Nostrand's Scientific Encyclopaedia, 5: 1957, 1976.
15. COTTON, F.A., Advanced inorganic Chemistry, 870, 1962.
16. UNDERWOOD, W.J., Trace Elements in Human and Animal

Nutrition, Academic Press, III, 1971.

17. SCHROEDER, H.A. and MITCHENER, M., J. Nutr., 101: 1431, 1971.

18. OEHME, F.W., Toxicity of Heavy Metals in the Environment I: 42, 1979.

19. KIRK-OTHMER, Encyclopaedia of Chemical Technology, 17: 143, 1968.

20. JACOBSON, C.A., Encyclopaedia of Chemical Reactions, Reinhold Publishing, 6: 1 - 18, 1959.

21. CLEVE, P.T., Vet. Ak. Handl. Ofvers, 4: 22, 1883. (Cited from Chemical Abstracts, American Chemical Society)

22. WEISER, A.B., J. Phys. Chem., 42: 677, 1938.

23. CARLA CASTELLANI BISI, et al., Gazz. Chim. Ital., 92: 447 - 53, 1962. (Cited from Chemical Abstracts, American Chemical Society)

24. BABESHKINA, Z.M., MARTYNENKO, L.I. and GRIGOREV A.I., Zh. Neorgan. Khim. 11:1282, 1966. (Cited from Chemical Abstracts, American Chemical Society)

25. SKORIK, N.A., et al., Tr. Tomskogo Gos. Univ. Ser. Khim. 157: 198 - 201, 1963. (Cited from Chemical Abstracts, American Chemical Society)

26. SIHVONEN, M.L., Ann. Acad. Sci. Fenn., A₂: 168, 1972. (Cited from Chemical Abstracts, American Chemical Society)

27. ERAMETSA, O., et al., Ann. Med. Exp. Biol. Fenn., 49: 35 - 37, 1971.

28. WESTER, P.O., Sci. Total Environ. 1: 97, 1972.

29. MATSUSAKA, N., INABA, J., ICHIKAWA, R., IKEDA, M. and OHKUDO, Y., Radiation Biology of the Fetal and Juvenile Mammal, U.S. Atomic Energy Commission, Washington D.C., 217 - 226, 1969.

30. BAALOGH, G., Ther. Hung., 22: 83 - 89, 1974.

31. GALOS, G., Ther. Hung., 22: 180 - 183, 1974.

32. LAWKONICZ, W., et al., Wiad Lek, 27: 1191 - 5, 1974. (Cited from Chemical Abstracts, American Chemical Society)

33. TURIN, M.Q., Pharmacology, 16: 301 - 5, 1978.
34. TURIN, M.Q., Jpn. J. Pharmacol., 27: 592 - 5, 1977.
35. TURIN, M.Q., Pharmacology, 15: 227 - 32, 1977.
36. TURIN, M.Q., Arch. Int. Pharmacodyn Ther., 230: 199 - 209, 1977. (Cited from Chemical Abstracts, American Chemical Society)
37. DOS REMEDIOS, C.G., Nature (London), 270: 750 - 1, 1977.
38. EPSTEIN, M., LEVITZKI, A. and BRUBEN, J., Biochemistry, 13: 1777 - 82, 1974.
39. KASTUER, J., et al., Proc. Bone Meas. Conf., 274 - 9, 1970.
40. O'MARA, R.E., McAFFEE, J.G. and SUBRAMANIAN, G., J. Nucl. Med., 10: 49 - 51, 1969.
41. GILYAZUTDINOV, I.A., et al., Kazan Med. Zh., 5: 45 - 7, 1974. (Cited from Chemical Abstracts, American Chemical Society)
42. HISADA, K. and ANDO, A., Igaku No Ayumi, 82: 635, 1972. (Cited from Chemical Abstracts, American Chemical Society)
43. HISADA, K. and ANDO, A., Radioisotopes, 21: 549 - 555, 1972.
44. HIGASI, T., FUJIMURA, T. and KANNO, M., Int. J. Nucl. Biol., 2: 98 - 101, 1973.
45. TARJAN, G., PAL, I., KARIKA, Zs. and FUZY, M., Izotopotechnika, 16: 440, 1973. (Cited from Chemical Abstracts, American Chemical Society)
46. SULLIVAN, J.C., FRIEDMAN, A.M., RAYUDU, G.V.S., FORDHAM, E.W. and RAMACHANDRAN, P.C., Int. J. Nucl. Med. Biol., 2: 44 - 45, 1975.
47. FRIEDMAN, A.M., SULLIVAN, J.C. and RUBY, S.L., Int. J. Nucl. Med. Biol., 3: 37 - 40, 1976.
48. THAKUR, M.L., et al., Proc. IAEA Symp. Copenhagen, March, 1973.
49. OEHME, F.W., Toxicity of Heavy Metals in the Environment, I: 558 - 561, 1979.
50. LEE, R.E., GORANSON, S.S., ENRIONE, R.E. and MORGAN,

G.B., Size Distribution Measurements of Trace Metal Components, Presented at the American Chemical Society 163rd Meeting, Boston, 1972.

51. SCOTT, J.R., In-113m Indium Oxinate: A New Possible Lung Scanning Agent, M.Sc. Thesis, University of Alberta, 1973.
52. BROWNING, E., Toxicity of Industrial Metals, Butterworks II, 1969.
53. STICHER, H., SPYCHER, M.A. and RUETTNER, J.R., Nature (London), 241: 49, 1973.
54. GENSCICKE, F. and NITSCHKE, H.W., Radiobiol. Radiother., 11: 57, 1970.
55. TERNER, U.K., WONG, H., NOUJAIM, A.A., LENTLE, B.C. and HILL J.R., Int. J. Nucl. Med. Biol., 6: 23, 1979.
56. WONG, H., TERNER, U.K., ENGLISH, D., NOUJAIM, A.A., LENTLE, B.C. and HILL, J.R., Int. J. Nucl. Med. Biol., 7: 9 - 16, 1980.
57. SEPHTON, R.G. and KRAFT, N., Cancer Res. 38: 1213 - 1216, 1978.
58. STEEL, G.G., Growth Kinetics of Tumors, Clarendon Press, Oxford, p.152 and 258 - 263, 1977.
59. SCHABEL, F.M. Jr., Pharmac. Ther. A., 1: 411, 1977.
60. DREWINKO, B. and HUMPHREY, R.M., Growth Kinetics and Biochemical Regulation of Normal and Malignant Cells, The Williams & Wilkins Company, p.547 - 557, 1977.
61. CREASEY, W.A., Antibiotics, 2: 420, 1979.
62. LLOYD, H.H., Cancer Chemother. Res., 54: 143, 1970.
63. STEEL, G.G. and ADAMS, K., Cancer Res., 35: 1530 - 5, 1975.
64. DUNNING, W.F., Natl. Cancer Inst. Monogr., 12: 351, 1963.
65. CLAFLIN, A.J., MCKINNEY, E. and FLETCHER, M.A., Oncology, 34: 105, 1977.
66. SEMAN, G., MYERS, B., BOWEN, J. and DMOCHOWSKI, L., Invest. Urol., 16: 231, 1978.

67. BIERMANS, HENRARD, Ind. Chim., 39: 6, 1952. (Cited from Chemical Abstracts, American Chemical Society)

68. HARRIS, D.C., Biochem., 16: 560, 1977.

69. HARRIS, D.C. and AISEN, P., Biochem., 14: 262, 1975.

70. KULPRATHIPANJA, S. and HNATOWICH, D., Int. J. Appl. Rad. and Isop. 28: 229, 1977.

71. TERNER, U.K., Unpublished Data.

72. SNYDER, W.S., Ford, M.R., Warner, G.G. and Fisher, H.L., Jr., J. Nucl. Med., 10, Supp. 3, Pamph. 5, 1969.

73. LOEVINGER, R., J. Nucl. Med., 9, Supp. 1, Pamph. 1, 1968.

74. DILLMAN, L.T., J. Nucl. Med., 10, Supp. 3. Pamph. 4, 1969.

75. ZALIK, S., Outline of Statistical Methods for Biological and Medical Research, University of Alberta, p.10 - 17, 1976. University of Alberta.

76. RADIOLOGICAL HEALTH HANDBOOK, U.S. Department of Health and Welfare, Revised Edition : 314, 1970.

77. LEDERER, C.M., HOLLANDER, J.M. and PERLMAN, I., TABLE OF ISOTOPES, John Wiley and Sons Inc. N.Y., 6: 307, 1967.

78. TANANAEV, I.V. and VASIL'EVA, V.P., Russ. J. Inorganic Chem., 8: 555, 1963.

79. TANANAEV, I.V. and VASIL'EVA, V.P., Zh. Neorgan. Khim. 9: 211, 1964. (Cited from Chemical Abstracts, American Chemical Society)

80. TANANAEV, I.V. and CHUDINOVA, N.N., Russ. J. Inorganic Chem., 8: 558, 1963.

81. TANANAEV, I.V. and CHUDINOVA, N.N., Russ. J. Inorganic Chem., 7: 1185, 1962.

82. MEL'NIKOV, P.P., EFREMOV, V.A., STEPANOV, A.K., ROMANOVA, T.S. and KOMISSAROVA, L.N., Russ. J. Inorganic Chem. 21: 26, 1976.

83. BLANCO, R.E. and PERKINSON J.D., J. Am. Chem. Soc., 73: 2696, 1951.

84. CHISHOLM, J.J., Pediatrics, 54: 441, 1974.

85. MARTELL, A.E. and CALVIN, M., Chemistry of the Metal Chelate Compounds, Prentice-Hall Inc., N.Y., 1952.
86. KRUPP, M.A., SWEET, N.J., JAWETZ, E., BIGLIERI, E.G. and ROE, R.L., Physician's Handbook, Lange Medical Publications, L.A., 7th Edition: 496, 1973.
87. TAKATA, M., PICKARD, W., LETTVIN, J.Y. and Moore, J.W., J. Gen. Physiol., 50: 461, 1966.
88. CUATRECASAS, P., FUCHS, S. and ANFINSEN, C.B., J. Biol. Chem., 242: 1541, 1967.
89. DURBIN, P.W., ASING, C.W., JOHNSTON, M.E., HAMILTON, J.G. and WILLIAMS, M.H., The metabolism of the lanthanons in the rat. USAEC Report, ORINS-12: 171, 1956.
90. WAGNER, H.N., Nuclear Medicine, HP Publishing Co., New York, 205 - 213, 1975.
91. FOREMAN, H., VIER, M. and MAGEE, M., J. Biol. Chem., 203: 1045, 1953.
92. FOREMAN, H. and TRUJILLO, T., J. Lab. Clin. Med. 43: 566, 1954.
93. MYERS, W.G. and DIENER, C.F., J. Nucl. Med., 1: 124, 1960.
94. WINTER, C.C. and MYERS, W.G., J. Nucl. Med., 3: 273, 1962.
95. HOSAIN, F., REBA, R.C. and WAGNER H.N., Radiology 93: 1135, 1969.
96. VINCKE, E. and OELKERS, H.A., Arch, Exptl. Pathol. Pharmakol., 187: 594, 1937.
97. SOULIER, J.P. and WEILLAND, C., Rev. Hematol., 11: 265, 1956.
98. HUNTER, R.B. and WALKER, W., Brit. Med. J., I: 227, 1957.
99. LARSON, S.M., RASEY, J.S., ALLEN, D.R. and NELSON, N.J., J. Nucl. Med., 20: 837, 1979.
100. CLOUTIER, R.J., WATSON, E.E. and HAYES, R.L., J. Nucl. Med., 14: 755, 1973.

Appendix 1

Derivation of equation:

U_d = percentage uptake by 10^6 dead cells

U_v = percentage uptake by 10^6 live cells

U_o = percentage uptake by 10^6 (live and dead) cells

V = viability of the cells

Let amount of nuclide be A

Uptake by 10^6 dead cells = $A \times U_d$

Number of dead cells in 10^6 live and dead cells

= $10^6 \times (100-V)/100$

Uptake by the $(100-V)/100 \times 10^6$ dead cells = $A \times U_d \times (100-V)/100$

Number of live cells in 10^6 (live + dead) cells = $10^6 \times V/100$

Uptake by 10^6 live cells = $A \times U_v$

Uptake by $V/100 \times 10^6$ live cells = $A \times U_v \times V/100$

Total uptake by the 10^6 live and dead cells

= $(A \times U_v \times V/100) + (A \times U_d \times (100-V)/100)$

Percentage uptake by 10^6 live + dead cells (= U_o)

= (total uptake / total amount of nuclide) $\times 100$

= $((A \times U_v \times V/100) + (A \times U_d \times (100-V)/100))/A \times 100$

= $(U_v \times V) + (U_d \times (100-V))$

$U_o = (U_v \times V) + (U_d \times (100-V))$

$U_v \times V = U_o - (U_d \times (100-V))$

$U_v = U_o/V - (U_d \times (100-V))/V$

Appendix 2

Calculations of The Absorbed Radiation Dose To The Bone,
Kidneys And Whole Body From Sm-153 EDTA

A. Absorbed Radiation Dose to the Bone

1. Radiation dose to bone from radioactivity in bone:

For 1 mCi administered, there were 213 uCi originally in the bone:

$$1/T_{\text{eff}} = 0.0512 \text{ hr}^{-1}$$

$$\lambda_{\text{eff}} = 0.0355 \text{ hr}^{-1} \quad \bar{D}(v + r) = \frac{A_r}{M_v} \left[\frac{1}{\lambda_{\text{eff}}} \right] \sum \Delta_i \phi_i(v + r) \text{ rad}$$

$$D(v \leftarrow r) = (213 \text{ uCi}/10,000g) \times [1/0.0355 \text{ hr}^{-1}]$$

$$\times [0.5263 \text{ g-rad/uCi-hr}]$$

$$= 0.3158 \text{ rads per mCi}$$

2. Radiation dose to bone from radioactivity originally in the liver:

For each mCi administered, 139.9 uCi were originally in the liver:

$$1/T_{\text{eff}} = 0.0388 \text{ hr}^{-1}$$

$$\lambda_{\text{eff}} = 0.0269 \text{ hr}^{-1}$$

$$D(v \leftarrow r) = (139.9 \text{ uCi} / 1833 \text{ g}) \times (1/ 0.0269 \text{ hr}^{-1})$$

$$\begin{aligned} & \times 0.0056 \text{ g-rad/uCi-hr} \\ & = 0.0159 \text{ rad / mCi} \end{aligned}$$

3. Radiation dose to bone from radioactivity in kidneys:

For 1 mCi administered, there were 38.5 uCi originally in the kidneys:

$$1/T_{\text{eff}} = 0.0585 \text{ hr}^{-1}$$

$$\lambda_{\text{eff}} = 0.0405 \text{ hr}^{-1}$$

$$D(V \leftarrow r) = (29.1 \text{ uCi} / 310\text{g}) \times [1/0.0405]$$

$$\begin{aligned} & \times [0.0076 \text{ g-rad/uCi-hr}] \\ & = 0.0176 \text{ rads per mCi} \end{aligned}$$

Therefore, the total absorbed dose to total bone is estimated as 0.3158 rads + 0.0159 rads + 0.0176 rads = 0.3493 rads per mCi.

B. Absorbed Radiation Dose to the Kidneys

1. Radiation dose to kidneys from radioactivity in kidneys:

$$\lambda_{\text{eff}} = 0.0405 \text{ hr}^{-1}$$

$$D(V \leftarrow r) = (29.1 \text{ uCi} / 310\text{g}) \times (1/0.0405)$$

$$\begin{aligned} & \times (0.5167 \text{ g-rad/uCi-hr}) \\ & = 1.1976 \text{ rads per mCi} \end{aligned}$$

2. Radiation dose to kidneys from radioactivity originally

in the liver:

$$\lambda_{\text{eff}} = 0.0269 \text{ hr}^{-1}$$

$$\begin{aligned} D(V \leftarrow r) &= (139.9 \text{ uCi} / 1833 \text{ g}) \times 1/0.0269 \text{ hr}^{-1} \\ &\quad \times 0.0034 \text{ g-rad/uCi-hr} \\ &= 0.0096 \text{ rads per mCi} \end{aligned}$$

3. Radiation dose to kidneys from radioactivity originally in the bone:

$$\lambda_{\text{eff}} = 0.0355 \text{ hr}^{-1}$$

$$\begin{aligned} D(V \leftarrow r) &= (213 \text{ uCi} / 10,000 \text{ g}) \times (1/0.0355) \\ &\quad \times 0.0006 \text{ g-rad/uCi-hr} \\ &= 0.0004 \text{ rads per mCi} \end{aligned}$$

Therefore, the total absorbed dose to kidneys is estimated as 1.1976 rads + 0.0096 rads + 0.0004 rads = 1.2076 rads per mCi.

C. Absorbed Radiation Dose to Whole Body

1. Radiation dose to whole body from radioactivity in the liver:

$$\lambda_{\text{eff}} = 0.0269 \text{ hr}^{-1}$$

$$\begin{aligned} D(V \leftarrow r) &= (139.9 \text{ uCi}/1833 \text{ g}) \times (1/0.0269 \text{ hr}^{-1}) \\ &\quad \times 0.0671 \text{ g-rad/uCi-hr} \end{aligned}$$

= 0.1904 rad per mCi

2. Radiation dose to whole body from radioactivity in the bone:

$$\lambda_{eff} = 0.0355 \text{ hr}^{-1}$$

$$D(V \leftarrow r) = (213 \text{ uCi}/10,000 \text{ g}) \times (1/0.0355 \text{ hr}^{-1}) \\ \times 0.0579 \text{ g-rad/uCi-hr} \\ = 0.0347 \text{ rad/mCi}$$

3. Radiation dose to whole body from radioactivity in the kidneys:

$$\lambda_{eff} = 0.0405 \text{ hr}^{-1}$$

$$D(V \leftarrow r) = (29.1 \text{ uCi}/310 \text{ g}) \times (1/0.0405) \\ \times 0.0662 \text{ g-rad/uCi-hr} \\ = 0.1534 \text{ rad/mCi}$$

Therefore, the total dose to the whole body is estimated to be 0.1904 rads + 0.0347 rads + 0.1534 rads = 0.3785 rads per mCi.

B30361